THE DESIGN OF FEED NETWORKS FOR ENHANCED BANDWIDTH OPERATION OF MICROSTRIP PATCH ANTENNAS

by

DAVID MARTIN DE HAAIJ

Submitted in partial fulfillment of the requirements for the degree

MASTER OF ENGINEERING

Department of Electrical, Electronic and Computer Engineering
Faculty of Engineering, Built Environment and Information Technology
UNIVERSITY OF PRETORIA

September 2003

Summary

This dissertation investigates a simple LC-matching network for the impedance bandwidth enhancement of microstrip patch antennas. Wideband impedance matching is a standard practice for active circuits. Simple impedance matching of antennas is also quite common, but data on wideband impedance matching of antennas is not found very much in the open literature. The matching circuit presented consists out of a resonant LC-circuit with a quarterwave matching line as part of the design. Results for a number of experimental antennas, on which the new technique was applied, are included in the report. A well-defined design procedure is also presented, and results in a relatively small circuit to implement. It is shown that the antenna VSWR bandwidth could be improved to more than double the original size in most of the antennas investigated.

Opsomming

Die verhandeling ondersoek 'n eenvoudige LC-aanpasnetwerk vir die impedansie bandwydte verbetering van mikrostrook antennas. Wyeband impedansie aanpasnetwerke word standaard toegepas op aktiewe hoëfrekwensie stroombande. Eenvoudige aanpasnetwerke word gereeld op antennes toegepas, maar die kombinering van wyeband aanpasnetwerke op antennes word nie baie bespreek in die literatuur nie. Die aanpasnetwerk wat in die verhandeling bespreek word bestaan uit 'n resonante LC-stroombaan met 'n kwartgolftransformator as 'n integrale deel van die stroombaan ontwerp. Die nuwe aanpasnetwerk is op 'n aantal eksperimentele antennas toegepas en die resultate word in die verhandeling bespreek. Die stroombaan, wat daarop gemik was om 'n eenvoudige en fisiese klein ontwerp te wees, se resultate toon dat die LC-aanpasnetwerk daartoe in staat is om die VSWR bandwydte van die oorspronklike antenne te verdubbel.

Acknowledgements

I would like to thank the God above for helping me through the time of my studies on this dissertation.

I would like to thank Professors Johan Joubert and Wimpie Odendaal for always being there to answer questions, support my studies and teaching me about antennas and electromagnetism in general.

Thanks to all my fellow students that helped during coffee breaks to discuss matters of interest on the topic.

Special thanks to my parents, Bram and Ank de Haaij, who showed me how to appreciate life and not take anything for granted. I thank you for giving me the opportunity to study at the university. Despite the many things I learned at Tuks, I don't believe I'll ever be able to equal the amount of things I learned at home.

Finally, I want to thank my girlfriend Yolanda Volsteedt for not dumping me when I had to study, my fiancée for not complaining when I had to study, and lastly my wife Yolanda de Haaij, for supporting me in the final stretch of finishing the dissertation.

To my parents, Bram and Ank de Haaij.

Thanks for the opportunity!

"Ywer sonder kennis deug nie;
oorhaastigheid bring foute."

- Spreuke 19:2

Contents

Chapter 1

Introduction

1.1 Background

The use of microstrip antennas has become increasingly popular. They have the advantages that they are compact in size, light in weight, low in cost and easy to fabricate [1]. Furthermore, these antennas can easily be integrated with microwave circuits and used for implementation in conformal arrays [2]. Despite these advantages they exhibit an inherently narrow bandwidth. A number of techniques to overcome this problem have been presented and work very effectively [1]. Some of the bandwidth enhancement techniques are thicker substrate, lower dielectric constant for the substrate or reactively loaded and multiple-resonator antennas.

The use of thicker, lower permittivity substrate, discussed in [3], results in a very effective increase in impedance bandwidth for the microstrip patch antenna. The problem associated with this technique, however, is the inductive component of the probe-feed. The series inductance is added to the RLC-equivalent impedance behaviour of the microstrip patch antenna [4], and if not compensated for in the design will lead to a substantial mismatch. The radiation pattern of the antennas is also affected by the thicker substrate, with higher cross-polarisation levels encountered, particularly in the H-plane. A remarkable increase in beam squint as a result of the probe is also sometimes introduced. A number of techniques for compensation of this problem have been discussed in the literature. One of these

techniques is probe compensation through capacitive feeding. The problem encountered with the input impedance is effectively solved with the capacitive feed, but the probe's influence on the radiation pattern remains [5-9]. Another feed structure mentioned in the literature is aperture coupling [10,11]. Aperture coupling has proven to work very effectively, lowering the cross-polarisation levels in the H-plane to negligible values. One drawback with this type of feed is that the aperture in the ground plane results in an increase in back lobe radiation.

Multiple resonators and reactive loading of the antenna are used to create more than one resonant frequency. A major design focus for this type of structure is dual-band antennas that will operate at two discrete frequencies [12 - 14]. By choosing the two resonant frequencies close to each other, it is possible to create a wider bandwidth due to the two overlapping resonant frequencies. The overall structure of this antenna is much more complex than a single patch antenna, thus leading to more intensive design procedures and less ideal radiation patterns [15].

The implementation of an impedance matching circuit to enhance the bandwidth of microstrip patch antennas was first introduced by Pues et al. [1]. Subsequent research led to the creation of the Simplified Real Frequency Technique (SRFT) [2,4]. This technique was used on passive antennas, and a bandwidth improvement factor in the range of 100% of the original impedance bandwidth was obtained. The SRFT was also implemented on active antennas, designing a matching circuit between the amplifier and the antenna [16]. This is named the dual-matching case, where both the load and system impedance consist of real and imaginary values.

The inclusion of the matching network in the feed has no effect on the radiation properties of the patch antenna itself. For a probe-fed microstrip patch antenna, the feed line with the matching network is hidden behind the ground plane of the antenna and there can be no physical coupling between the reactive circuit and the radiating element. The radiation pattern remains fairly constant for a frequency range often wider than the Voltage Standing Wave Ratio (VSWR) bandwidth of the patch antenna [1]. However, a remarkable loss in gain is encountered over the bandwidth considered. Although part of the loss is due to the

fact that one moves away from the resonant frequency, drop in gain can also be attributed to mismatch losses encountered at the feed point. The aim is to reduce these losses at the feed point by using a wideband feed network.

Recently, coupled transmission lines as a means to increase the bandwidth of patch antennas have been discussed [17, 18]. Coupled lines as matching networks for implementation in patch arrays are discussed in [17]. The resonant nature of the feed line results in an improvement of the 2:1 VSWR bandwidth of the array of about 110%. The structure proposed in [17] consists of two coupled quarterwave sections. The transmission line required to feed the antenna would then be more than half a wavelength long. In view of this relatively large size the coupled line matching technique is recommended mainly for antenna arrays where the antenna itself is already larger in size. A second coupled line structure presented in [18] implements a resonant feed on the same side of the substrate as the antenna. There is no physical connection between the antenna and the feed line, effectively resulting in two quarterwave coupling sections as well. The technique does, however, occupy less space than the structure presented in [17]. The bandwidth improvement factor given for this technique is considered to be three times the original bandwidth. The fact that the feed network is on the same side as the radiating element limits the usability of this technique, since the antenna cannot be placed on thicker substrate with lower relative dielectric constant than the microstrip feed network allows.

1.2 Contribution of this dissertation

Impedance matching of microstrip antennas proved to be a viable solution to the bandwidth limitation problem encountered with microstrip patch antennas. The SRFT is a matching technique for microstrip patch antennas that presented promising results, but the numerical optimisation and calculation of the matching circuit is a tedious process [17]. The coupled quarterwave matching circuit provided a simple solution to the wideband matching problem. Space occupancy proved a major drawback for this technique, as well as limitations on the choice of possible dielectric substrates.

In this dissertation a relatively simple matching circuit, consisting of a parallel capacitor-inductor combination and a phase transformator, is proposed. The design of the matching circuit is called the Single LC-Resonator Matching Technique. The Single LC-Resonator Matching Technique is able to increase the VSWR bandwidth of probe-fed patch antennas to almost double the original bandwidth. The matching circuit can be designed to provide an increase in VSWR bandwidth for any predefined VSWR specification.

An improved version of the proposed matching technique, named the Optimum Bandwidth Single LC-Resonator Matching Technique (SRMT), is also presented [19, 20]. This technique includes impedance transformation, and the design procedure of the originally obtained Single LC-Resonator Matching Technique is revised. Results comparable to the SRFT and the coupled quarterwave matching lines are obtained, with the VSWR bandwidth improved to more than double the original bandwidth.

The SRMT is compact and does not occupy much space. It is easy to design and implement in microstrip line.

1.3 Organisation of this dissertation

In Chapter 2 a general overview of previous impedance matching techniques is presented. The SRFT is described with specific attention paid to the components used and the circuit lay-out in microstrip line. The resonant feed with coupled lines [17, 18] is also considered, as well as two additional example antenna configurations that implement the feed network as the main contributor for an enhanced VSWR bandwidth.

Chapter 3 discusses the whole design procedure of the proposed matching circuit. The discussion is undertaken with the aid of a patch antenna example. The SRMT is explained on a step-by-step basis, with a brief explanation given with each new step.

The example published for the SRFT is considered in Chapter 4. The results obtained using respectively the SRFT and the SRMT are directly compared on the patch antenna

implemented as test case for the SRFT in [2, 4]. Results for other standard matching techniques are also included, namely the quarterwave stub, single stub, double stub and triangular matching network.

Chapter 5 includes full-wave simulations as well as actual measurements for a number of different types of microstrip patch antennas. A summary of the results obtained for the SRMT is presented at the end of Chapter 5.

Chapter 6 concludes the dissertation, and provides a brief summary of the results shown in the dissertation. Some ideas for future work and expanding the basic matching circuit are also included.

Chapter 2

Background

The use of matching networks to enhance the properties of microstrip patch antennas has not received much attention in open literature. The aim with this dissertation is to shed some light on the possibilities that exist when one includes a matching feed network as part of the antenna design. Chapter 2 presents a brief overview of current antenna impedance matching techniques. Specific attention is paid to the circuit layout, the origin of the technique and the level of impedance bandwidth improvement obtained with each of the techniques.

2.1 Concepts of impedance matching

The most basic impedance matching network consists mainly of circuits with an open or shorted stub transmission line section [21], a quarterwave transformer or in amplifier design a T- or Π-section impedance matching circuit [22]. In active circuit design where transistors and other circuit components are used, impedance matching is very important, the reason being that transistors are not necessarily, if ever, matched to the required system impedance. To accomplish a basic match a T- or Π-section is implemented, resulting in a match at the required frequency, but not necessarily at other frequencies. Figure 2.1 shows an example of a Π-section impedance matching circuit. The fact that the circuit is only matched at a single frequency can be a problem. Normally a system is not meant to work at

a single frequency, but over a designated frequency range. Having a 50 Ω match at a single frequency does imply that there will be a frequency range around the matched point where the VSWR will fall below a certain value, thus resulting in a matched frequency range. The problem is that there will be no control over the frequency range impedance behaviour other than the centre frequency. Numerous techniques have been developed to address this problem.

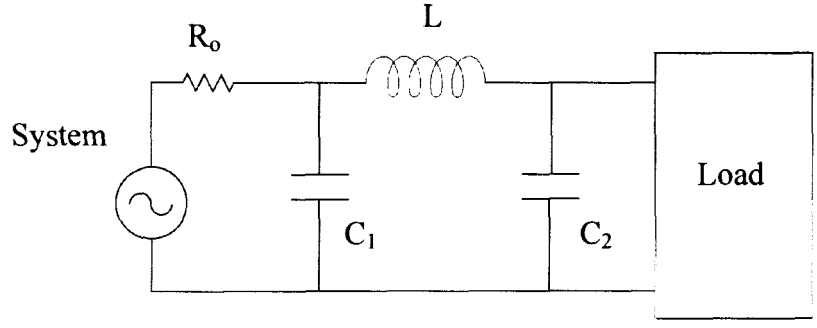

Figure 2.1 Implementation of a Π-section to match a load with arbitrary impedance to a specific system

2.2 The Real Frequency Technique

The Real Frequency Technique, known in short as the RFT, has been developed by H.J. Carlin in 1977 [23]. The method uses real frequency impedance data (for example experimental results), so that no model or prior knowledge of the load is required. This implies that the technique's aim is to find a matching solution for any arbitrary load. The load might either be a specific model, or it could be a set of tabulated load impedance values with no clearly visibly relation between them. The transducer gain $T(\omega^2)$ is taken as the starting point for the design of the matching circuit, and the gain through the matching circuit is optimised for maximum power transfer over a designated frequency range (Equation (1), taken from [23]).

$$T(\omega^2) = \frac{\text{Power to load}}{\text{Power available from generator}} = 1 - |\rho|^2 \qquad (1)$$

Transducer gain is a term often used in amplifier circuit design and is not a commonly used definition for antennas. The gain is simply a reference to the power transferred through the matching network considered, and is also known as G_T [22].

$$G_T = T(\omega^2) = |S_{21}|^2 \tag{2}$$

The whole procedure is described in [23], and examples are presented. The circuits considered consist of an LC-ladder network, as shown in Figure 2.2.

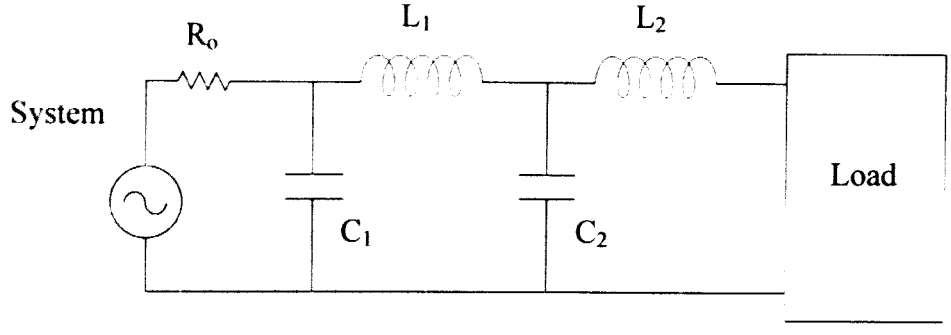

Figure 2.2 Circuit topology used for the examples given in [23]

In amplifier circuits the active circuit normally acts as an intermediate stage between two parts of the system. Figure 2.3 illustrates how a Field Effect Transistor (FET) is placed in a circuit, and how two matching circuits are required to create an overall matched system. This topology is discussed in [24]. The RFT is once again considered in this paper, but generalised for implementation in circuits such as the one shown in Figure 2.3 instead of circuits terminated in a load (Figure 2.2).

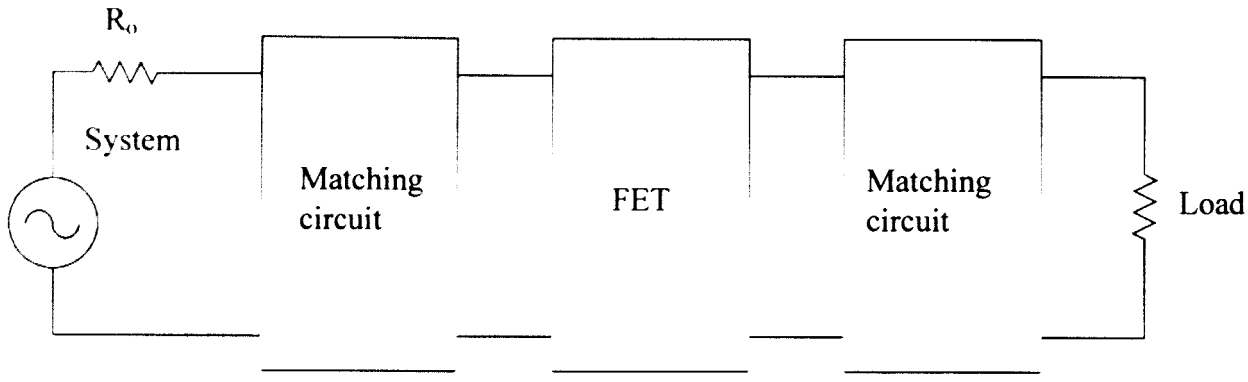

Figure 2.3 Matching of an active amplifier circuit, with a real impedance load on the right-hand side

For amplifier circuits a maximally flat transducer gain (i.e. close to constant gain over the required frequency band) is normally required [25]. Prior to the publication of [25], Chebychev gain functions were commonly used to match complex loads to resistive generators. According to [25] this method does result in an optimum response (transducer gain with the inclusion of the whole circuit) provided the load is terminated in a resistive load. Examples are presented in [25], proving the fact that the current knowledge at that stage was insufficient to provide optimum solutions for complex loads. A discussion on matching in the case where the load impedance is not resistive is found in [26]. The circuits discussed in [26] consisted of a number of microwave amplifiers and the authors provided answers to the questions they presented in [25]. The main issue addressed was multistage amplifiers, where intermediate matching was required but the transistors never reflect resistive impedances only over a wide frequency range. This presented another situation where the matching required not only matches a resistive generator to a complex load, but also a complex generator (the previous amplifier step) to a complex load (the next amplifier step). This specific scenario was addressed in [27].

The implementation of the RFT with an alternative set of circuit components is presented in [28]. In this article transmission lines are implemented as part of the design and the circuit is applied to an amplifier circuit with a frequency range of 0.1 – 5 GHz.

Alternative matching techniques have also been developed in the field of microwave circuits. Some of these techniques are described in [29 - 33]. They focus mainly on numerical techniques to optimise and design LC-ladder configurations similar to the circuit shown in Figure 2.2, although some different configurations are shown in [30]. The background given in this section is applicable to microwave circuits, with all the examples presented in the papers being active amplifier circuits of some kind. The difference between having an amplifier that is not properly matched and an antenna that is not near its fundamental resonant frequency is that antennas exhibit almost perfect mismatches (VSWR > 10:1 is not uncommon) when they are non-resonant. It is very difficult, if not impossible, to match an antenna if the element in itself is not reasonably close to its resonant frequency. Transistors, as part of amplifier circuits, on the other hand, are not that extreme. They are in a workable region over a much greater frequency range than antennas and general approaches to match a configuration are viable options.

2.3 The Simplified Real Frequency Technique

The concept of using a matching feed circuit to enhance the bandwidth of microstrip patch antennas for the first time actively received attention in 1989 from Pues et al. [1]. A study was undertaken on the possibility of designing a matching circuit for a patch antenna that would enhance the antenna's impedance bandwidth. With the technique described, an improvement factor of 3.2 compared to the original bandwidth was obtained.

Important to note at this stage is how the improvement factor is specified. For this dissertation, a specification is set, for example a VSWR of 2:1. When comparison is made between the bandwidth before and after a matching circuit is included, the results for the specified VSWR (2:1) are presented. This would probably not result (percentage-wise) in the optimum answer, but it does provide a constant repeatable result. The result presented in [1] is compared between the matched and unmatched patch antenna for the optimum improvement point. Data analysis provided in [1] showed that the best improvement was obtained at a VSWR of 2.14:1. Therefore the published result for this VSWR is stated as the improvement factor, although this is only valid for the single VSWR value.

Although the improvement factor of 3.2 might seem very little when compared to the results of the previous section where amplifier matching was discussed, it is in fact a substantial improvement for single element microstrip patch antennas.

The above-mentioned technique [1] is an analytical procedure, and the same group furthered their research and came up with the Simplified Real Frequency Technique (SRFT). The procedure for the SRFT is described with examples in [2, 4]. The SRFT is derived from the Real Frequency Technique (RFT) [23]. It is a simplification, requiring less computation than the original RFT, but keeping all the advantages normally associated with the original technique [4]. An example is presented in the paper that uses an LC-ladder similar to the circuit shown in Figure 2.2. The antenna in this example is designed for operation around 3.5 GHz. The antenna is a square probe-fed antenna, with a foam substrate of thickness 6.35 mm and ε_r = 1.03 beneath the supporting substrate with thickness t = 0.5 mm and ε_r = 2.17. The example patch antenna is shown in Figure 2.4, with the matching network and its equivalent etched version as described in [2, 4] shown in Figure 2.5.

The circuit consists of three inductors and one capacitor, as shown in Figure 2.5. The values obtained with the SRFT are L_1 = 6.46 nH, L_2 = 8.381 nH, L_p = 2.606 nH and C_1 = 0.531 pF.

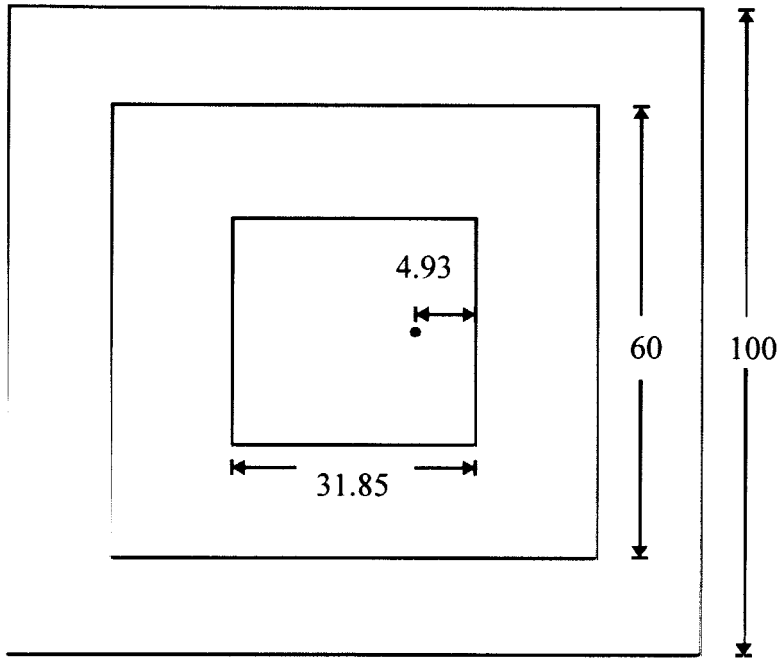

(a)

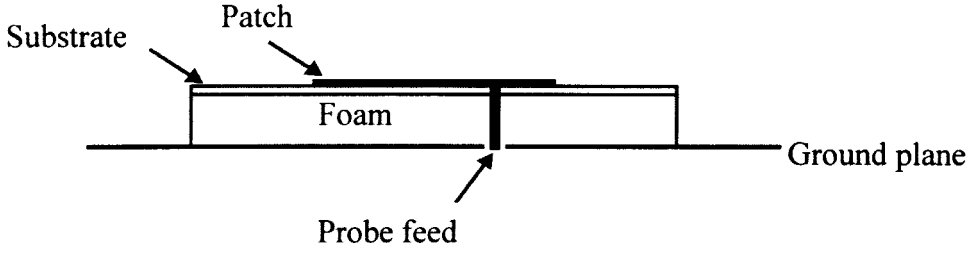

(b)

Figure 2.4 Antenna example for the SRFT [2, 4]. In (a) the top view of the patch is shown, with the side view given in (b) . All dimensions are presented in millimeters

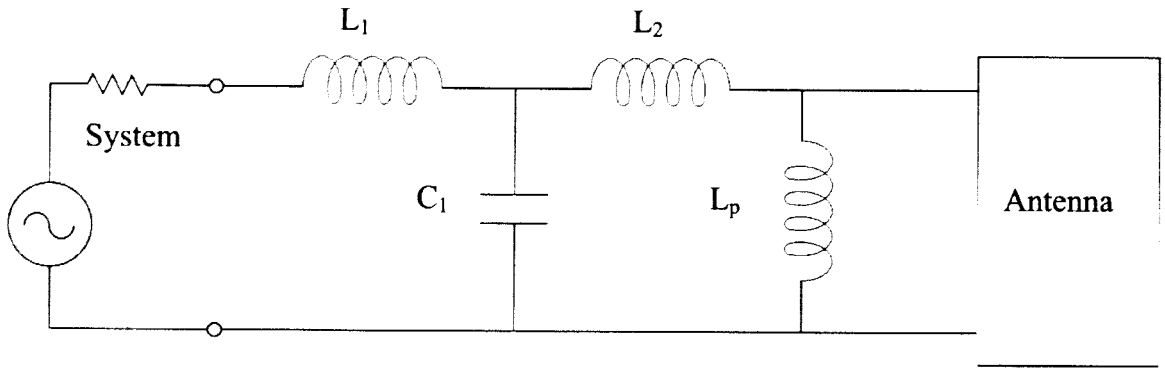

(a)

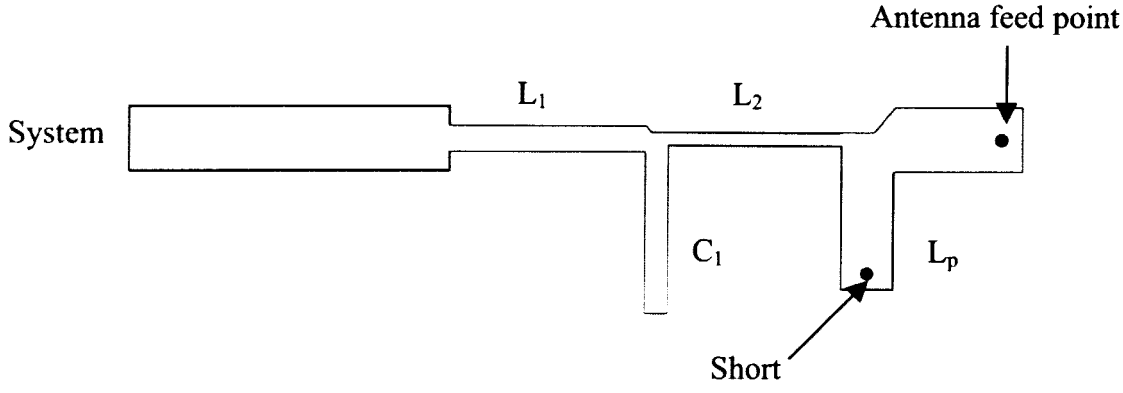

(b)

Figure 2.5 Matching network designed and presented in [2, 4] with the SRFT. Figure 5(a) presents the circuit resulting from the technique, and Figure 5(b) shows the actual circuit that was implemented on microstrip material

In Figure 2.4(a) the size of the ground plane is 100 x 100 mm and the substrate on which the patch antenna is placed is 60 x 60 mm. The etched circuit shown in Figure 2.5(b) was placed on the back of the ground plane of the antenna illustrated in Figure 2.4. The substrate used for the feed network consists of similar dielectric as the patch antenna, but the thickness is 1.575 mm instead of 0.5 mm. The $\varepsilon_r = 2.17$. No dimensions of the circuit are included in [2, 4]. The calculated results with and without the matching network are presented graphically in Figure 2.6. The aim with the matching circuit was to create a

wideband matched antenna system. The antenna alone is not matched for a VSWR < 1.5:1 anywhere in the frequency range considered. The addition of the matching circuit resulted in the antenna being matched over a 12.1% bandwidth. The same antenna was also optimised for a VSWR < 2:1 and the bandwidth obtained for this example was 16.8%.

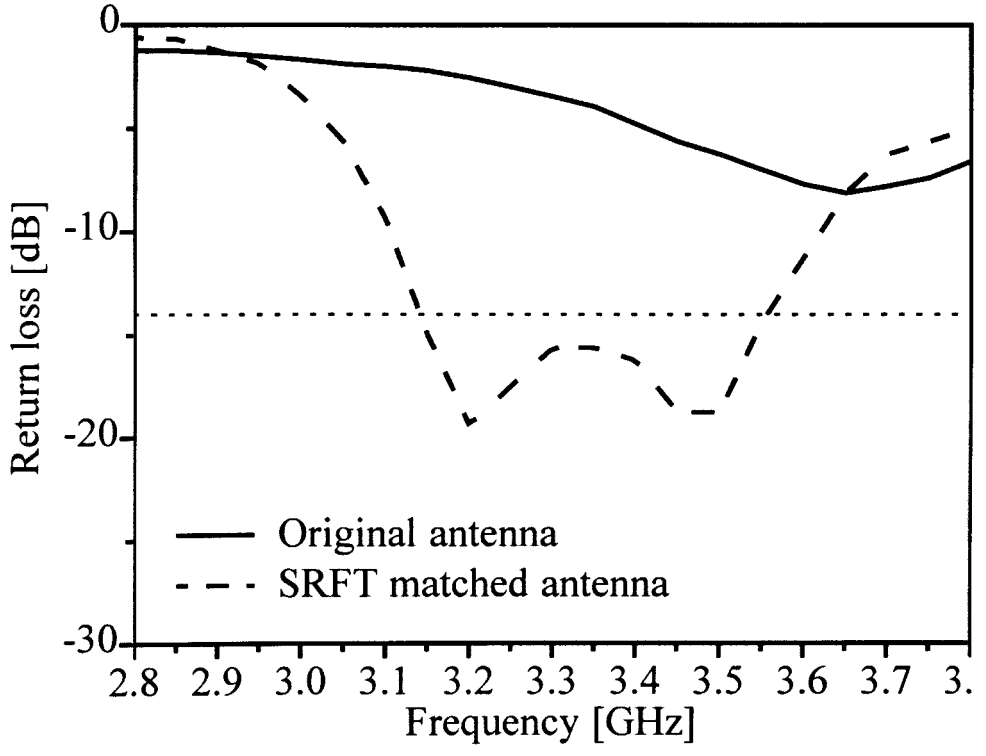

Figure 2.6 Return loss for the patch antenna discussed in [2, 4]

The RFT was first presented in [23] and has been developed with the specific aim of creating a broadband amplifier design. The implementation of the SRFT in microstrip patch antenna technology was done with good results, but the integration of the two applications (amplifiers with patch antennas) was the main aim with the development of the SRFT. This is evident from the range of publications written by the authors and inventors of the SRFT, as well as the final thesis published by An [34]. In [16] a wideband patch was designed, with the aid of the SRFT, to integrate with a wideband amplifier circuit and obtain an overall broadband active antenna. Good results were obtained, and the patch antenna used for the publication was exactly the same one described in both [2] and [4] and shown in Figure 2.4.

The RFT and the subsequent SRFT proved to work very effectively for their specific application, i.e. amplifier and microstrip patch antenna design, respectively. Many of the current matching circuits and the techniques with which they are designed aim to find an optimum solution for an LC-ladder. The LC-ladder is most often (but not always, as evident from the SRFT example) made up of series inductors and parallel capacitors. In microstrip patch antenna development several alternative ways to improve the impedance bandwidth of the antenna have been identified. Some of the techniques will be discussed in the following section. Most of the time the technique is an alteration of the radiating element to improve the impedance bandwidth, but often this is at the expense of other characteristics such as radiation properties of the antenna. Some of the current technologies will be presented in the next few sections.

2.4 Microstrip antenna array bandwidth improvement

The use of resonant circuits to enhance the bandwidth of patch array antennas significantly has recently come under investigation. One such matching technique was presented in [17]. The idea that coupled lines can be used to increase the impedance bandwidth of microstrip patch arrays was presented. Detail about the working of coupled lines can be found in [21]. The main argument presented in [17] is the ease with which one can design this matching structure when compared to techniques such as the SRFT. The circuit discussed in [17] is shown in Figure 2.7. Although no design procedures were presented, it is assumed that the resonant frequency of the coupled lines must be the same as the resonant frequency of the patch array. Later in this dissertation it will become clearer why this is probably the case.

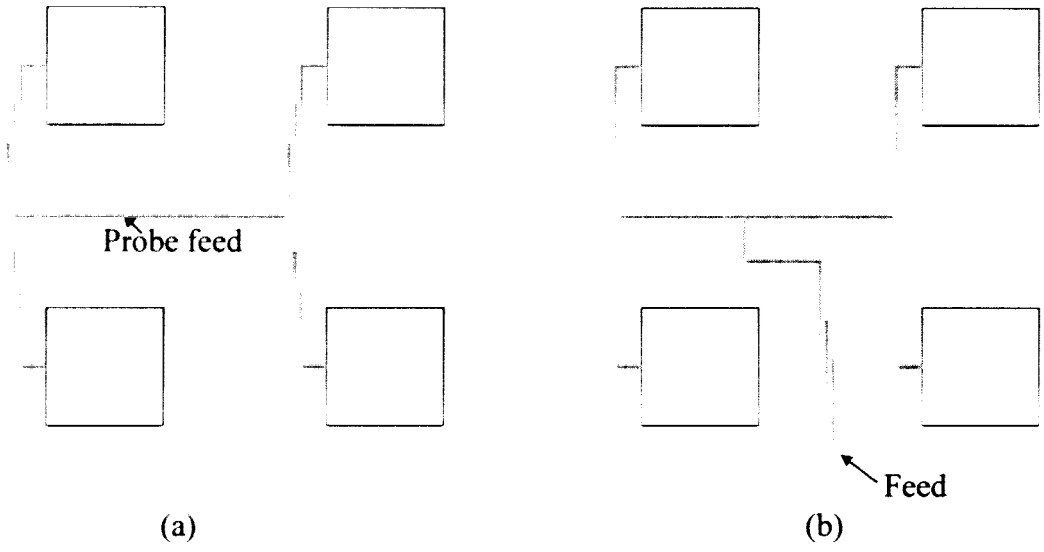

Figure 2.7 Implementation of quarter wave coupled lines for impedance bandwidth improvement. In (a) a probe excitation is used at the same position as where the transmission line connects to the horisontal line in (b)

A problem encountered with this technique is mainly the physical space occupied by the coupled structure. This is overcome in [17] by implementing the feed in an array, where there is a lot of extra space not being used between the patch elements. Two feed structures are discussed and shown in Figure 2.7(a) and Figure 2.7(b) respectively. The different quarterwave coupled arrays present similar impedance and radiation bandwidth. The gain for the array without the matching feed network, as well as with the structure shown in Figure 2.7(a) and (b), is only shown at three discrete frequency points. From the data shown in [17] it is, however, clear that the gain tends to drop rapidly once a frequency other than the resonant frequency is considered. A reason provided in [17] is possible spurious radiation obtained by the quarterwave feed lines included in the matched antenna arrays. The VSWR bandwidth increased by a factor of 2 after addition of the coupled quarterwave.

2.5 Single antenna-element bandwidth improvement

The use of coupled lines for bandwidth improvement is also presented by van Wyk et al. in [18]. The proposed technique is shown in Figure 2.8. The coupled lines are implemented in a similar manner as in [17], but the feed network is used to feed a single edge-fed patch element. There is no physical connection between the antenna and the feed line. The last coupling quarterwave section is taken between the feed line and the radiating patch. This reduces the overall space required for the feed line considerably. An edge-fed patch, similar to the patch used in [1], has been built and tested. The simulated bandwidth improvement is more than double the original impedance bandwidth (VSWR < 2:1) and the radiation pattern shows good similarity between the edge-fed and coupled patch. The main difference is the beam squint obtained. This can be attributed directly to the coupling lines that are placed on the same side as the radiating patch antenna.

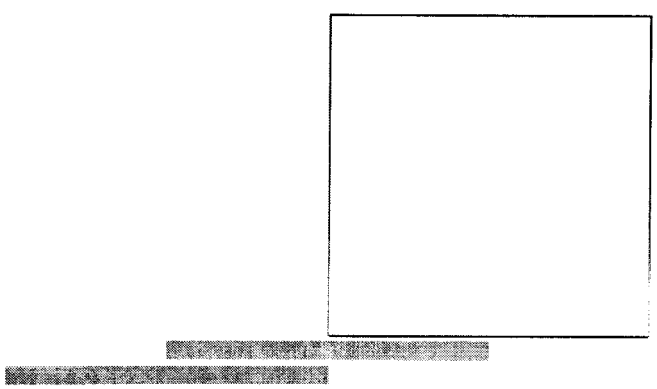

Figure 2.8 The use of a resonant coupling structure to feed a patch on the non-radiating side of the patch antenna. The coupling lines overlap by a quarter wavelength as described in [18]

A discussion on single element electromagnetically coupled microstrip patch antennas with a tuning stub is presented in [35]. The feed is presented graphically in Figure 2.9. The advantage of this technique is that the tuning stub is placed directly underneath the radiation element. The tuning stub is designated in Figure 2.9 by the length L2. The length L2 starts at the split and is considered till the end of the line. A great degree of freedom in

tuning is provided with this antenna, since a number of variables are provided. L1 is mainly used for matching and L2 for the resonance in conjunction with the patch size.

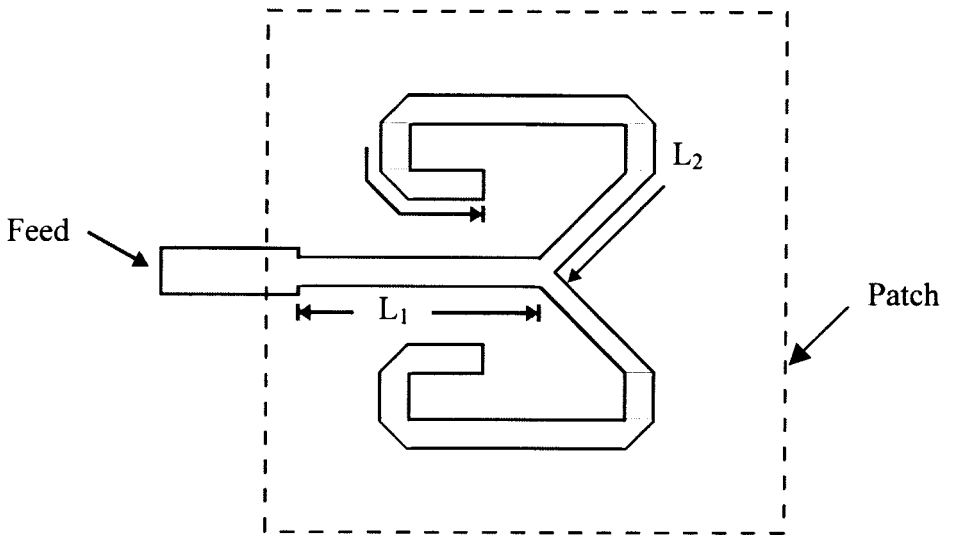

Figure 2.9 Coupled line wideband patch presented in [35]. L1 is a quarter wave transformer and L2 the coupling line having a half wave length at the desired centre frequency

Bandwidth improvement of 1.25 over the original band was obtained. No physical connection between the patch and the feed is made, reducing the margin of construction error possible when adding a probe, for instance. The technique was applied to normal coupling feed structures as well as aperture-coupled antennas. The aperture-coupled patch obtained an increase in backlobe radiation, although only 1.5 dB worse than the original.

2.6 Conclusion on impedance matching

In this section a number of impedance matching techniques are summarised. The need for bandwidth improvement becomes evident in the literature, where numerous papers that have something to do with the impedance of microstrip patch antennas highlight the narrow impedance bandwidth property of the antennas. The SRFT is a very effective technique with good results. The circuit that results from the SRFT is not predefined, and possibilities arise that the circuit might become physically large. The coupling structure presented in [35] is a solution for a number of patch configurations. The main working mechanism is coupling that might become difficult when the patches become electrically too thick.

The coupling lines presented in [17, 18] are the first actual references where a purely resonant circuit is used to implement a matching structure. The results in terms of impedance bandwidth enhancement are very good, and the only possible problems encountered with this idea might be the physical space occupied by the feed or degradation of the radiation pattern. The physical space problem is effectively dealt with in [17]. The fact that the matching feed line is etched on the same side of the dielectric substrate as the patch antenna, imposes a height restriction on the antenna [17, 18]. This limits the number of antennas possibly considered for the quarterwave coupled line matching technique as well as the maximum bandwidth obtainable with the circuit.

Chapter 3

Theory

In this chapter the theory behind the SRMT will be presented. The first section will be devoted to a discussion of the equivalent network model for patch antennas. The foundation of the SRMT is the fact that the network model consists of a resonant parallel-RLC circuit. The influence of the probe on the input impedance and the network model is discussed in section 3.2. Sections 3.3 and 3.4 describe the basic working of the SRMT, and the improvement to end up with the Optimum Bandwidth Single LC-Resonator Matching Technique (SRMT) is provided in section 3.5.

3.1 Equivalent network model for patch antennas

The design of microstrip patch antennas consists mainly of two parts. Firstly, the patch antenna must be resonant. Figure 3.1 shows a probe-fed and a microstrip-fed patch, showing the main design parameters available to design a patch antenna. The resonant length (L) of the radiating structure, i.e. the patch, will normally be slightly shorter than half a wavelength at the centre frequency. The length depends on a number of variables, some of which are the substrate chosen as well as the electrical thickness of the patch antenna, i.e. the substrate height. The definition of this length is explained in terms of field distribution underneath the patch in [36]. Another important parameter to keep in mind with patch antenna design is the impedance at the feed position. The feed position (d) and

patch width (W) are the main contributors to this parameter, although the resonant frequency and input impedance cannot be designed independently. The width, length and feed position all have some level of influence on one another.

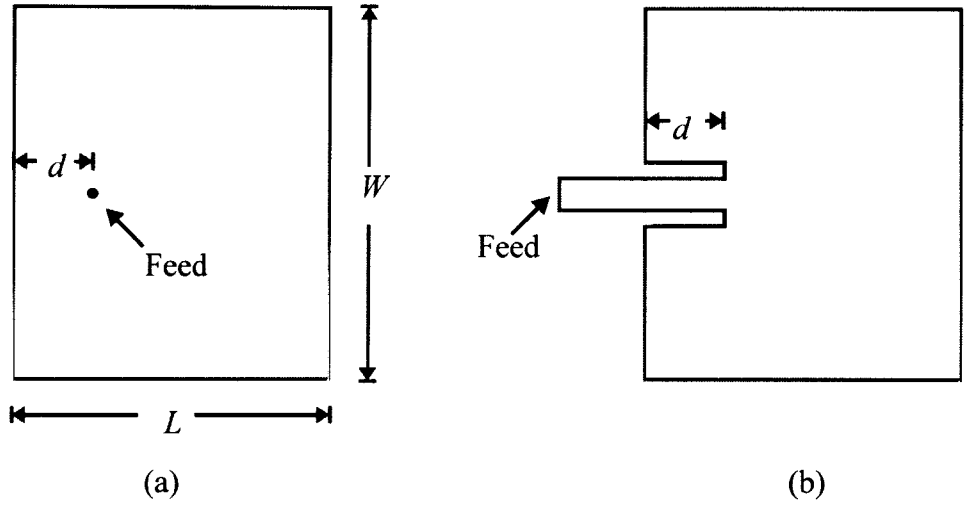

Figure 3.1 Main design parameters for a rectangular microstrip patch antenna. (a) shows a probe-fed patch antenna, and (b) a microstrip-fed patch antenna

The input impedance of a microstrip patch antenna has an RLC-circuit behaviour near its fundamental resonant frequency [1]. The feed mechanism (being either probe- or microstrip-fed) then further alters the impedance response. Mainly the probe-fed patch antenna will be considered in this dissertation. The probe adds a series inductance to the RLC-impedance. The simplified equivalent circuit of the input impedance of a probe-fed microstrip patch antenna, taken from [1], is shown in Figure 3.2.

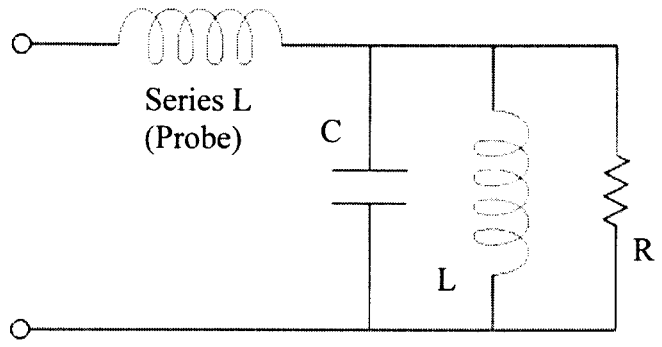

Figure 3.2 Approximate equivalent circuit of the input impedance of a probe-fed patch antenna

The impedance frequency response of a parallel RLC-circuit is shown in Figure 3.3. In illustration the following component values were used: R = 50 Ω, C = 17.5 pF and L = 0.47 nH.

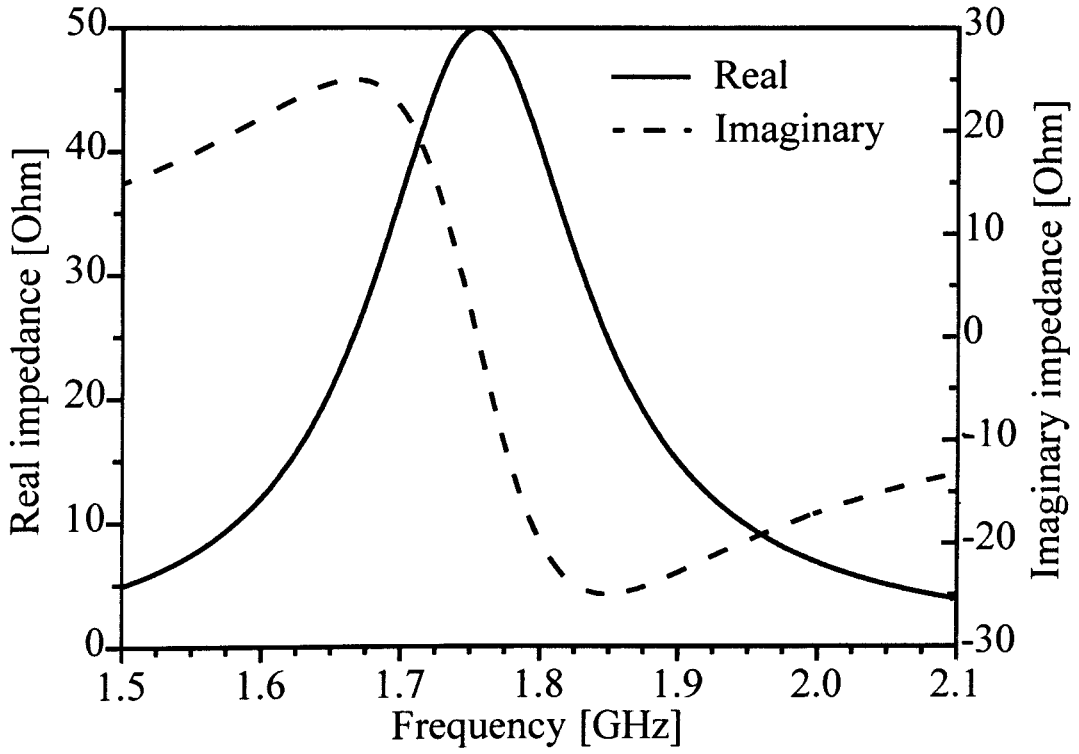

Figure 3.3 Frequency response of a parallel RLC-circuit with a resonant frequency close to 1.8 GHz

In Figure 3.3 the resonant frequency is clearly visible at 1.8 GHz as the imaginary impedance reaches zero. Incidentally the real impedance is also a maximum value at the resonant frequency for a pure parallel RLC-circuit. The real part of the impedance is symmetric around the resonant frequency, and the peak value of 50 Ω is the same as the resistor used in the example circuit. The imaginary part of the impedance shows odd symmetry around the resonant frequency. It is equal in size, but opposite in sign around this frequency. The RLC-circuit's impedance is thus equal in magnitude around its resonant frequency, but the impedance is inductive below and capacitive above the centre frequency. This type of frequency response is shown graphically on a Smith chart in Figure 3.4.

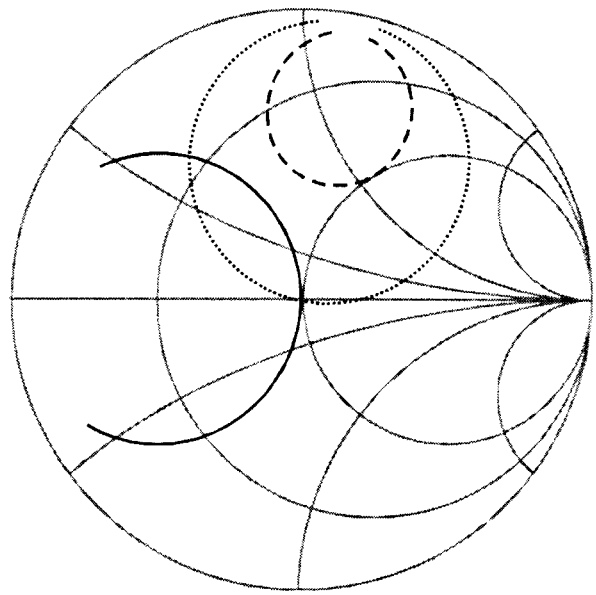

——— Parallel RLC
– – – – Parallel RLC with series L
..... Parallel RLC with series L and R increased

Figure 3.4 Smith chart representation of impedance versus frequency behaviour for the various circuits discussed in this section

The probe feed, commonly used for patch antennas, can be modelled as an additional series inductance to the patch input impedance. For the RLC-circuit discussed in the previous paragraph, a series inductor value of 5.2 nH is chosen to represent a probe-feed. The value is also for illustration only. In order to explain what is seen in Figures 3.4, 3.5 and 3.6 the

circuit shown in Figure 3.2 is mathematically derived. The final derived expression for the parallel-RLC circuit with a series inductor is given in (2). It is assumed that the reader has a basic knowledge of reactive impedance expressions as well as parallel and series component theory. Therefore the steps in between the derivation are omitted and only the initial and the final expression are presented.

$$\begin{aligned} Z_{in} &= Z_{Lserie} + Z_{RLC} \\ &= Z_{Lserie} + \frac{1}{\frac{1}{R} + \frac{1}{Z_L} + \frac{1}{Z_C}} \\ &= j\omega L_{serie} + \frac{j\omega RL}{j\omega C(j\omega RL) + j\omega L + R} \\ &= \frac{\omega^2 RL^2}{(R - \omega^2 RLC)^2 + \omega^2 L^2} + j\omega L_{serie} + j\frac{\omega RL(R - \omega^2 RLC)}{(R - \omega^2 RLC)^2 + \omega^2 L^2} \end{aligned} \quad (3)$$

The series inductance is added to the impedance of the parallel-RLC circuit. In equation (3) the final expression illustrates how the term obtained with the series inductance is imaginary, and the term can be considered part of the imaginary impedance only. The real impedance has no reference to the component (L_{serie}) and is therefore unaffected by the addition of the series inductance. In the region of 1.8 GHz an inductor of 5.2 nH results in a series imaginary impedance of 58.8 Ω being added to the imaginary impedance. Figure 3.5 graphically illustrates how the imaginary curve is literally lifted. The amount that the curve is lifted varies (i.e. the impedance added from L_{serie}), because the inductor impedance is frequency sensitive. On the Smith chart in Figure 3.4 the dashed line graphically illustrates the real and imaginary curves obtained from (3) with the series inductor included. Interesting to note is the major reduction encountered in the size of the locus on the Smith chart, from the solid curve representing the original parallel RLC-circuit, to the identical parallel RLC-circuit with the series inductor added. There is no region where the locus gets close to the real axis. In Figure 3.5 the imaginary curve is also very high above the $j0$ Ω value over the whole frequency range considered.

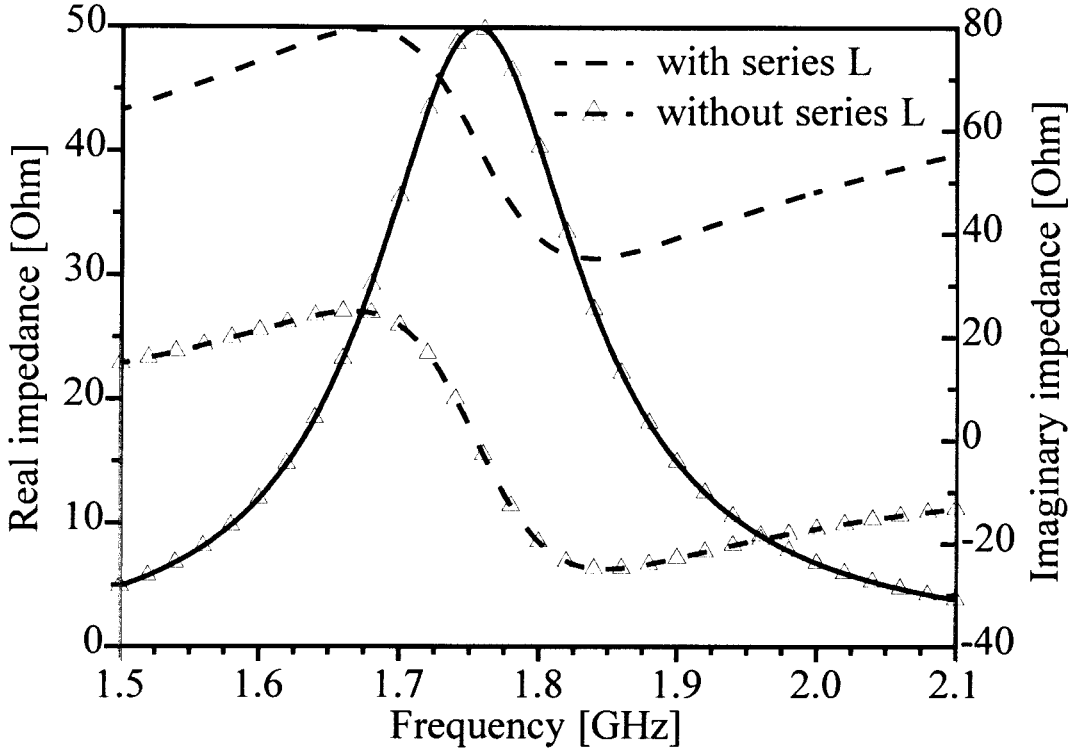

Figure 3.5 Comparison of the impedance of a parallel RLC-circuit with and without the addition of a series inductor

Electrically thicker patch antennas often have real impedance peaks that are higher than the required value. The frequency point where the antenna is matched to 50 Ω is then not at the peak of the real impedance curve, but on the slope. The series inductor with the parallel-RLC model discussed so far in this section is part of a building block to try to understand this impedance behaviour of electrically thick patches. Equation (3) shows that the imaginary term of the input impedance includes all the elements (R, L, C and L_{serie}) used in the model. Varying either L or C will ultimately alter the resonance of the parallel RLC-circuit and changing L_{serie} will only result in the imaginary curve lowering or lifting. Variation in R proved to be a viable option. The value of R was increased to 120 Ω, and the dotted locus shown in Figure 3.4 illustrates the effect of doing this. The curve passes through the 50 Ω point. More important to note is the graph presented in Figure 3.6. The imaginary curve has changed dramatically. The offset of the imaginary curve is still 58.8 Ω as originally obtained from L_{serie}, but the curve has much lower and upper limit values and

reaches *j*0 Ω in the frequency range considered. In conjunction with the imaginary curve that has changed, the real impedance has inevitably also changed with the increased R.

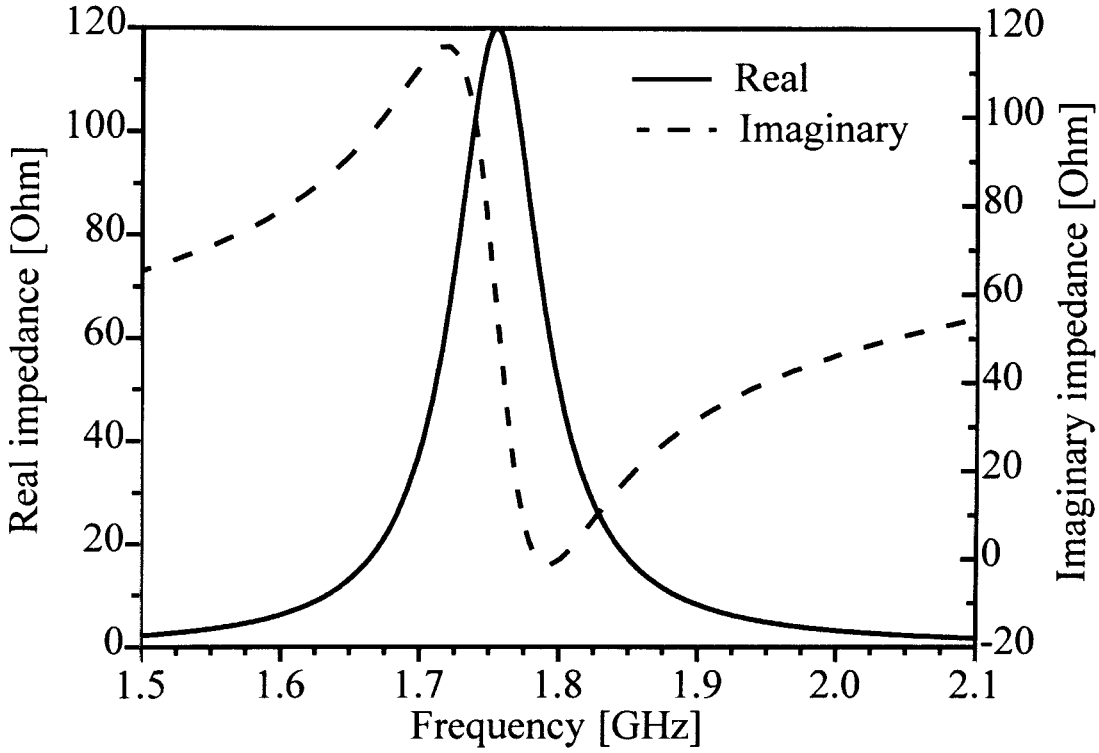

Figure 3.6 Impedance response versus frequency with the addition of a series inductor and increased real impedance

The impedance of the RLC-circuit that the section started was symmetric around the resonant frequency. Resonant frequency is defined as the frequency where the imaginary part of the impedance reaches zero and the total input impedance is purely real. Figure 3.6 and the coinciding Smith chart locus in Figure 3.4 show how a series inductance disturbs this symmetry, and an increased R in effect restores a level of resonance, but with no symmetry around the centre frequency anymore. This type of input impedance, with no real noticeable symmetry, is a very common sight in microstrip patch antenna design. In the next section it will be shown how symmetry can actually still be obtained, and that it can then be used to one's advantage.

3.2 Retrieval of symmetry in the impedance curves around the minimum reflection frequency point

Section 3.1 started with a simple parallel RLC-circuit, and ended with a more complicated circuit, shown in Figure 3.2. It was shown how one can initially have an ideal impedance curve (Figure 3.3 and 3.4) and how this curve is almost never the graph one ends up to work with (Figure 3.6). In this section it will be shown how the effect of the series inductor and increased R of the input impedance can be reversed in terms of frequency impedance behaviour. This will be done with actual simulated patch antenna data.

The patch used as design example for the matching circuit principle is shown in Figure 3.7.

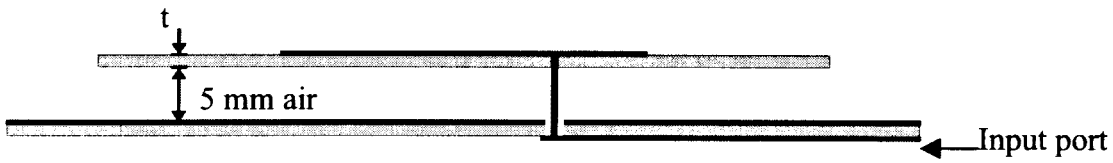

Figure 3.7 Probe-fed patch antenna example. The input impedance is measured and referenced at the ground plane interface

The patch antenna presented in Figure 3.7 is etched on dielectric substrate with dielectric constant ε_r = 3.05, loss tangent $tan\delta$ = 0.003 and thickness t = 1.524 mm. The material is GML-1000 and supplied by GIL Technologies [38]. The feed line and matching network considered later are etched on dielectric substrate with ε_r = 3.53, $tan\delta$ = 0.017 and t = 1.575 mm. Material is MC3D, also by GIL Technologies [39]. Figure 3.8 presents the real and imaginary impedance curves of the patch antenna of Figure 3.7 near its designed resonant frequency, chosen to be 1.8 GHz. The graphical response is shown on a Smith chart in Figure 3.9. The solid black line on the Smith chart is the response coinciding with the curves presented in Figure 3.8. Take note of the close correlation between the curves shown in Figures 3.8 and 3.6.

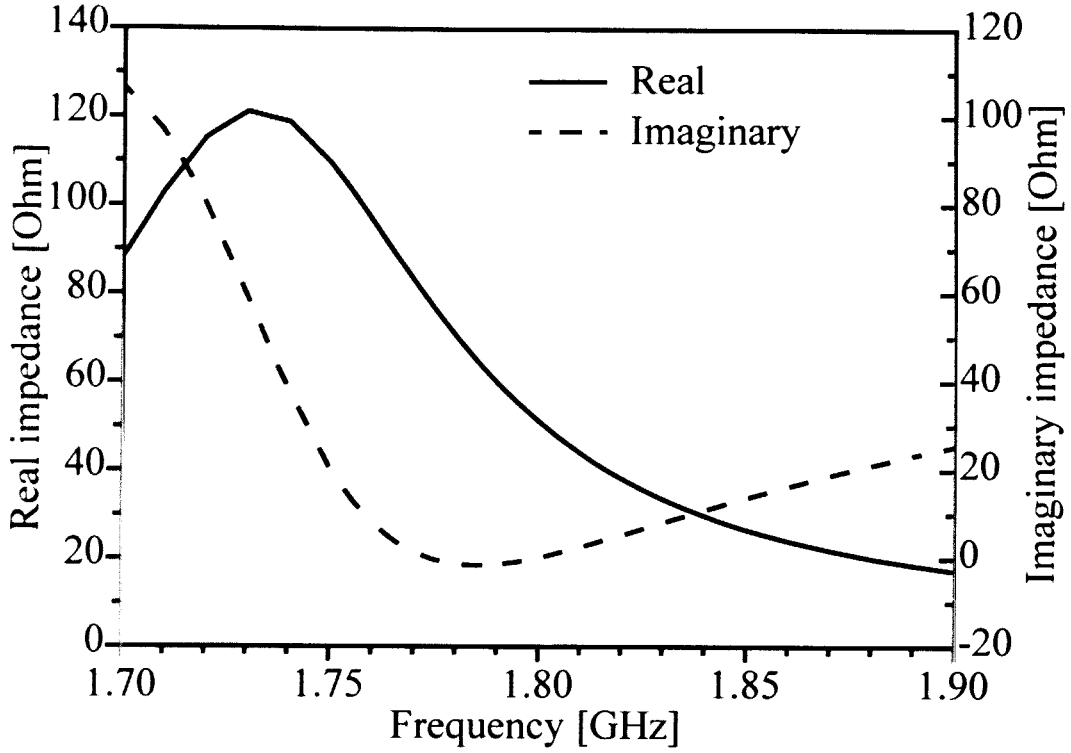

Figure 3.8 Simulated input impedance of the probe-fed microstrip patch antenna shown in Figure 3.7

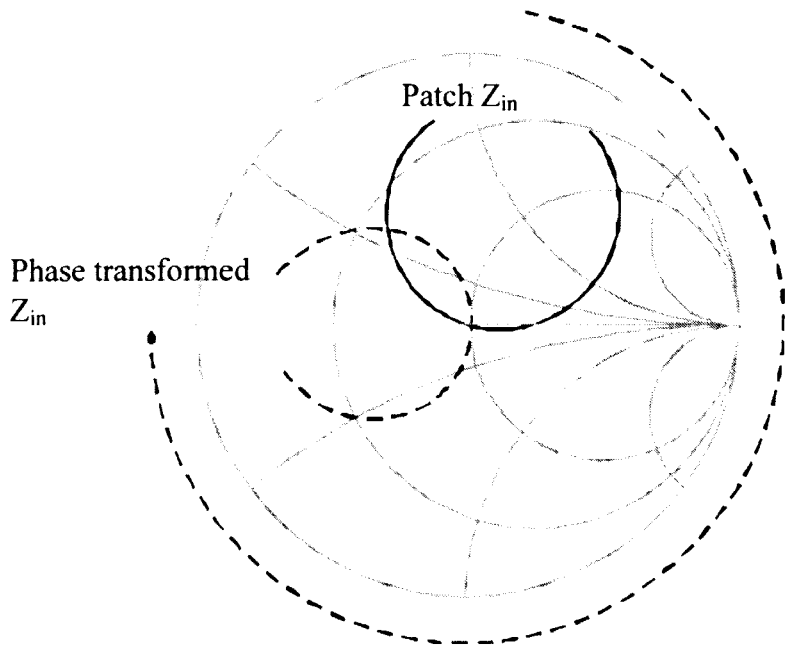

Figure 3.9 Input impedance of the example patch antenna as plotted on the Smith chart

In the previous section emphasis was placed on the fact that no symmetry is available in the impedance response. The series inductance associated with the probe-feed acts as a transmission line with some level of impedance transforming. This becomes evident as the Smith chart is considered as graphical aid. The phase and impedance transforming effect of the inductor can be seen in Figure 3.4. Additional phase transforming will result in an impedance response that is again similar to a response expected from a relatively simple parallel RLC-circuit. Figure 3.10 shows the analogy of phase transforming the impedance.

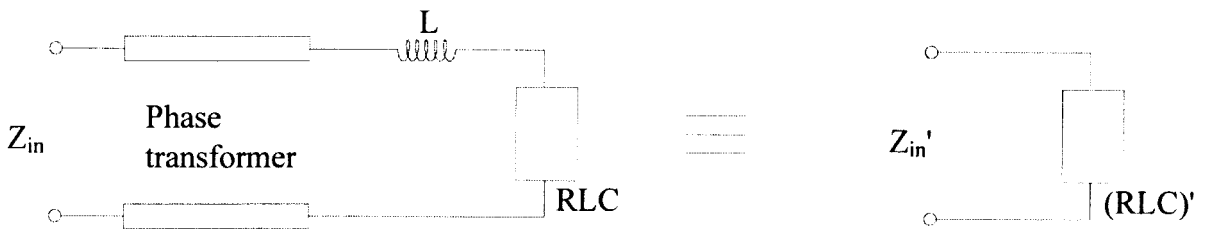

Figure 3.10 Effective result of phase transformation applied to patch antenna input impedance

The phase transformed data for the patch antenna is included on the Smith chart in Figure 3.9. The locus changes somewhat in shape. This is due to the fact that the phase transformation is a function of frequency, and only the centre frequency has the exact numerical transformation expected.

The real and imaginary impedance curves of the newly obtained input impedance are shown in Figure 3.11. A peak real impedance value is obtained at the resonant frequency and the imaginary impedance curves resemble odd symmetry around the resonant frequency, i.e. opposite in sign but equal in magnitude.

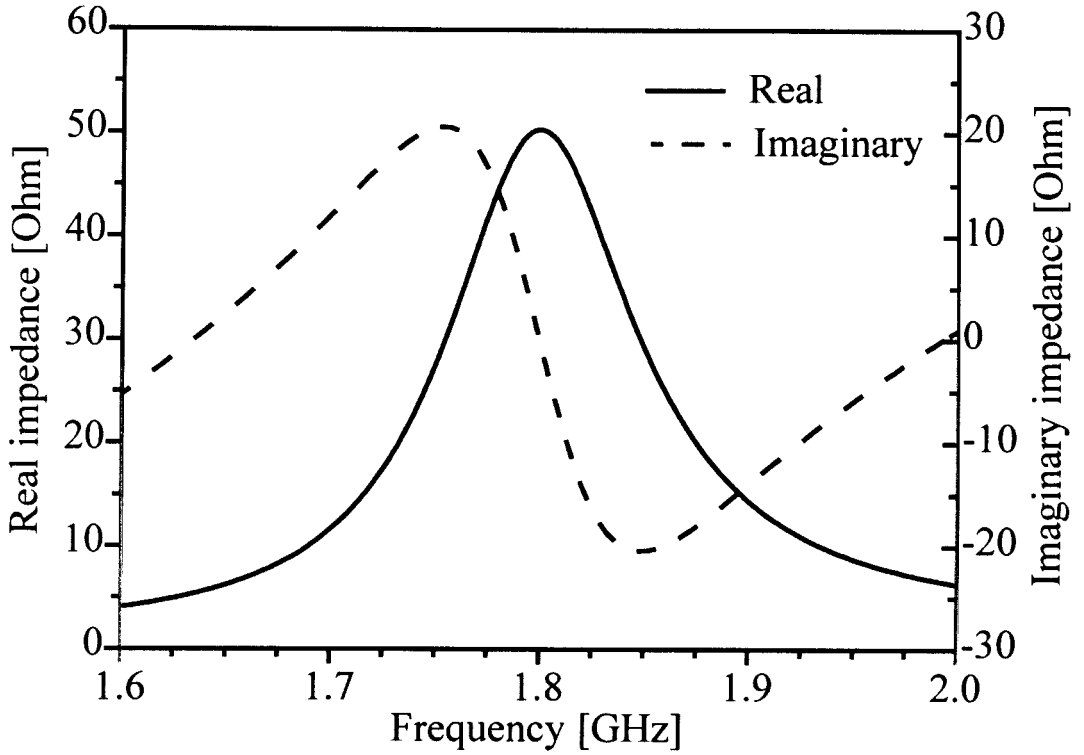

Figure 3.11 Impedance curves of the phase transformed patch antenna input impedance

3.3 Reduction of imaginary impedance

The imaginary impedance of the phase transformed patch antenna is inductive at frequencies lower than the resonant frequency and capacitive at frequencies higher than the centre frequency. If one considers a parallel LC-combination without the resistor and series inductance in the circuit diagram as presented in Figure 3.2, this is precisely what would happen with this combination at and around its resonant frequency. The matching technique presented in this dissertation aims to obtain a bandwidth improvement by effectively cancelling the imaginary component of the input impedance at frequencies close to the resonant frequency.

A parallel LC-combination is inductive at low frequencies and capacitive at high frequencies, where low and high are defined relative to the resonant frequency. This means that a parallel combination of the LC-circuit and a load that is inverse, i.e. capacitive at low frequencies and inductive at high frequencies, will result in a cancellation of the total reactive component. A patch antenna impedance locus as presented in Figure 3.11 is phase transformed to obtain an RLC-equivalent response. When the phase transformation is not taken as far as in Figure 3.9, but rather a line length at centre frequency of 90° shorter, the curve shown in Figure 3.12 is obtained.

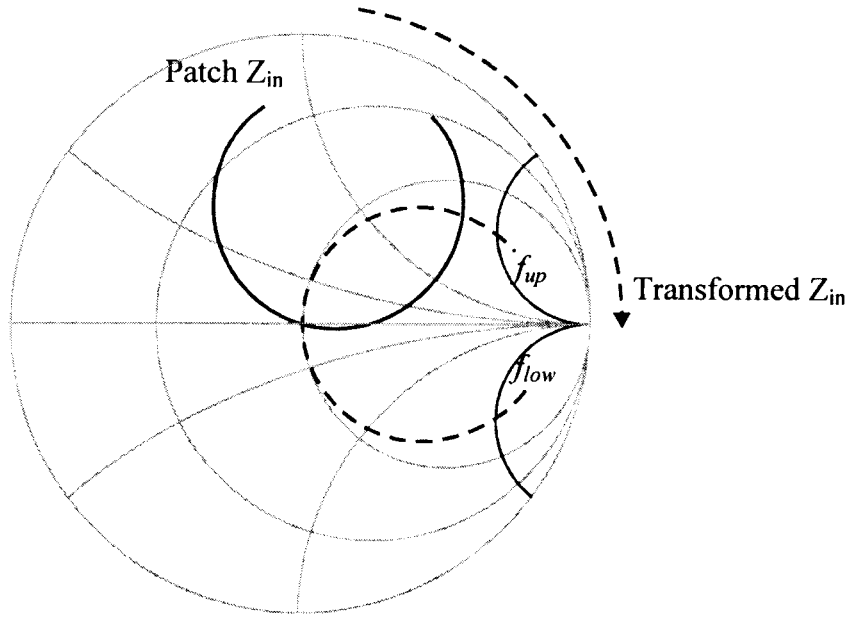

Figure 3.12 Phase transformation of patch antenna to obtain a capacitive reactive component at low and inductive component at high frequencies

It is mentioned in the previous paragraph that one would like to work with a parallel combination between the proposed LC-circuit and the load impedance. Therefore it might prove more useful to work with admittance instead of impedance values. When placing components in parallel the total admittance will be a simple summation of each component's individual admittance value, as is shown in equation (4).

$$Y_L + Y_C + Y_{Load} = Y_{Total} \tag{4}$$

The admittance curves obtained with the phase transformation illustrated in Figure 3.12 are shown in Figure 3.13. The shape is similar to the ideal parallel RLC-circuit. In other words, a peak real admittance value is obtained at the centre frequency, and the imaginary admittance is equal in magnitude but opposite in sign around the centre frequency. Also, a positive imaginary value now implies a capacitive component while a negative reactive value represents an inductive component.

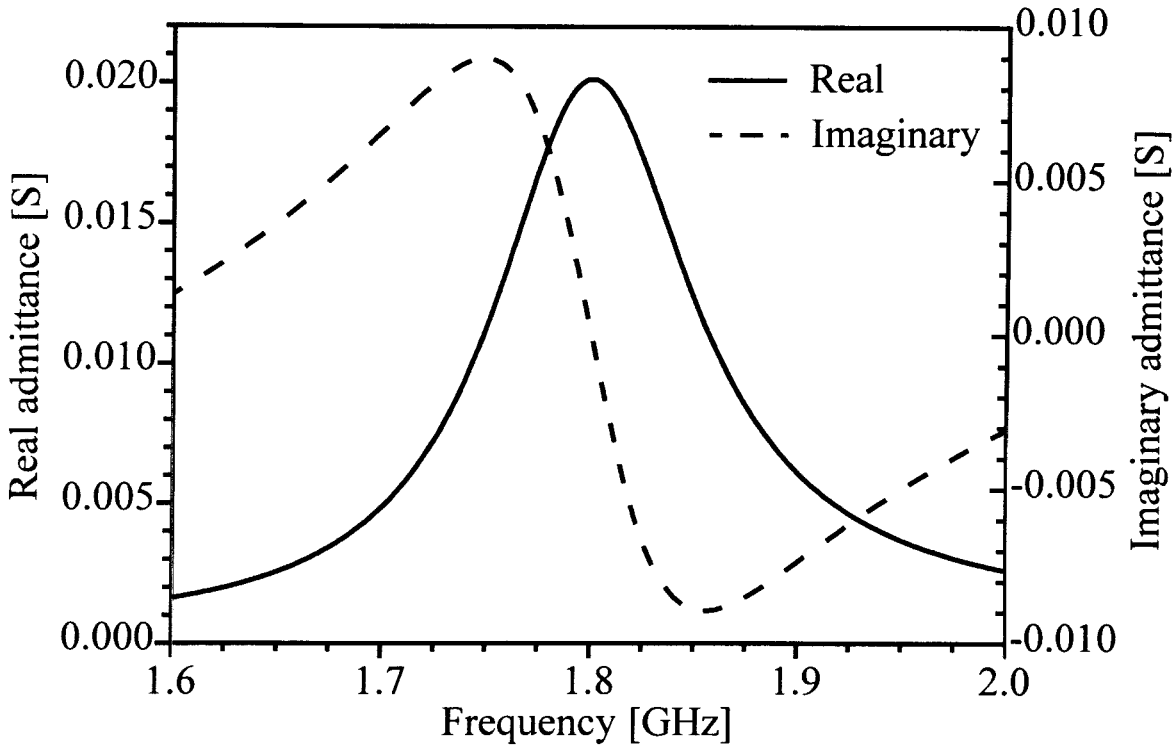

Figure 3.13 Admittance curves associated with the phase transformation done in Figure 3.12

An LC-circuit has a straight-line admittance frequency response crossing the zero admittance value at its resonant frequency. The solid line in Figure 3.14 represents the admittance of a parallel LC-section with a resonant frequency of 1.8 GHz. When a LC-circuit is used to cancel out overall reactive components, care must be taken that resonance for both the load and the added LC circuit occurs at the same frequency. This will result in the LC-circuit added in parallel having no effect on the admittance at the centre frequency, while cancelling the antenna imaginary admittance values at other frequencies. This is mathematically presented in equation (5).

$$\mathrm{Im}[Y_{fc_{LC}}] = \mathrm{Im}[Y_{fc_{Load}}] = 0 \tag{5}$$

The subscript -*fc*- denotes centre frequency, and the subscripts -*LC*- and -*Load*- denote the LC section and load admittance respectively.

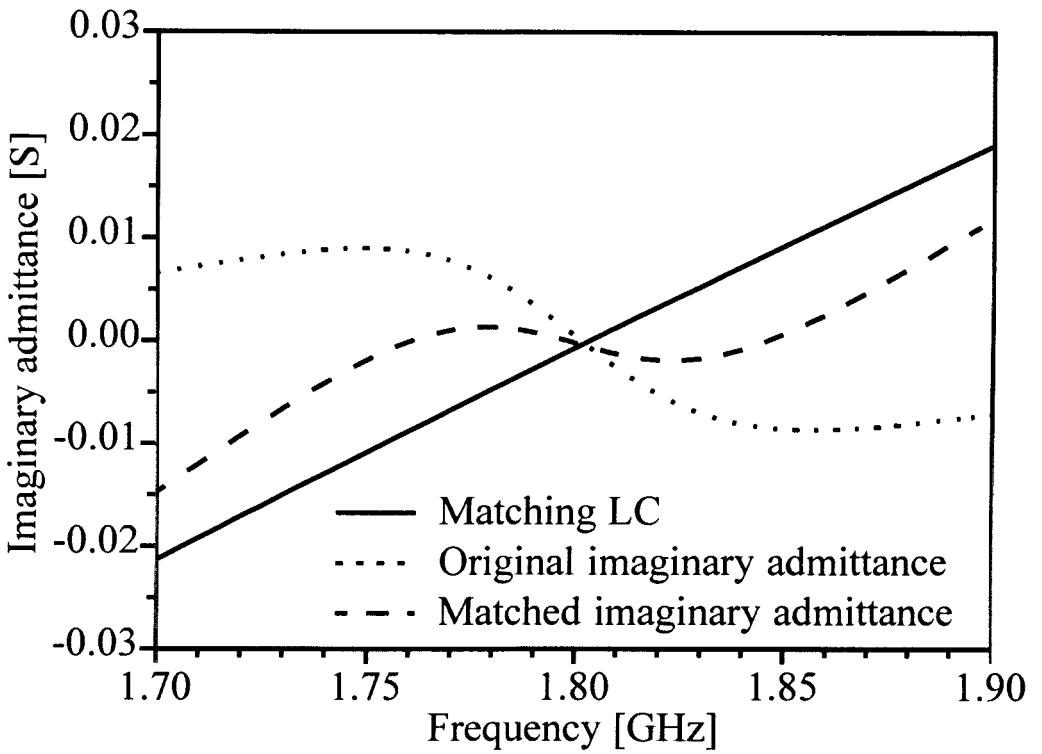

Figure 3.14 Effective cancellation of the imaginary part of the load admittance with the addition of a parallel LC-section

The addition of a parallel LC-section means that only the imaginary component of the admittance will change and the real part will remain the same. This is shown in equations (6) and (7).

$$\mathrm{Im}[Y_{Total}] = Y_L + Y_C + \mathrm{Im}[Y_{Load}] \tag{6}$$

$$\mathrm{Re}[Y_{Total}] = \mathrm{Re}[Y_{Load}] \tag{7}$$

Figure 3.15 includes the real admittance obtained in Figure 3.14 and shows what happens to the parameter before and after the LC-section is added to the phase transformed load.

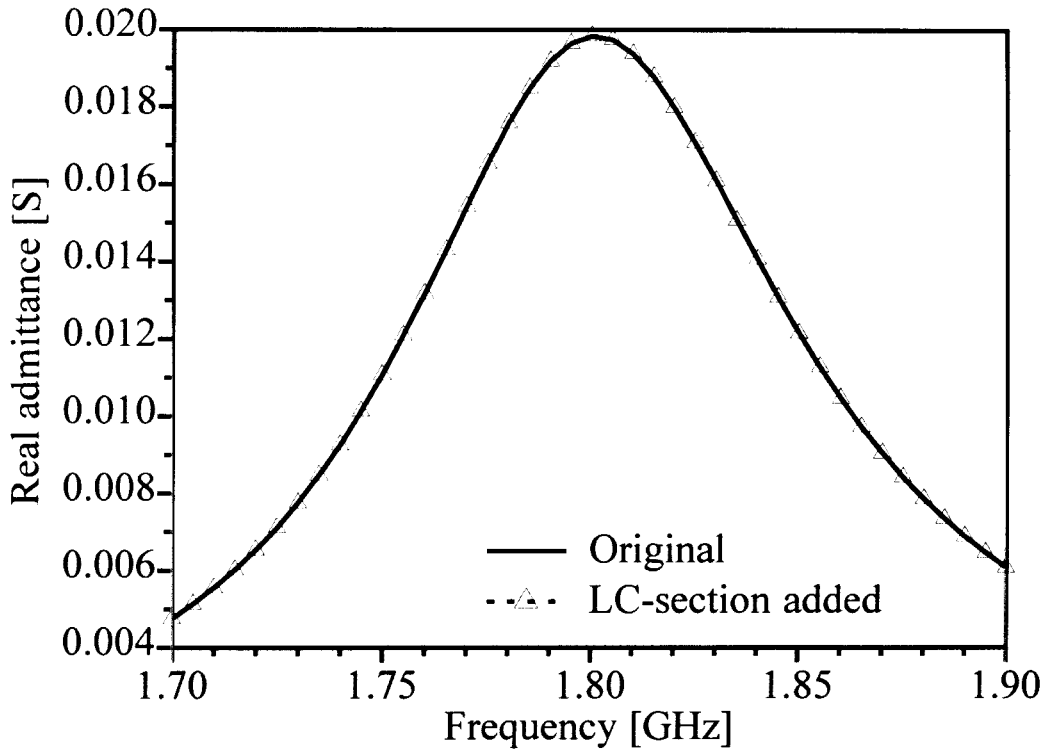

Figure 3.15 Effect on the real admittance with the addition of a parallel LC-section to the load admittance

In the last two figures it can be seen clearly how the admittance of a phase transformed patch antenna was changed in such a way that the imaginary admittance varies less around the centre frequency, while the real admittance remains virtually unchanged. The Smith chart representation illustrating the effect of this addition of the LC-section is shown in Figure 3.16. An eye-shaped locus is created on the Smith chart. This eye is the result of the unchanged real admittance, while the reactive component is now more constant around the centre frequency than before.

The Smith chart representation in Figure 3.16 illustrates how the eye-shaped locus makes a loop that remains within a certain VSWR circle on the Smith chart. The reflection coefficient simulated for this circuit, before and after the addition of the LC-section, is presented in Figure 3.17.

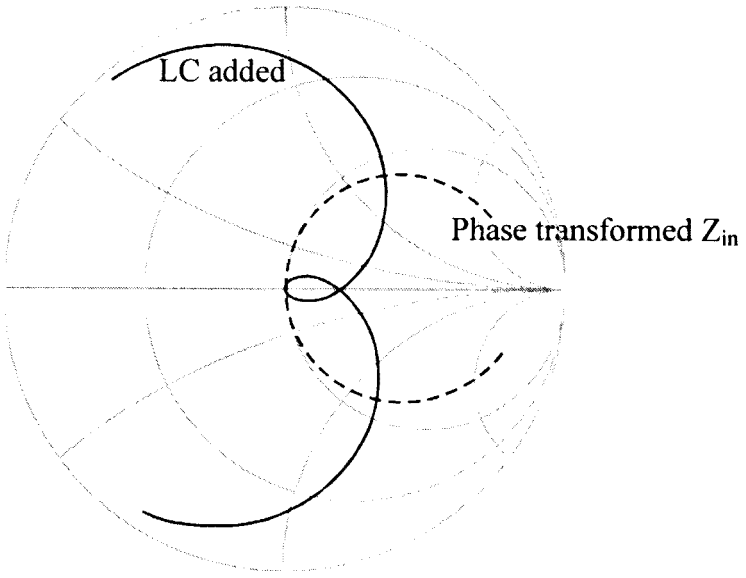

Figure 3.16 Addition of a parallel LC-section to the phase transformed load impedance

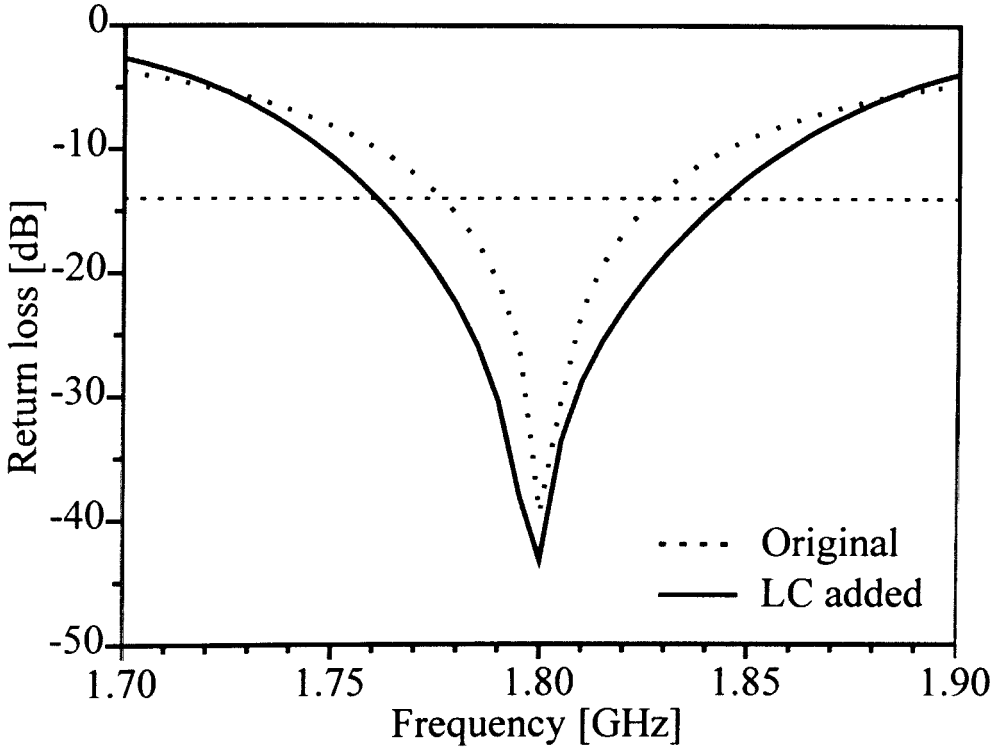

Figure 3.17 Effective improvement of the return loss with the addition of an LC-section to the phase-transformed load

In Figure 3.17 it is clear that there is a bandwidth improvement. More precise design procedures will be discussed in the following section, including additional improvement as well as design criteria.

3.4 Design of the LC-network for bandwidth improvement

In the previous section the fact that an added parallel resonant circuit can result in a patch antenna having an improved impedance bandwidth was illustrated. This is the underlying principle on which the coupled lines matching circuit discussed in [17, 18] is also based. The mathematical approximation of the coupled lines is a resonant circuit similar to a parallel LC-circuit with a transformer [21]. This additional resonator is then effectively responsible for the improvement in impedance bandwidth of the patch antenna and array. In [17, 18] not much detail of the working of the feed circuit is presented.

The first step in the design of a matching LC-section is to find the length of the phase transforming transmission line that will lead to symmetry in the real admittance, and odd symmetry in the imaginary admittance around the centre frequency. For this basic condition two possibilities are valid and must therefore be defined in more precise detail. The real admittance should have a maximum value at the centre frequency and the imaginary admittance should be positive below and negative above the resonant frequency. This definition is presented graphically in Figures 3.12, 3.13 and 3.16. This is a part of the design process where the graphical aid of the Smith chart is of great advantage, and it is suggested that this method (the graphical method) be used to find the correct line length.

The guidelines for the phase transformation mentioned in the previous paragraph should be used in conjunction with the graphical aid of the Smith chart. The statement of the maximum real admittance shows one the exact point where the locus on the Smith chart tends to turn away from the centre again, provided that one is relatively close to the correct phase position. In conjunction with the real admittance, the imaginary admittance should exhibit close to identical values but opposite in sign around the resonant frequency. The unmatched curve in Figure 3.16 illustrates this scenario, where the maximum real

admittance will be at the left-hand side of the locus, also being the centre frequency of the curve. Similarly, the curve is identical above and below the real axis.

The next step is to find the parallel LC-combination that will result in the most effective reduction in the reactive components around the centre frequency leading to an improved impedance bandwidth. Figure 3.14 illustrates what happens to the final imaginary admittance when the resonant admittance is added to the system. In the area close to the resonant frequency the imaginary admittance has a negative slope. The LC-circuit on the other hand has a positive slope. Summation of these two functions results in a reduction in the slope of the imaginary component. There are now three frequency points where the reactive components are zero. The centre point is the resonant frequency, where both the phase-transformed antenna admittance and the LC-circuit should have a zero reactive component. The other two frequency points are in the ideal case spaced equally far from the centre value at a lower and higher frequency. These two points, in conjunction with the resonant frequency, are the main design parameters for the LC-circuit. A simple set of equations can be implemented to calculate what the required capacitor and inductor values should be. The equations are shown in (8) and (9) and should be used in conjunction with (10) and (11).

$$Y_{low} = Y_{C_{low}} + Y_{L_{low}} \tag{8}$$

$$Y_{up} = Y_{C_{up}} + Y_{L_{up}} \tag{9}$$

The admittance of the capacitor and inductor are defined as follows:

$$\begin{aligned} Y_C &= j\omega C \\ \therefore Y_C &= j2\pi fC \end{aligned} \tag{10}$$

$$\begin{aligned} Y_L &= \frac{-j}{\omega L} \\ \therefore Y_L &= \frac{-j}{2\pi fL} \end{aligned} \tag{11}$$

The symbol Y denotes the admittance, with the subscript -*C*- and -*L*- indicating whether it is for the capacitor or inductor respectively. The further defined subscripts -*low*- and -*up*- show the frequency, in other words for the lower or upper frequency edge of the matching circuit. In equations (10) and (11) the -*low*- and -*up*- subscripts are omitted. To find the required admittance (Y) one must substitute the specific frequency (f) that is needed, being either the lower or upper frequency. From these equations one ends up with two unknowns, L and C, and two basic equations, (8) and (9). Solving them simultaneously results in the required solution. Equation (12) now gives the resonant frequency of the LC- circuit.

$$f_c = \frac{1}{2\pi\sqrt{LC}} \tag{12}$$

Earlier in this section it was mentioned that the LC-circuit and the antenna should have resonant frequencies, f_c, that are ideally exactly the same. Despite this important fact, it is not part of the actual design process. The reason is that when the phase shift as shown in Figure 3.12 is done accurately, the resonant frequency (f_c) will automatically be correct. If one uses a slightly incorrect phase shift the resonant frequency will not be precise. This will lead to a marginal capacitance or inductance when the LC-circuit is added where the system was assumed to be resonant, and a slight asymmetry in the final return loss can be seen. Fine-tuning of the component values once the matching network is combined with the patch antenna will solve this.

In equations (8) and (9) two frequencies were defined, namely f_{low} and f_{up}. These are the frequencies where the parallel-resonant circuit must cancel the imaginary component of the phase transformed antenna admittance completely in such a way that total admittance becomes real. These frequency values are not chosen arbitrarily, but are chosen according to the real admittance curve. In Figure 3.15 it is evident that the addition of the LC-network to the circuit does not alter the real admittance. This property of the LC-circuit provides the solution for choosing the frequency points where the imaginary component should be zero. When the reactive component of the input admittance is effectively cancelled with the addition of the resonant section at the frequencies where the real admittance would just fall within the required VSWR specification when considered alone,

the best bandwidth improvement is obtained. Results for a test conducted on the patch example shown in Figure 3.7 to verify the validity of this statement is shown in Figure 3.18. The bandwidth was tested for a VSWR less than or equal to 1.5:1. Without the addition of an external circuit the antenna itself has a return loss better than –14 dB between 1.773 and 1.825 GHz, a bandwidth of 2.89%. The phase-transformed admittance was considered and various LC-combinations were chosen to reduce the overall reactive component of the admittance. The capacitance and inductance values are chosen to cancel the imaginary admittance at a specific frequency (assuming symmetry in impedance, i.e. the lower and upper real admittance is roughly the same) is plotted against percentage bandwidth improvement in Figure 3.18. For a VSWR < 1.5:1 the real admittance when considered alone should be either 0.0133 S or 0.03 S.

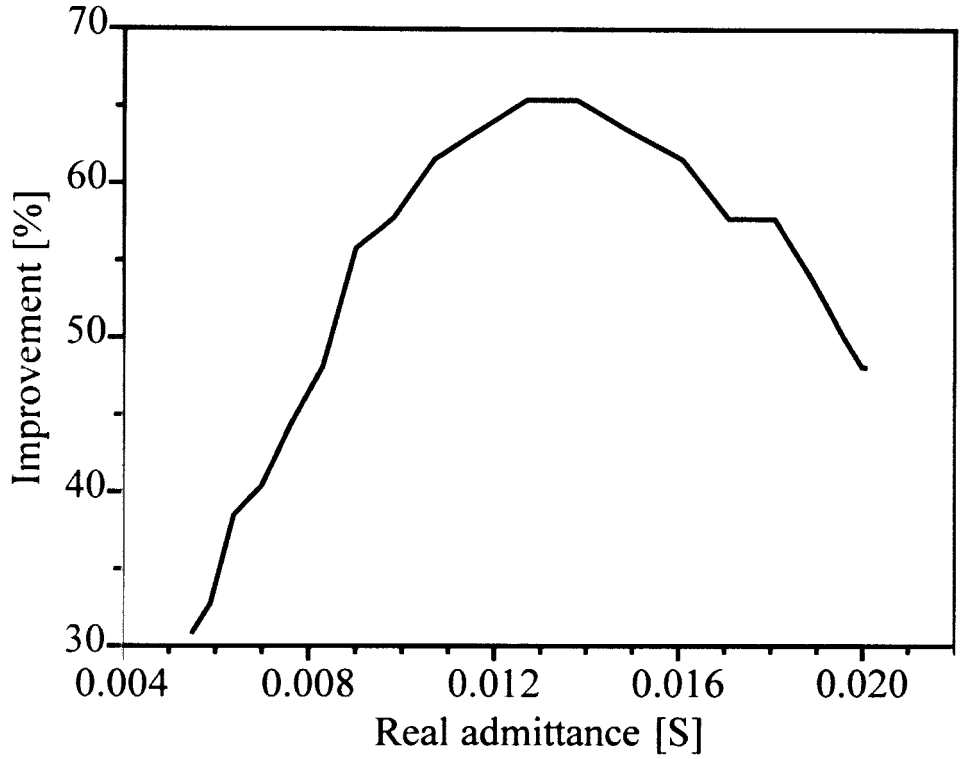

Figure 3.18 Percentage improvement obtained for real admittance values where the LC-circuit is designed to cancel the imaginary component

From Figure 3.18 it is clear that a bandwidth improvement in the order of 65% can be obtained when the LC-circuit is designed in such a way that it will result in real admittance values that fall just within specifications when considered alone. The lower edge for a VSWR < 1.5 is 0.0133 S. The actual percentage (i.e. 65%) is a value that is only valid for this patch antenna example, and it will vary for different types of antennas. The most important deduction that can be made from the graph in Figure 3.18 is that the maximum possible improvement will be obtained when the matching LC-section is chosen to cancel the imaginary admittance at the frequencies where the real admittance considered alone will fall just within the VSWR specification.

3.5 Transformation of the real admittance

In the previous section it was explained in detail how it is possible for the LC-section not only to improve the impedance bandwidth of a microstrip patch antenna, but also that an optimal solution can also be found for an LC-circuit. In Figures 3.16 and 3.17 the result is shown on both the Smith chart and the Cartesian plane. When the mentioned technique is suggested as an impedance enhancement method, a quick glance at these two graphs suggests some room for additional improvement. On the Smith chart a so-called eye is created when the LC-circuit is added. At the centre frequency the impedance locus passes through 50 Ω. A better bandwidth improvement factor is possible when the centre frequency does not pass through 50 Ω, but when the centre of the eye is located at 50 Ω. The displacement of the eye-shaped locus on the Smith chart to the centre of the chart will result in the graph of Figure 3.17 not having a near perfect match at the centre frequency, but rather a more steady and broader frequency band response below a certain reflection coefficient value. This section is devoted to explaining and illustrating how this is done, and what the effect on the effective bandwidth improvement of this extra step is.

The accomplishment of an optimally wide impedance bandwidth by creating a mismatch at the centre frequency is a relatively simple procedure. It is done by transforming the real part of the impedance (alternatively admittance) as part of the matching procedure. As a result of the symmetric nature of the matching technique discussed, a quarterwave matching section poses the simplest solution. A few factors that one needs to keep in mind are that the quarterwave transformer will transform the real admittance to another form, and that the quarterwave length in itself is only valid at the centre frequency. At any other frequency the line will either be electrically longer or shorter.

First the issue of line length is considered. The quarterwave match is known to be fairly wideband in its performance. Although the term wideband is commonly used, and generally understood, it must be defined more precisely. A wideband microstrip patch is most often a patch with a 20 to 30% impedance bandwidth. On the other hand, wideband antennas can reach bandwidths with a frequency ratio of up to 40:1. For the real wideband

antenna range, quarterwave matching will not provide an answer, but for patch antennas these transformers are wider than the antenna and will provide a good match.

The second consideration for quarterwave matching circuits is the phase transforming property of the transmission line. The 90° section of transmission line results in a real admittance with a minimum value at the centre frequency and higher values being reached at the edge of the frequency ranges considered. This is shown in Figure 3.19. This phase-transforming property of a quarterwave section must be kept in mind when designing a matching circuit. The next few paragraphs will illustrate how this is done.

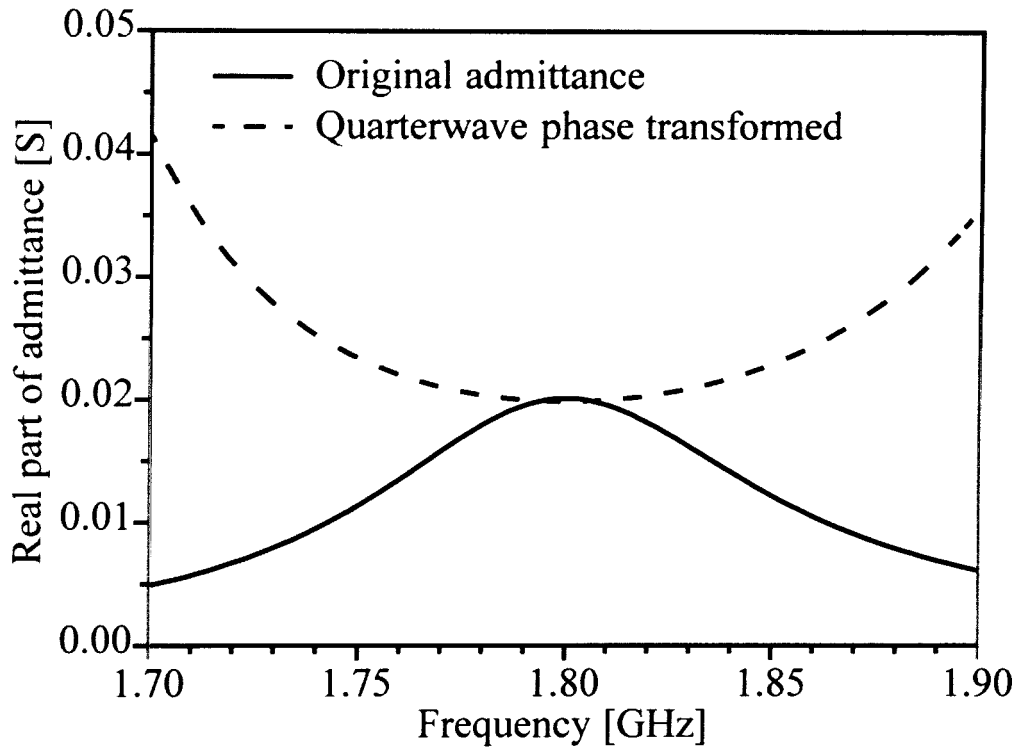

Figure 3. 19 Phase transforming of the real admittance with a 90° line

The inclusion of a quarterwave transmission line in the matching circuit leads to a slightly enlarged circuit. At first glance the possibility of including the impedance transformer in the first phase transforming line section seems to be the best option. The problem encountered is, however, that the line length for phase transformation will not reach a value of 90°. The only alternative position for the quarterwave impedance (admittance) transformer is after the LC-circuit.

The design of the transformer can be integrated as part of the matching circuit design process. The procedure will change slightly, since the real impedance must first be transformed before the LC-section can be calculated.

Considering the so-called eye on the Smith chart (Figure 3.16) it becomes clear that the front end of the locus (the left-hand side of the eye in Figure 3.16) can move left to the specified VSWR circle on the Smith chart. The effect of this left-sided movement in Figure 3.16 will possibly be an increase in VSWR bandwidth, but more importantly the original band considered (Figure 3.17) will remain below the predefined VSWR. In conjunction with the displacement of the locus on the Smith chart, an increase in diameter of the locus can also contribute to an improvement in bandwidth operation. This is possible when the LC-circuit is designed for a lower f_{low} and higher f_{up}.

The inclusion of the quarterwave transformer line results in a 90°-phase transformation. The curve will then be orientated in similar fashion to the locus included in Figure 3.9. The implication is that the real admittance curve has a minimum value at the centre frequency, instead of the maximum value that was intended originally (Figure 3.19). The LC-section is placed before the transformer, and the matching principle will remain the same. The only difference will be that the anticipated real admittance (after the transformer) will determine f_{low} and f_{up}.

Working with the edge of the VSWR circle on the Smith chart, the centre frequency real admittance must be transformed to the minimum allowable value, according to (13).

$$Z_{\lambda/4} = \frac{1}{\sqrt{Y_{Load} \cdot Y_{\min}}} \tag{13}$$

Equation (13) is an alternative formulation of the standard quarterwave transformer expressed in terms of load admittance (Y_{Load}) for the phase-transformed admittance and the required minimum admittance ($Y_{\min}$) used for improved bandwidth. For the test case considered previously the minimum value for a VSWR of 1.5:1 is 0.0133 S, and for a VSWR of 2:1 it is 0.01 S. Assuming that the original admittance is 0.02 S, this results in a transmission line impedance of 61.2 Ω or 70.7 Ω respectively.

The transformer line impedance calculated with (13) is initially used for the centre frequency transformed admittance. In addition, the transmission line also determines the newly obtained edge frequencies, f_{low} and f_{up}, where the imaginary component can be cancelled so that the real value that is left will fall within the VSWR specification. The impedance (admittance) transformer is normally designed to work mainly for real impedance values. In this matching technique the aim is to create two additional frequency points where the admittance will also be a real value. From Figure 3.19 it is clear that the edge value for the transformed admittance is at a maximum allowable value. For a VSWR of 1.5:1 this is 0.03 S and for a VSWR of 2:1 it is 0.04 S. $Z_{\lambda/4}$ is a known parameter from (13), and it is also known that the admittance will be real at the maximum value due to resonance. In order to find the frequencies where the LC-circuit must cancel the imaginary admittance equation (14) is implemented (derived from (13)).

$$Y_{Load} = \frac{1}{Y_{\max} \cdot Z_{\lambda/4}^2} \tag{14}$$

The phase-transformed (before admittance transformation) admittance of the patch antenna (Y_{Load}) is now considered to be the unknown parameter. The impedance of the transformer ($Z_{\lambda/4}$) and the maximum admittance ($Y_{\max}$) that falls within specification are used in (14) to determine what admittance in the original curve (Y_{load}) will be transformed to the required load after the transformation. With a VSWR of 1.5:1 and $Z_{/4} = 61.2\ \Omega$ the admittance in the original curve is 0.0089 S. A VSWR of 2:1 represents an admittance in the original curve of 0.005 S. The two edge frequencies, f_{low} and f_{up}, can be found where the phase-transformed admittance (Y_{Load}) is one of the above. The design of the LC-section should be done so that the imaginary admittance will be cancelled at these frequencies for close to optimal impedance enhancement (for this technique). This technique works since the LC-circuit cancels the imaginary component at the three frequencies where the transformation is anticipated for, and thus real admittance (or impedance) transformation is effectively obtained.

In order to illustrate the design procedure in full, the patch antenna example shown in Figure 3.7 with the subsequent impedance data presented in Figures 3.8 and 3.9, is

matched for close to optimal impedance bandwidth with a single LC-section. The patch antenna will be matched for two conditions, VSWR of 1.5:1 and also VSWR of 2:1. The first step in the design is to find the phase-transforming transmission line length that will result in the required admittance response. A graphical approach is taken by using the Smith chart and judging when the curve exhibits symmetry around the real axis as shown in Figure 3.13. This step is identical for both bandwidth requirements, so there is no need to repeat it. The line length to accomplish this for the patch antenna considered is 37° at the centre frequency, 1.8 GHz.

The first design is for optimum VSWR 2:1 bandwidth. The admittance edges for this VSWR are between 0.01 S and 0.04 S. The original real admittance is 0.02 S, so a transformer is needed to transform 0.02 S to 0.01 S using (13).

$$Z_{\lambda/4} = \frac{1}{\sqrt{0.01 \cdot 0.02}}$$
$$= 70.7\Omega$$

To obtain the maximum admittance that will be transformed to acceptable admittance edges, (14) is implemented with the now known impedance $Z_{\lambda/4}$.

$$Y_L = \frac{1}{0.04 \cdot 70.7^2}$$
$$= 0.005S$$

The frequencies where the admittance is 0.005 S (Refer to Figure 3.15) are at 1.702 GHz and 1.916 GHz. These are the frequencies where the LC-circuit must cancel the imaginary component of the admittance. The imaginary admittances at these frequencies are 0.0067 and –0.0066 S respectively (Refer to Figure 3.14). The frequency with its imaginary admittance is taken and substituted into (8) and (9) for the different frequencies considered. This leaves one with two unknowns (L and C) and two equations (an equation for the lower and upper frequency). A capacitance of 4.936 pF and inductance of 1.572 nH result in the

required LC-combination. The proposed feed network for the antenna is shown in Figure 3.20.

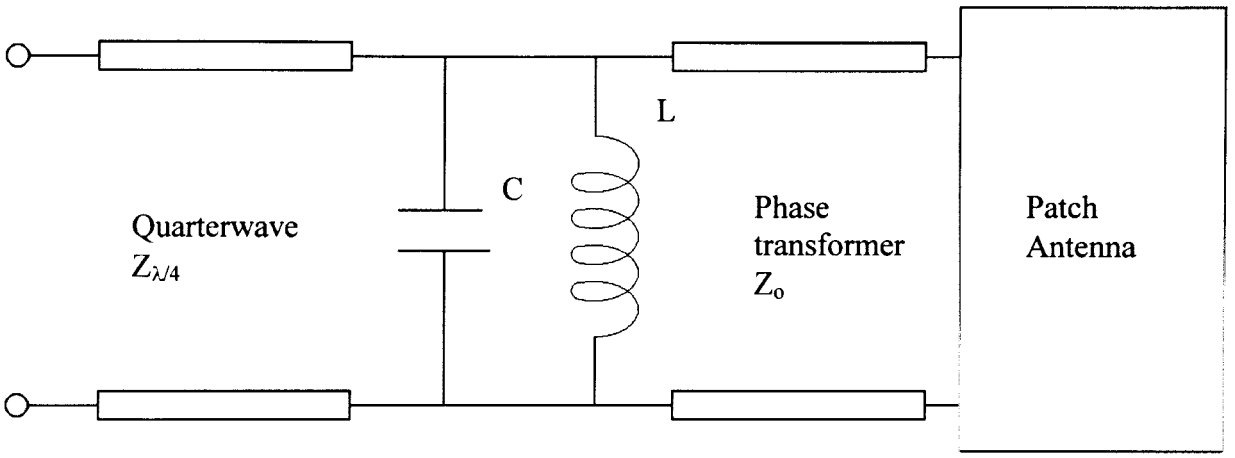

Figure 3.20 Final feed network layout for the enhancement of microstrip patch antennas

A summary of the resulting values for the circuit shown above with the patch antenna example of this chapter is given in Table 3.1. The quarterwave transformer value was changed from 70.7 Ω to a slightly lower value of 70.4 Ω for the VSWR of 2:1 design. The Smith chart graphical presentation is shown in Figure 3.21.

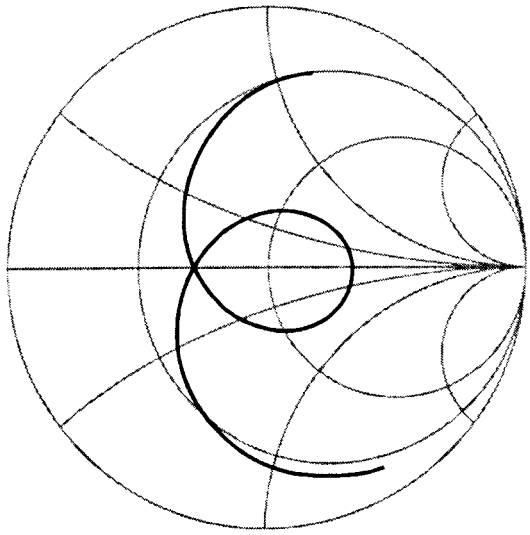

Figure 3.21 Graphical presentation of the matching result for a VSWR < 2:1

The return loss of the matched antenna and the original return loss of the antenna are shown in Figure 3.22. The results presented are for ideal components. The values are exact and the transmission lines lossless. In Figure 3.22 it is evident how close the centre frequency is to the VSWR specified value. For this the transforming impedance was changed slightly from 70.7 to 70.4 Ω. It is a slight variation, and resulted in the return loss at the centre frequency being just below specification instead of slightly above.

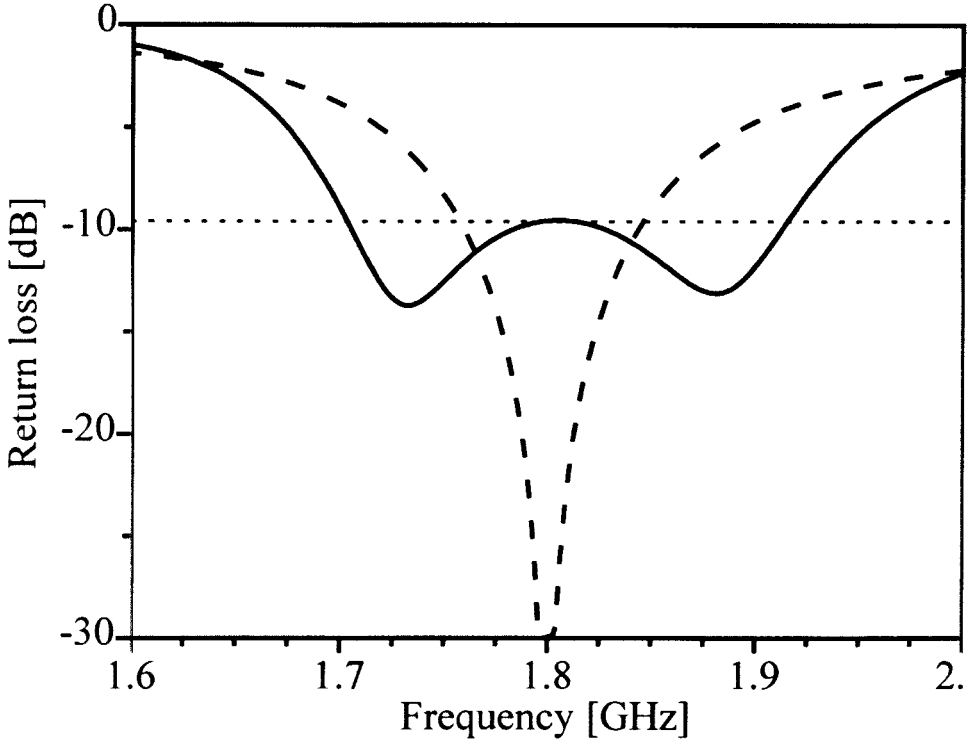

Figure 3.22 Return loss for the matched antenna with VSWR < 2:1

The frequency range of the antenna changed from 1.758 - 1.846 GHz to a frequency band of 1.704 - 1.914 GHz. This is an improvement from 4.89% to 11.67%, an improvement factor of 138.6%, for a VSWR of 2:1.

The same design procedure was followed for a VSWR specification of 1.5:1. The phase transformation for both scenarios remains the same. The second part of the design, to obtain a value for the capacitor and inductor, has to be repeated. From (13) the transmission line characteristic impedance for the transformer is 61.2 Ω. Substituting this impedance in (14) and using the edge's highest allowable admittance, 0.03 S, the

admittance on the real curve to be considered is 0.0089 S. The frequencies where this admittance is obtained are 1.736 and 1.87 GHz. The phase transformed imaginary admittances at these frequencies are 0.0087 and –0.0087 S respectively. The calculated component values are C = 10.142 pF and L = 0.768 nH. The characteristic impedance for the transformer was lowered from 61.2 to 61 Ω, since the return loss is very close to the maximum allowable VSWR. The impedance curve is shown in Figure 3.23 on the Smith chart, and the return loss for direct comparison of the original and matched antenna is shown in Figure 3.24.

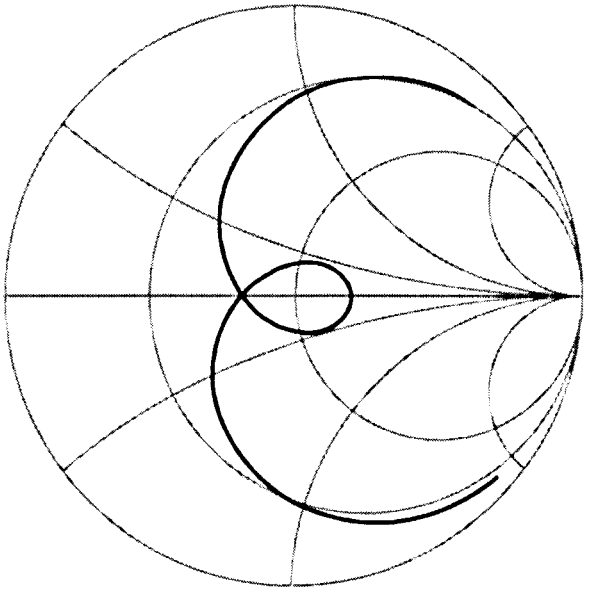

Figure 3.23 Graphical presentation of the matched result for a VSWR < 1.5:1. The locus shown reaches the 1.5:1 VSWR circle on the right hand side of the chart, and the crossing on the left is also aimed to be right on the VSWR 1.5:1 circle.

The frequency band of the antenna without the matching network for a VSWR of 1.5:1 is between 1.774 and 1.826 GHz. After the inclusion of the matching network with the impedance transformers a new frequency band was obtained, being 1.738-1.87 GHz. This is an improvement of 153.8%, from a bandwidth of 2.89% to 7.33%. All the results for the example presented in this section are given in Table 3.1.

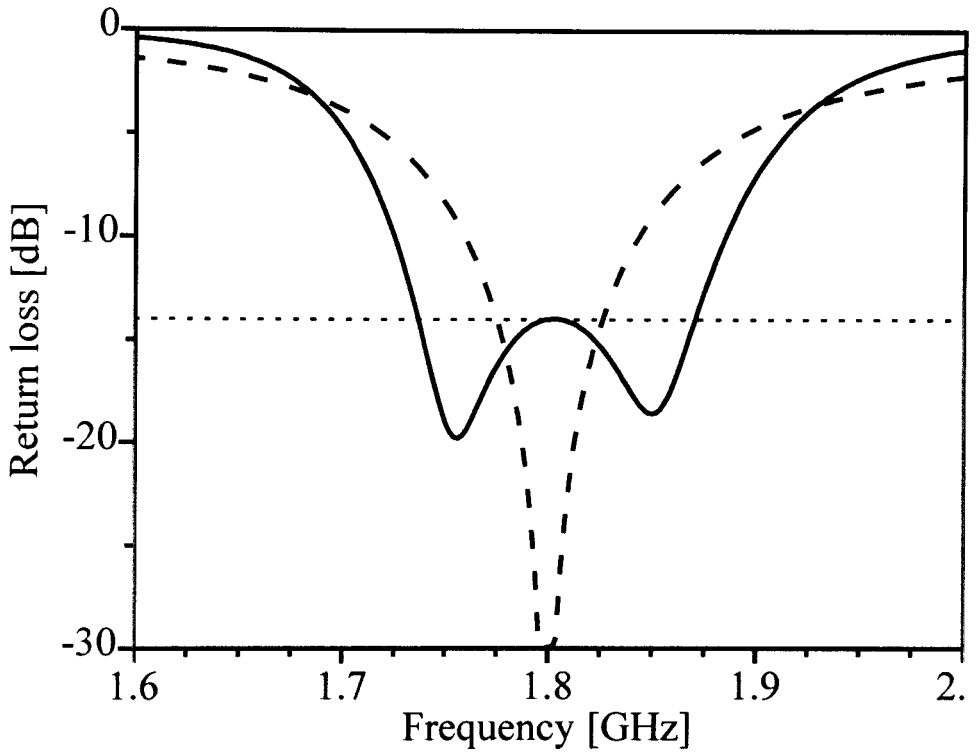

Figure 3.24 Return loss for the matching circuit and patch antenna with VSWR < 1.5:1

Table 3.1 Results for the matching circuit applied on the patch antenna shown in Figure 3.7

Parameter	VSWR < 2:1 Match	VSWR < 1.5:1 Match
Phase transmission line length [°]	37	37
Capacitor [pF]	4.936	10.142
Inductor [nH]	1.572	0.768
Quarterwave transformer $Z_{\lambda/4}$ [Ω]	70.7	61.2
Implemented $Z_{\lambda/4}$ [Ω]	70.4	61
Original bandwidth [MHz]	88	52
Matched bandwidth [MHz]	210	132
Improvement factor [%]	138.6	153.8

3.6 Conclusion on the SRMT theoretical design

From the patch antenna examples it is evident that in theory an improvement in the order of 140% can be obtained with a single LC-resonant matching circuit and some additional impedance transforming (SRMT). A comparison between the current technique (the SRMT) and results from the SRFT will be presented in the next chapter.

In chapter 4 and 5 results obtained with IE3D by Zeland Software [40] and Sonnet Lite [41] will be shown. IE3D is a full wave simulation package that implements moment method to solve microstrip circuits and antennas. Sonnet Lite is the shareware version of Sonnet. This package is specifically aimed at solving microstrip circuits. In the Lite version limitation are imposed on the circuit size one can simulate, but fortunately the SRMT presented in this dissertation is small enough so that Sonnet Lite can simulate the circuit. The theoretical designs (with ideal components) presented in this dissertation were computed with the aid of a network simulator that is part of Sonnet Lite.

Three main antenna examples, consisting of an antenna made with substrate only, the 5 mm air spaced antenna already discussed in this chapter and a 10 mm air spaced antenna are also manufactured to verify the validity of the SRMT. An antenna similar to the quarterwave coupled line structure presented in [18] is also discussed and verified against the SRMT.

Chapter 4

Theoretical comparison to known matching circuits

The SRMT presented in Chapter 3 is relatively simple to implement. In order to be able to evaluate the ease and effectiveness of this proposed technique, it must be directly compared to other standard and wideband matching techniques. In this chapter a direct comparison is made between standard matching techniques often used in the industry and the SRMT. The examples presented include the single and double stub matching techniques, called the parallel-element matching technique in this chapter. Furthermore, a comparison is made with the quarterwave matching section and a triangular matching line. They are referred to as series matching since the matching element is in serie with the patch antenna. Lastly the SRFT example presented in [2, 4] is taken as reference, and the LC-matching circuit is applied on a similar microstrip patch antenna.

4.1 Parallel-element matching circuits

These standard matching techniques are aimed at matching an arbitrary impedance to a specified impedance. In order to be able to compare different techniques a patch antenna

with a minimum return loss at 1.8 GHz was used with an optimum return loss of only -11 dB. The response of this test case is shown in Figure 4.1.

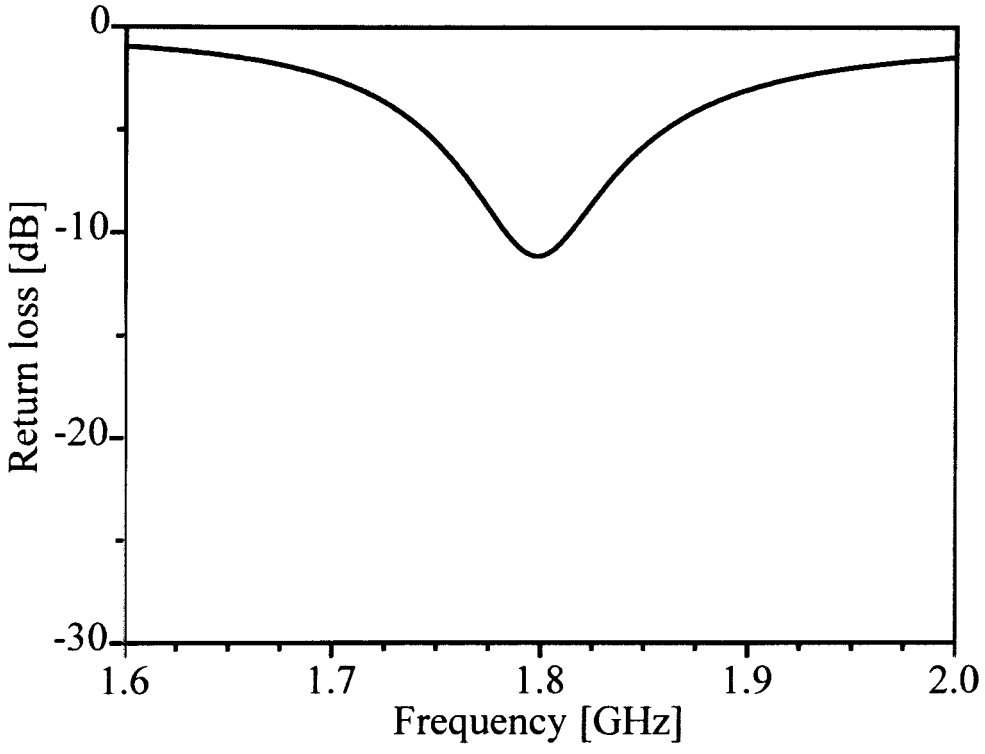

Figure 4.1 Example patch impedance for implementation of standard matching circuits

The input impedance at 1.8 GHz for the patch antenna is 47.3-*j*27.9 Ω. The first matching circuit implemented on this test case is a single stub matching circuit. In order to be able to match this impedance to 50 Ω, a circuit consisting of a series transmission line of length 166° (at centre frequency) with characteristic impedance 50 Ω is needed. A parallel open circuit transmission line of length 30° will transform the impedance to 50 Ω at the centre frequency. Please note that there are a number of alternative ways of implementing this technique. The aim is not to evaluate the single stub matching technique, but instead simply to obtain a proper result with the technique so that it can be compared to the SRMT. The result obtained with the single stub circuit is presented in Figure 4.2.

Also shown in Figure 4.2 is the result obtained when a double-stub matching circuit is implemented. The double-stub circuit used to obtain this result consisted of an open stub of

length 14° followed by a 50 Ω-transmission line of length 135° and another parallel open stub of length 23°.

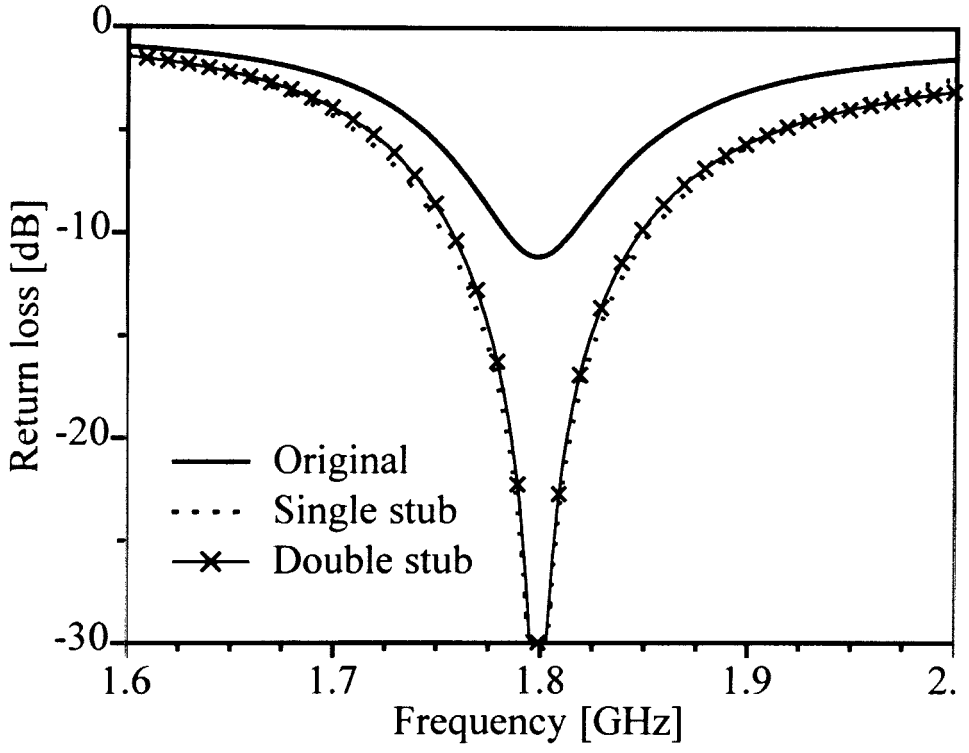

Figure 4.2 Single and double stub match implemented on an arbitrary impedance to match to 50 Ω

From Figure 4.2 it is evident that the results for the two techniques correspond very closely. The unmatched return loss was below –10 dB between 1.783 GHz and 1.815 GHz. This represents a bandwidth of 32 MHz. The single stub matched circuit has a bandwidth of 100 MHz and the double stub matched circuit an 89 MHz bandwidth. For a –14 dB matched criterium the original load has no bandwidth, but the single stub and double stub matching techniques resulted in a 59 MHz and 54 MHz bandwidth respectively. The difference between the results of the two techniques is minimal.

4.2 Series-element matching circuits

A very popular matching structure is the quarterwave matching transmission line. It is very easy to design and takes up no space in a feed network when a transmission line length of more than 90° is used. The unmatched patch (centre frequency) input impedance used in the previous section for illustration, 47.3-*j*27.9 Ω, is again used for the next example. The quarterwave matching line only works for resistive loads. To ensure that the quarterwave matching line transforms a resistive load, the original load impedance is first phase-transformed to a real value. A 50 Ω transmission line of electrical length 40° is inserted between the load and the quarterwave matching transmission line. The phase-transformed impedance is now 88.4 + *j*0 Ω. With a newly obtained load impedance of 88.4 Ω a quarterwave matching section of 66.5 Ω will result in a 50 Ω matched circuit. The return loss as function of frequency for the quarterwave section is shown in Figure 4.3.

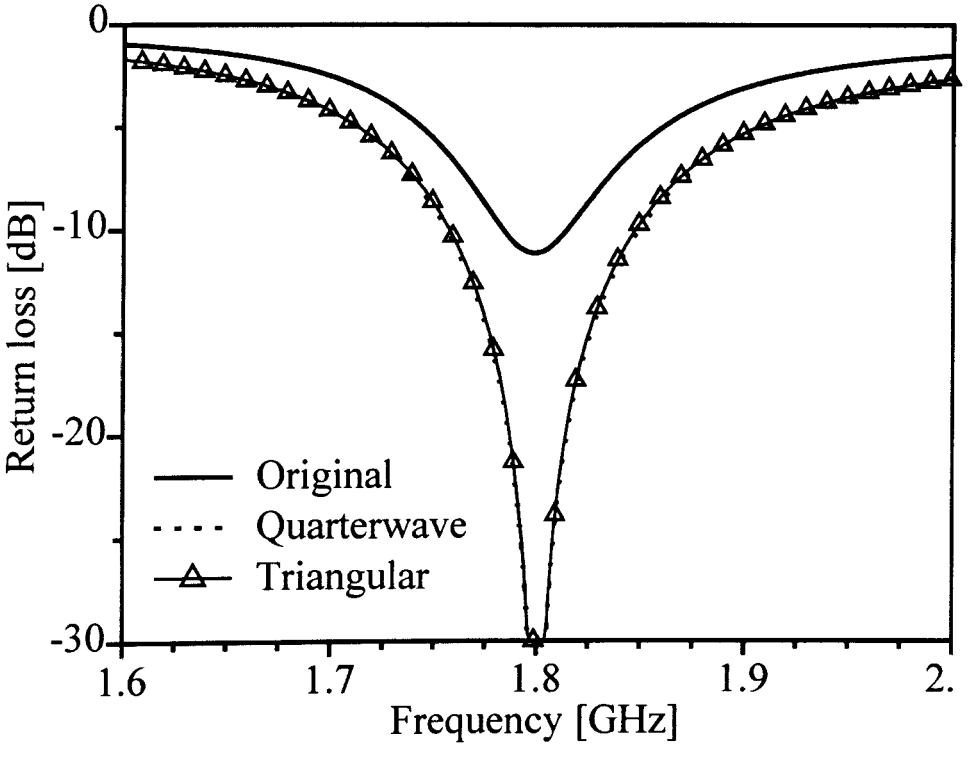

Figure 4.3 Results for the series type of matching circuits

The continuously tapered types of matching circuits are discussed in Chapter 5.8 of [21]. The types of structures discussed in [21] include the exponential taper, the triangular taper and the Klopfenstein taper. They all have similar-looking circuit layouts and particular responses. The triangular taper circuit is taken as an example. The impedance Z of the transmission line as a function of position x down the matching is described by the following relation [21]:

$$Z(x) = \begin{cases} Z_0 e^{2\left(\frac{x}{L}\right)^2 \ln\frac{Z_L}{Z_0}} & \text{for} \quad 0 \le x \le \frac{L}{2} \\ Z_0 e^{\left(\frac{4x}{L} - \frac{2x^2}{L^2} - 1\right)\ln\frac{Z_L}{Z_0}} & \text{for} \quad \frac{L}{2} \le x \le L \end{cases} \tag{15}$$

A phase-transforming section of line is required for the triangular taper since it also works with real load impedances only. The 40° line used for the quarterwave transmission line is again implemented in this circuit. A line with a total length of 360° is chosen, consisting of 10° subsections. The final results for both the quarterwave and triangular taper, shown in Figure 4.3, are very close to each other in terms of frequency bandwidth. The quarterwave section has a –14 dB bandwidth of 56 MHz and the triangular taper 54 MHz.

A very important fact to keep in mind specifically when considering the taper match circuits is that they are known to be very frequency insensitive and can achieve large bandwidths. However, this is only valid for a frequency insensitive load impedance. Yet, as is shown in the two graphs, all the matching techniques have a relatively similar response for a load impedance that varies over frequency.

4.3 SRMT applied to load

Finally, the mismatched patch example is matched with the SRMT. In order to be able to compare the new matching technique to the standard matching techniques (as described in the previous paragraphs) the LC-resonant match is done with two different approaches.

4.3.1 Single LC-resonant match without optimum bandwidth

The resonant technique considered in this dissertation requires a matched load to function. The SRMT would not operate if the original load impedance of 47.3-*j*27.9 Ω is considered alone. Therefore, the quarterwave matched load designed in the previous paragraph is considered the load impedance. This implies that the quarterwave matching transmission line is again part of the matching circuit. The single LC-resonant circuit that results in the required match consists of a capacitor of 8.4 pF and inductor of 0.93 nH. The return loss result for this circuit is presented in Figure 4.4. The –14 dB return loss bandwidth is 83 MHz, in comparison to the original quarterwave matching circuit that resulted in 56 MHz.

4.3.2 Optimum Bandwidth Single LC-Resonant Matching Technique

The second test case application for the LC-resonant circuit is done with the real impedance transformation as described in Chapter 3.5. The circuit will also consist of a 50 Ω phase-transformer of 40°, followed by the LC-circuit and a quarterwave matching transmission line. A capacitor of 4.98 pF, inductor of 1.56 nH and quarterwave matching line of impedance 81 Ω resulted in the return loss response presented in Figure 4.4. The bandwidth for –14 dB return loss is 134 MHz.

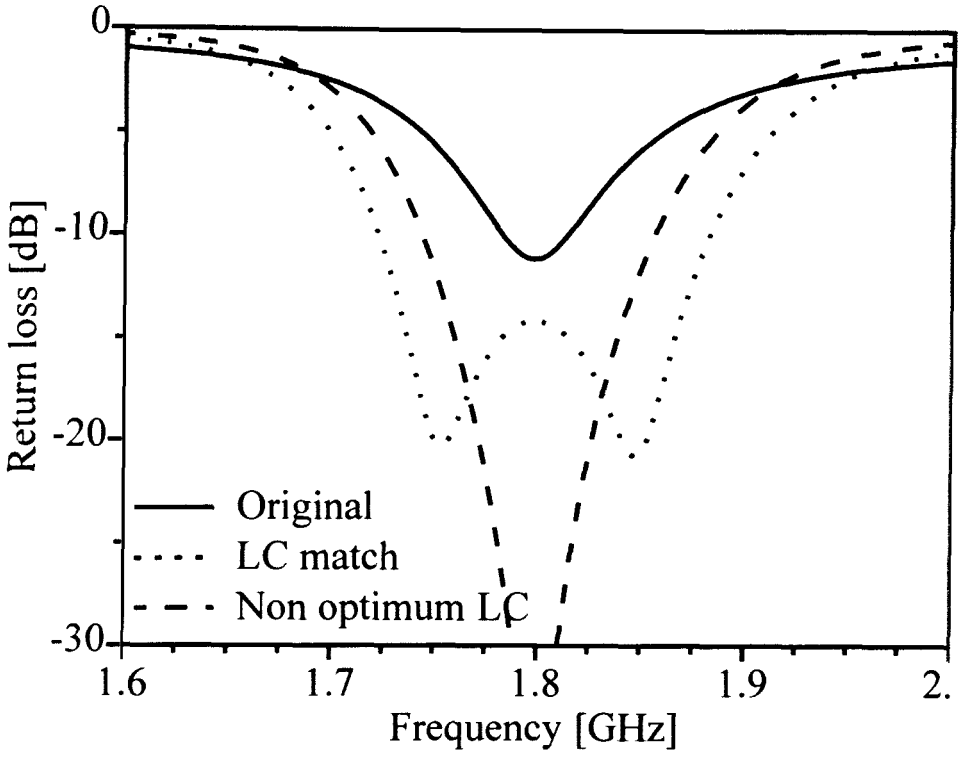

Figure 4.4 Matching results with the implementation of the proposed LC-circuit

It is evident from Figure 4.4 and the previous two sections that the LC-matching circuit can result in a vast improvement in bandwidth results. One must keep in mind that the standard techniques are mostly aimed at either a single frequency match (the quarterwave matching circuit when considered alone as well as the single and double stub matching circuits) or matching of a constant load impedance over a relatively wide frequency range (the tapered transmission line structures, as well as the quarterwave matching circuit to some extent). It would therefore be incorrect to state that the SRMT is an improvement for matching circuits in general, but any circuit or load with a similar frequency response to the examples illustrated so far can be significantly improved with the SRMT.

4.4 Patch example from the SRFT

The SRFT is mentioned in Chapter 3 as one of the commonly discussed microstrip patch antenna wideband impedance matching techniques found in open literature. The publications that presented this technique [2, 4] were also included in a very popular compendium of papers concerning microstrip patch antennas [37]. For this reason it is very important to measure the presented LC-matching technique to the SRFT, so that one can be able to make a proper judgement on the working of the LC-technique and whether it would work as effectively as the well-known SRFT. The authors of the SRFT publications implemented the technique on a single patch antenna for all their publications on the SRFT [2, 4 and 16]. The graphical representation of the patch antenna presented in all the above-mentioned papers is shown in Figure 2.4 and for ease of reference repeated in Figure 4.5. The microstrip antenna is a square patch. On the ground plate a foam sheet of thickness 5 mm and ε_r = 1.03 is placed. On the foam sheet a substrate with thickness 0.5 mm, ε_r = 2.17 and $tan\delta$ = 0.0009 is placed. A similar type of dielectric substrate is used for the feed network on the back plane of the ground plate, but with thickness t = 1.575 mm instead of 0.5 mm. Since the antenna is described in detail in all three the papers regarding the SRFT, it was decided to take this same antenna and simulate it in IE3D. The resulting return loss obtained from the simulation and the published results from [2, 4 and 16] is shown in Figure 4.6.

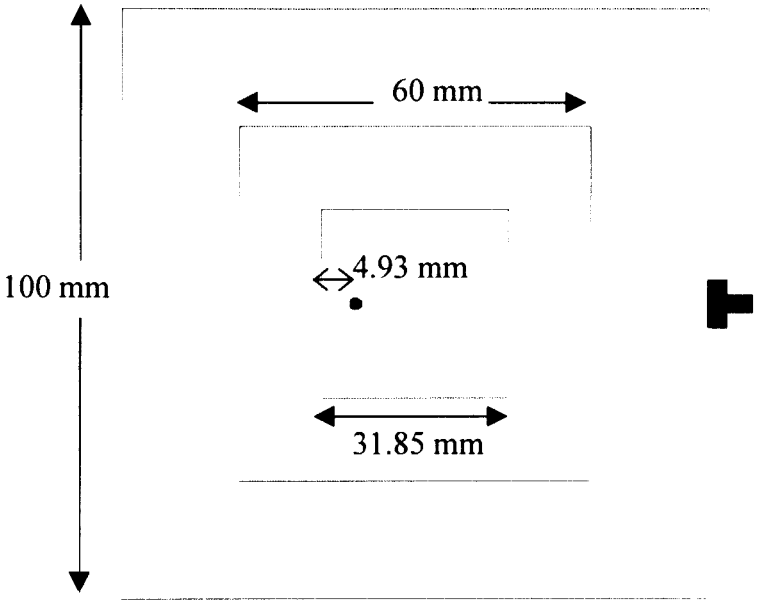

(a)

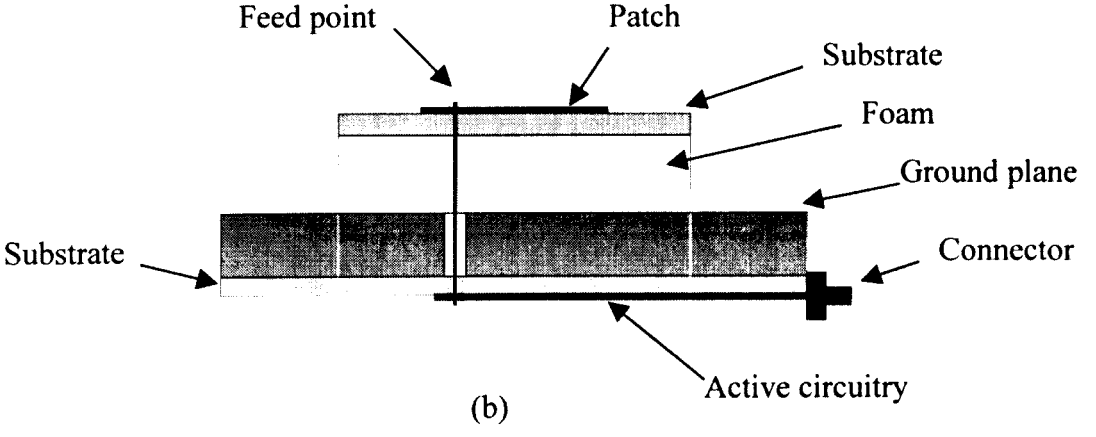

(b)

Figure 4.5 Example patch antenna described and wideband matched in [2, 4 and 16]

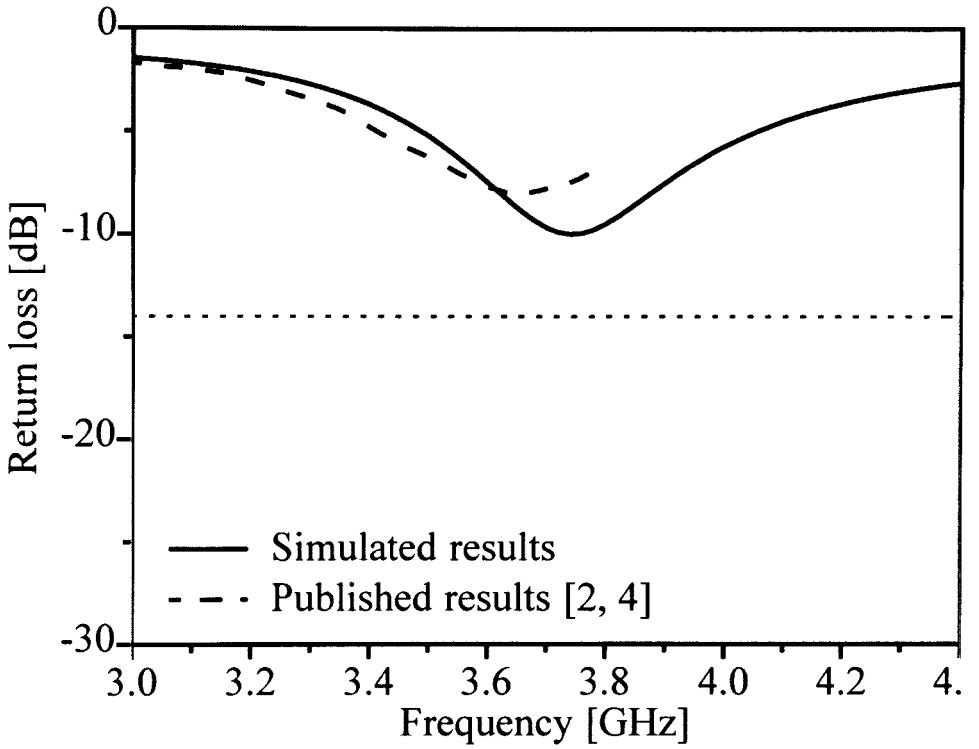

Figure 4.6 Published and simulated results for the example patch antenna implemented for the SRFT

Figure 4.6 shows reasonable correlation between the simulation and the published data for the patch antenna shown in Figure 4.5. A frequency shift in the order of 4% is encountered, and the simulation shows 2 dB better return loss when compared to the published results. The published results from [2, 4] end at 3.8 GHz. When comparing the results of the two techniques this deviation must be kept in mind before a final comment is made about the results that will be shown in this section.

The SRMT was applied to the simulated patch antenna data. The results are shown in Figure 4.7. The circuit implemented consists of a 14° phase transforming line, a capacitor of 0.637 pF, an inductor of 2.77 nH and a quarterwave transmission line of 83 Ω. The design frequency was 3.74 GHz. Also included in Figure 4.7 is the result that was obtained when the SRFT was applied [2, 4]. The SRFT circuit consists of (seen moving away from the load) a parallel inductor of 1.993 nH, a series inductor of 7.7336 nH, parallel capacitor of 0.516 pF and a series inductor of 6.9056 nH (Refer to Figure 2.5).

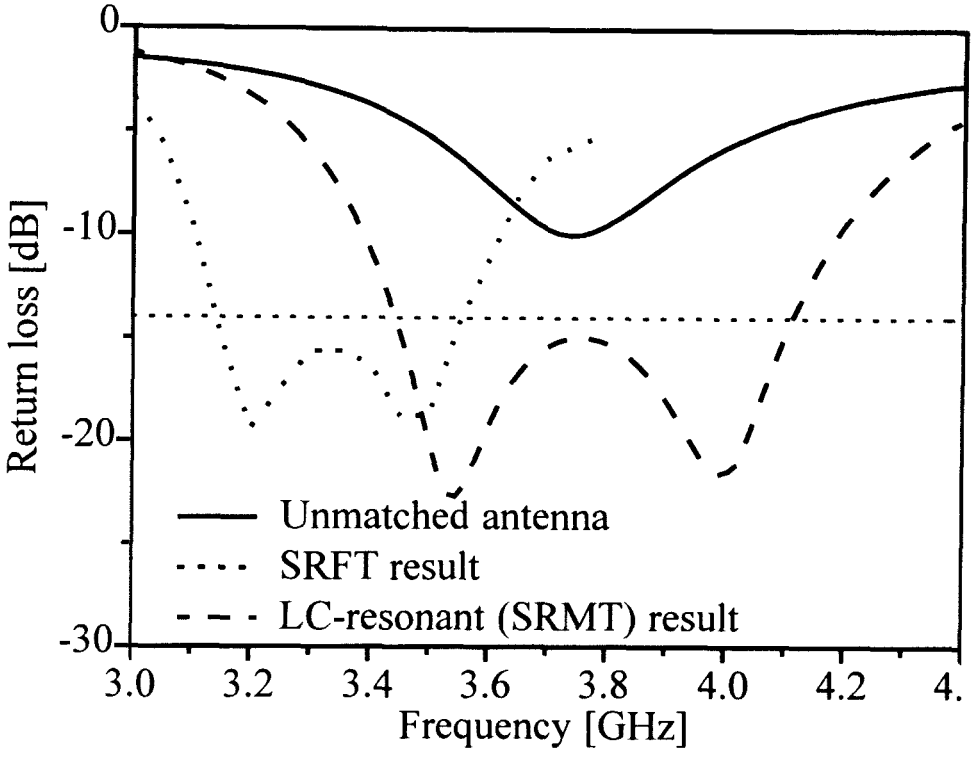

Figure 4.7 Return loss results for the published SRFT patch antenna example, matched with the mentioned technique and the LC-resonant network

Figure 4.7 presents some important results. The SRMT manages to establish a VSWR < 1.5:1 bandwidth of 680 MHz, between 3.44 GHz and 4.12 GHz. The SRFT result that was published had a bandwidth of 400 MHz, between 3.15 GHz and 3.55 GHz. The main difference is the choice of frequency range for the SRFT matching network to match the antenna. In Figure 4.7 it is evident that the centre design frequency for the SRFT case is close to 3.3 GHz. A statement made in [4], where the result from Figure 4.7 is obtained, reads as follows. "The fundamental resonant frequency of the patch is 3.3 GHz." This statement might be somewhat confusing, but it leads one to the final conclusion as to why the published result was not taken at the frequency where the return loss for the unmatched antenna was already a minimum, namely 3.74 GHz. [3] states the following:

"In fact, for the thicker antennas, the reactance curve never passes through zero at all. For this reason, the resonant frequency has been redefined as the point at which the resistance reaches a maximum, independent of the value of the reactance."

The real part of the simulated impedance of the unmatched antenna is shown in Figure 4.8 together with the SRFT-matched return loss response obtained in [4]. The article in which the statement about the resonant frequency presented in the previous paragraph is made, is also referred to in [4]. One can only assume that the choice of matching frequency for the authors of the SRFT in [4] is based on the real impedance of the patch antenna, and not so much the frequency where minimum reflections are originally obtained.

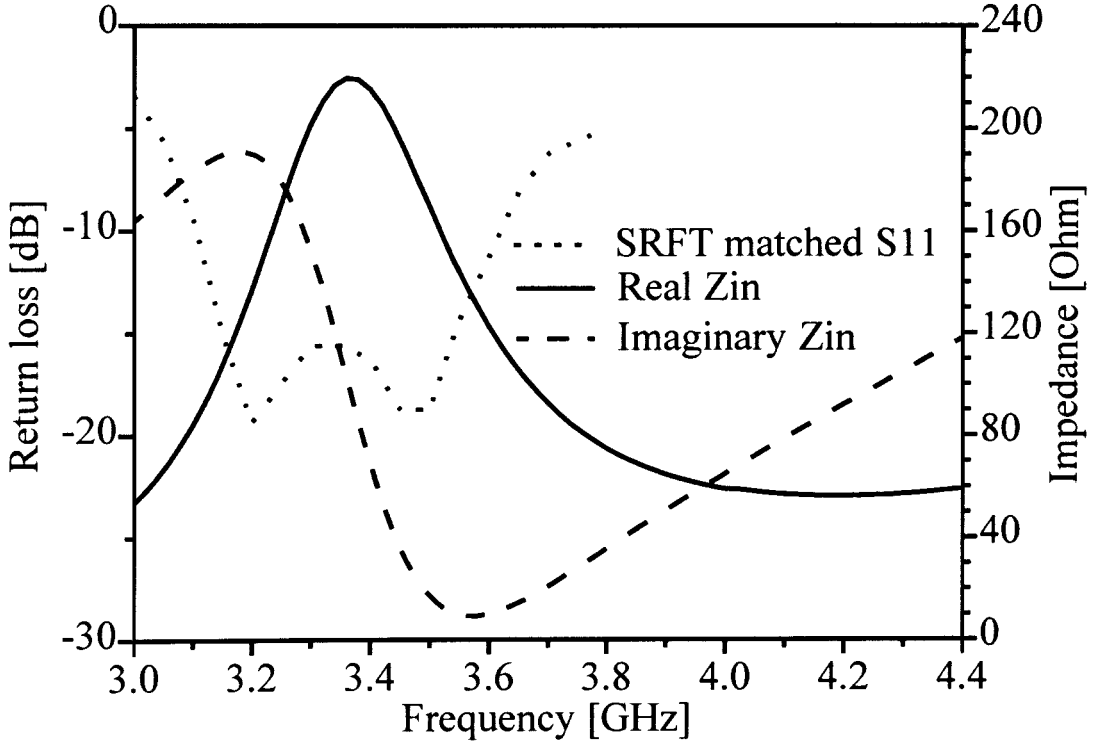

Figure 4.8 Input impedance simulated for the patch antenna presented in [2, 4]

The results obtained and presented in Figure 4.7 show that the LC-matching technique is comparable to the SRFT in terms of bandwidth enhancement results. It also shows that the deviation obtained between the simulation done and the published results is not particularly crucial since there are a number of other parameters that also play a very important role in determining the final match. The selection of frequency range where the wideband match must be done is one of these parameters. It is evident that a different approach is taken for the LC-resonant match, which aims at enhancing the minimum return loss already available. The published results for the SRFT, on the other hand, show that this is not the

case for the SRFT. An in-depth study of the SRFT would probably provide more information.

An alternative design with the SRMT was done on the patch antenna example presented in this section to establish whether it would be possible to obtain a frequency shifted match as well. The result is academic in nature, since the circuit obtained is difficult to realise in practice. The steps taken to obtain the required match are shown and explained with the aid of a number of Smith charts. Figure 4.9 shows the original impedance locus of the unmatched antenna on the Smith chart.

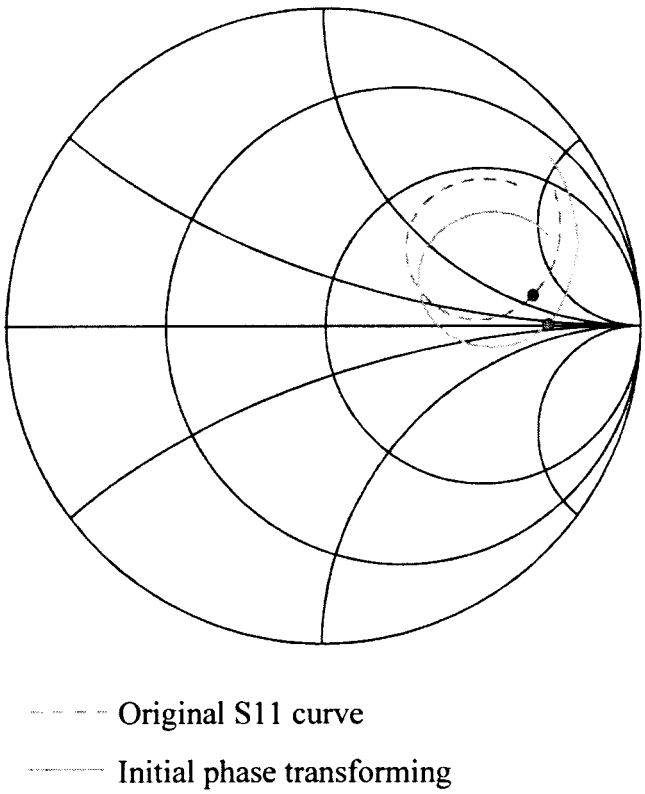

Figure 4.9 Return loss of original patch antenna and phase transforming to obtain real impedance at new design frequency

The dots shown on the locus on the Smith chart represent the new frequency positions where the antenna will now be matched. This is the frequency where the antenna has a maximum real impedance, irrespective of the reactance value. The first aim for the new circuit was to get the newly defined center frequency on the real axis. This was done with a

50 Ω transmission line of 5° at center frequency, now considered to be 3.35 GHz. This is different from the value of 3.3 GHz stated in [2, 4] because of the slightly shifted frequency response obtained with the IE3D simulation. Figure 4.10 shows the next two steps taken to match the patch antenna to the required level.

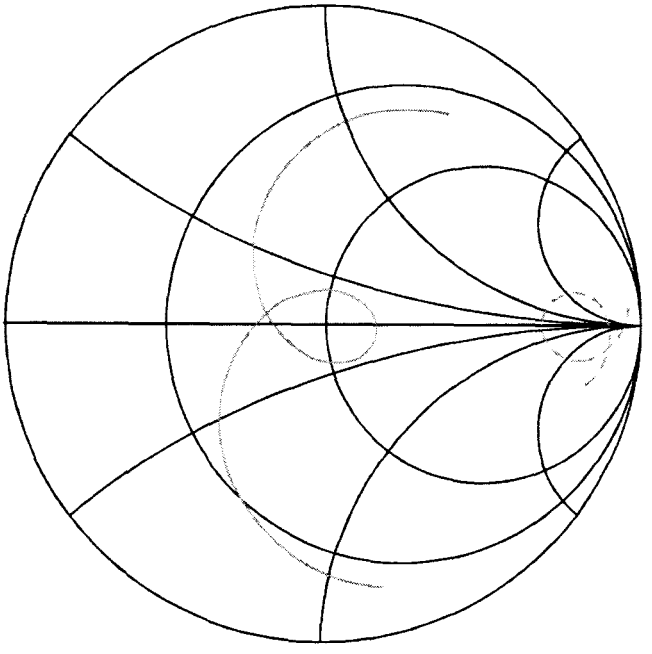

Figure 4.10 Phase transformed impedance and final matched result for center frequency 3.35 GHz

The actual impedance encountered after the 5° phase transformation was 270 + *j*0 Ω. This is a very high real impedance value and becomes difficult to work with. The next step in the matching sequence is the phase transformation so that the imaginary admittance curve will lie favourable around the design centre frequency. The easiest way to get this done while using the minimum amount of space was to turn the locus around its new impedance value, 270 Ω. The correct phase transformation, shown in Figure 4.9, was obtained with a transmission line of length 65° at 3.35 GHz and characteristic impedance 270 Ω. This part of the circuit would be extremely difficult to realise in practice. The final design of the circuit to match the antenna to 50 Ω over an optimum frequency band around 3.35 GHz

was done with a capacitor of 0.187 pF and an inductor of 11.73 nH. The quarterwave matching transmission line for optimum bandwidth from 270 Ω to 50 Ω was 139 Ω. The final resulting return loss with comparison to the SRFT result is shown in Figure 4.11.

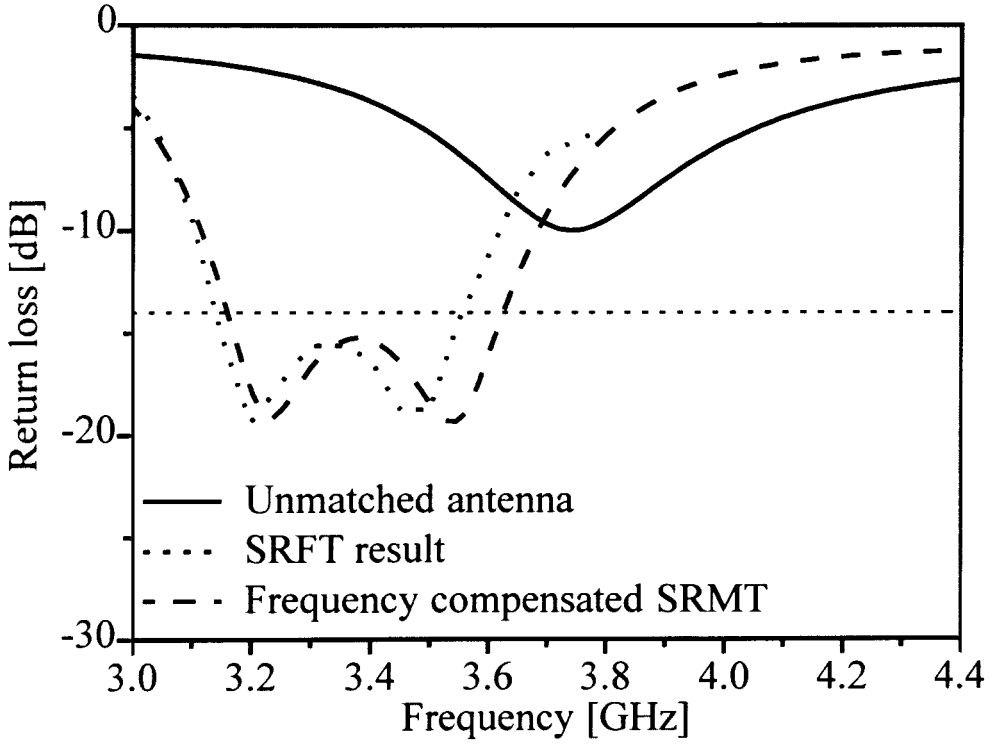

Figure 4.11 Adapted LC-match for direct comparison with the SRFT

The result obtained by implementing the frequency compensated matching circuit results in a frequency band of 470 MHz, between 3.16 GHz and 3.63 GHz. The SRFT-match presents a 400 MHz matched bandwidth. For the specific antenna the adjusted LC-resonant matching circuit resulted in a wider bandwidth than the SRFT. One must keep in mind that there was a slight difference between the simulated patch antenna and the initial antenna presented in [2, 4]. Therefore it is more fair to state that the SRMT provides comparable results with that published in [2, 4] for the SRFT, since there are number of unknown variables between the simulation and the publication. For this specific example the SRFT result is more practical to implement than the SRMT circuit, due to the frequency shifted match.

4.5 Summarising statement on comparing analysis

The SRMT is a technique aimed specifically at matching single resonance antennas. Probe-fed patch antennas have a distinctive resonant impedance behaviour, and the SRMT can improve this load impedance very effectively. Different loads do not necessarily present similar frequency behaviour and alternative matching techniques should be considered for these loads. Examples of this are the single and double stub matching structures applied to an arbitrary load impedance to match it to any required impedance at a single frequency. Quarterwave matching lines and tapered matching lines can match a constant load impedance very effectively over a much broader frequency band than the stub matching circuits. The load impedance example presented in this chapter illustrates how the SRMT is just as easy to design as the above-mentioned matching techniques, and that it is superior for the specific example used. Other scenarios, as mentioned in this paragraph and in the chapter, will obviously reign superior in their respective applications.

In the second part of the chapter the SRFT was taken and compared to the SRMT. The results proved that the improvement obtained is similar in terms of percentage improvement, but that the procedure for the design of the SRFT leads to another frequency range. A brief discussion of this phenomenon is presented in the chapter.

Chapter 5

Measured results

Results for the SRMT designed with IE3D and Sonnet Lite and applied to actual patch antennas are presented in this chapter. It is shown that the impedance bandwidth of a patch antenna can easily be doubled when the LC-resonance is added to the feed line. Full-wave simulation comparison between the proposed matching circuit and already published techniques and structures is also presented.

5.1 Example 1: 5 mm air gap patch antenna

In Chapter 3 a patch antenna is presented in Figure 3.7 with its input impedance presented in Figure 3.8. This antenna was built as the first patch antenna example. This same antenna is now further analysed in this section. For convenience the cross-sectional geometry of the antenna is reproduced in Figure 5.1.

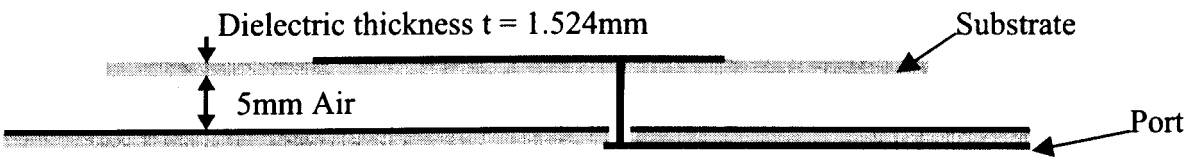

Figure 5.1 Cross-sectional geometry of the primary example patch antenna. The antenna dielectric substrate used has properties $\varepsilon_r = 3.05$ and $tan\delta = 0.003$

The dielectric substrate used for the patch antenna is GML-1000 [38] and for the feed network MC3D [39]. The dimensions of the patch antenna are W = 63 mm, L = 65.6 mm and d = 15.85 mm. The various dimensions are explained in Figure 3.1(a). The simulated and measured return loss is compared in Figure 5.2. There is good correlation between the simulated and measured results.

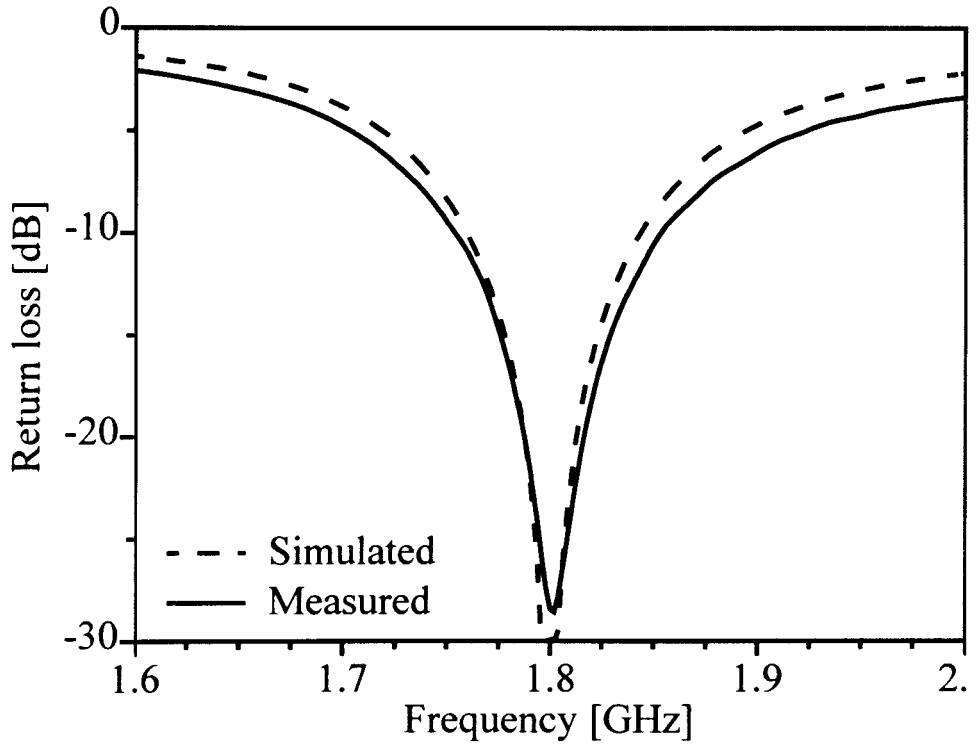

Figure 5.2 Unmatched return loss data for the 5 mm air gap patch antenna

The patch antenna is the same example as was used for the theory in Chapter 3. The various elements and transmission lines used for the SRMT on this patch have therefore already been calculated in Chapter 3. The capacitor and inductor are implemented as microstrip stubs. The capacitor is constructed as an open–ended parallel stub and the inductor is a short-circuited parallel stub. The starting values for the parallel-stub combination are obtained with equations (16) and (17).

$$Z_{OL} \tan(\beta l) = X_{HL} \qquad \text{(inductive)} \qquad (16)$$

$$\frac{Z_{OL}}{\tan(\beta l)} = X_{HC} \qquad \text{(capacitive)} \qquad (17)$$

The patch antenna example was designed to obtain optimum VSWR < 1.5:1 bandwidth. The required components for the matching circuit consist of (refer to Table 3.1) a 50 Ω transmission line of 37°, a parallel LC-section with element values of 0.768 nH and 10.45 pF, and a quarterwave transformer with $Z_{\lambda/4}$ = 61.2 Ω.

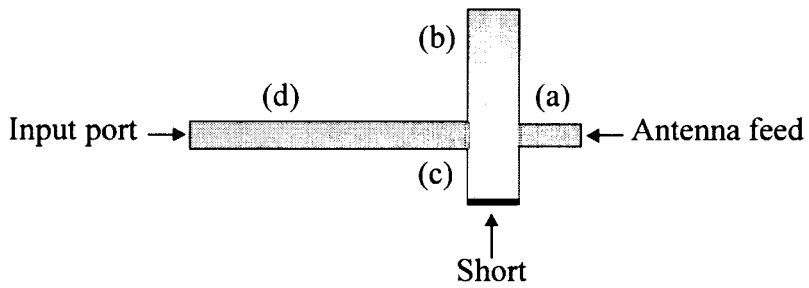

Figure 5.3 Circuit layout for the SRMT. The components are placed in the following order: (a) phase transformer, (b) and (c) capacitor and inductor respectively, and (d) quarterwave transformer

A number of problems were encountered when the circuit shown in Figure 5.3 was first simulated. The main issue was uncertainty regarding the reference position of the stubs. The exact location where the phase transforming transmission line and the quarterwave matching circuit should start and end was not accurately known when starting with the theoretically calculated values for all the elements in the circuit. With these unknown parameters in mind it was decided to do the conversion from theoretical component values to microstrip line step by step. These steps are explained in the next paragraphs.

The first step in the design is to ensure that the phase transforming circuit is correct. The desired transformation is a known parameter, and with the aid of this information the microstrip version of this transmission line can be optimised. In IE3D the transmission line

was combined with the patch antenna shown in Figure 5.1. The 50 Ω line is then tweaked to exactly the right length so that the phase transformation is correct.

The resonance and placement of the capacitor and the inductor are the next step. The distributed LC-section is first optimised to obtain the correct resonance, after which the placement with respect to the phase-transforming transmission line is considered. If all the elements are placed close to a third of the tangential line width inwards, good starting values were obtained. Figure 5.4 illustrates the position of this "one third".

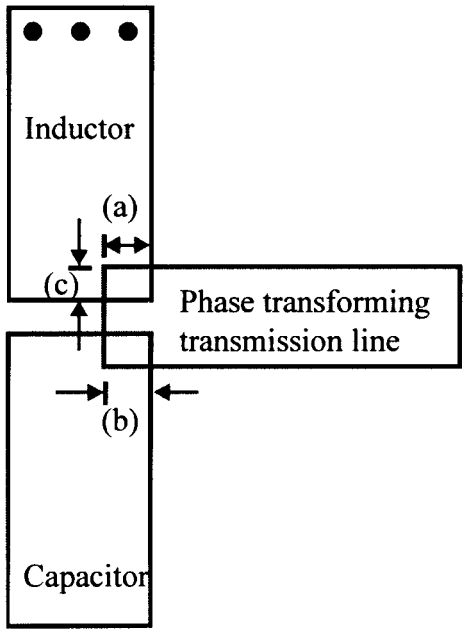

Figure 5.4 Illustration to show where the distributed components are placed before final optimisation. Positions (a) and (b) show how the phase transformation line is placed one third of the elements' width into the junction, and (c) shows how the distributed elements are placed one third of the transmission width inwards from the edge

The positions described here are not based on any previously published research. It is simply a starting value from where the capacitive and inductive stub lengths and positions are tweaked further.

Lastly the quarterwave transformer is added to the circuit. The transformer is normally close to correct without too much tweaking.

An important issue encountered is the pronounced effect of the probe connecting the microstrip feed network to the antenna port, situated on the ground plane (see Figure 5.5 for a graphical representation).

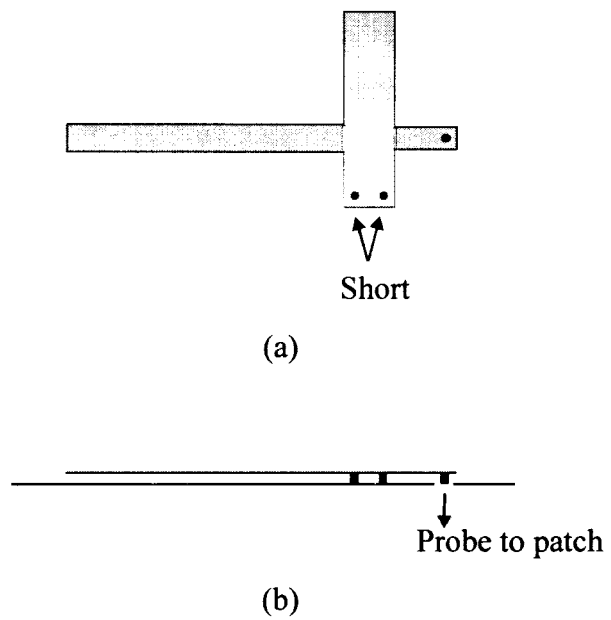

Figure 5.5 Top view of the fully modelled microstrip feed line (a) and a side view to illustrate the position and layout of the shorting pin and feed probe (b)

The connection line between the patch antenna feed probe and the microstrip line is important to include in the design. The importance of the connection line lies in the fact that it is effectively a small piece of transmission line. This piece of line does not exhibit the required characteristic impedance of 50Ω and contributes to the phase and impedance transformation of the input impedance. Compensation for this component can be done by simply including the probe (as shown in Figure 5.5) in the network design from the start. The inclusion is very simple to do in IE3D, and results in the length and width of the phase transforming transmission line changing slightly from the initially predicted dimensions.

The reason for using two shorting vias (as opposed to one) in the inductor stub (Figure 5.5) is that the stub width is fairly large compared to the shorting via. The ideal case would be to have a shorting plane at the end of the stub.

For all the probe-fed antenna examples presented in this dissertation, an evaluation of the resonant section of the matching circuit is included. This was done in order to verify that it is possible to implement the parallel-LC circuit section with the proposed open and shorted stubs. Figure 5.6 presents the imaginary admittance response obtained with the parallel capacitor and inductor required for the 5 mm air gap patch antenna.

Figure 5.6 illustrates how one can closely obtain the ideal resonant response for the matching circuit with distributed components. The most important factor in the resonant design is the straight-line frequency response, since this is the essence of the SRMT. As described earlier in this section, it is good to consider the phase transforming transmission line alone at first. Also, as shown in Figure 5.6, it is good to get the resonance close to the correct level in terms of resonant frequency and imaginary admittance values. One must, however, keep in mind that the most important result is the final return loss for the antenna integrated with the feed network. Therefore it is important to get the individual components close to the correct values, as in Figure 5.6. Once the individual components are satisfactory it is more important to combine the system and tweak the components for optimum overall results. A guideline for satisfactory results for the resonant section is that the centre frequency should be at least within 10% accurate, and the imaginary admittance values at the design frequency should also be within this margin. This guideline is applicable to the 5 mm air gap patch antenna, and will also work for wider bandwidth patch antennas. The second example of this chapter is an extremely narrow band patch antenna (1% bandwidth), and in that case much more care must be taken to obtain accurate results. More will be said about this in the next section.

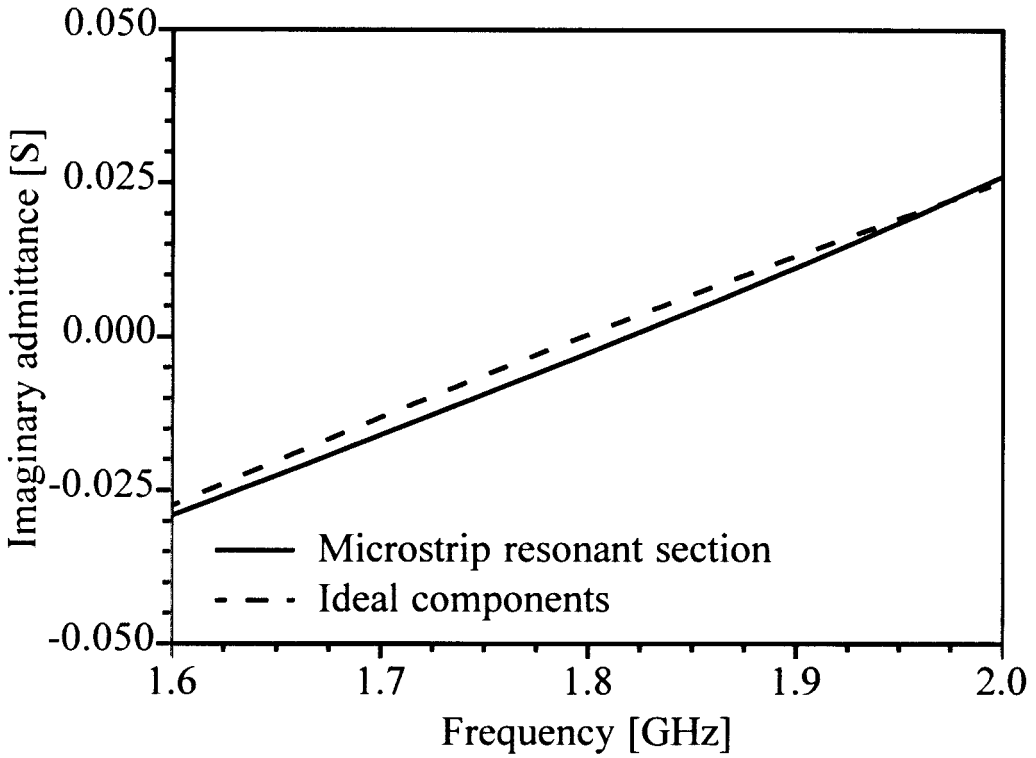

Figure 5.6 Comparison obtained in initial design between the theoretical parallel-LC section, and the implemented open- and short-circuited stubs. Both are for the 5 mm air gap patch antenna

The simulated results for the patch antenna with and without the matching circuit are shown in Figure 5.7. The response shown is for the final simulated circuit, in other words no additional tweaking is required for this circuit anymore. The design VSWR specification is 1.5:1. In Figure 5.7 one can see that the aim is not to be too close to maximum return loss value, since manufacturing tolerances should be kept in mind.

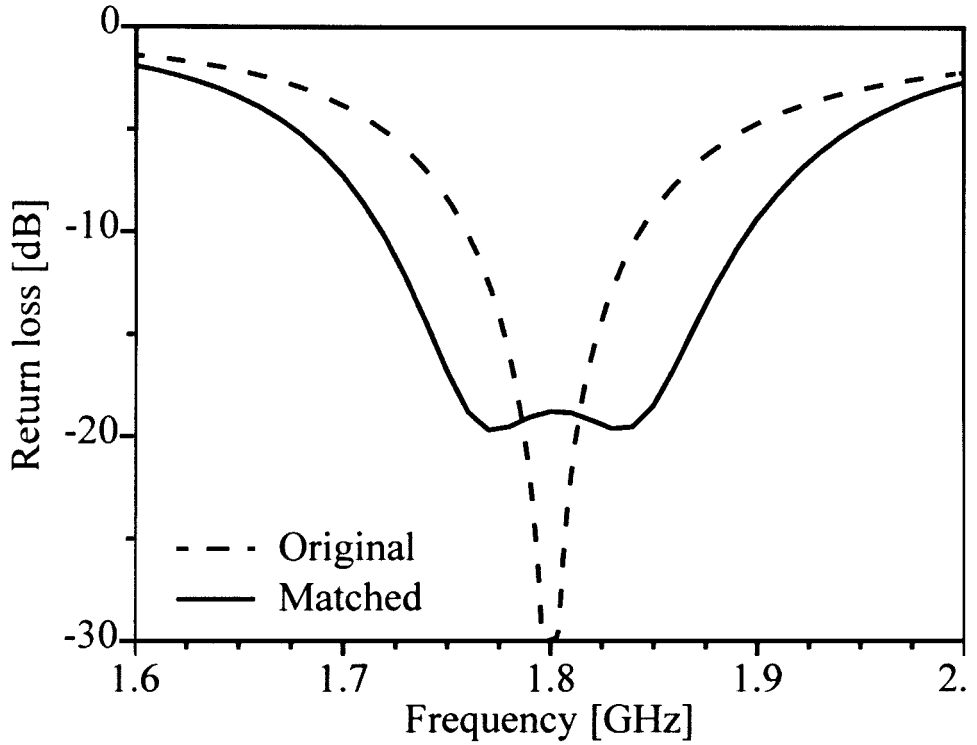

Figure 5.7 Simulated results for the patch antenna with the inclusion of the matching network for bandwidth improvement

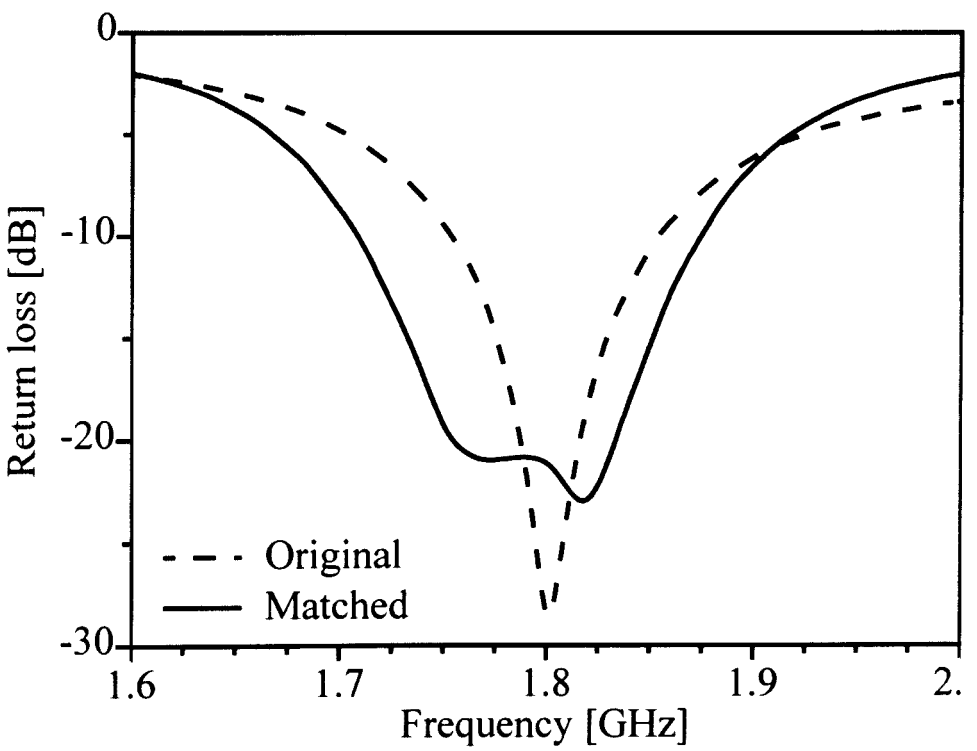

Figure 5.8 Measured results for the matching network when applied to the patch antenna example

The original simulated antenna in Figure 5.7 has a bandwidth of 50 MHz, between 1.78 and 1.83 GHz. The addition of the SRMT matching section resulted in an improved bandwidth of 130 MHz, from 1.74 GHz to 1.87 GHz.

Figure 5.8 shows the measured return loss for the antenna. The measured bandwidth of the antenna without the matching network was 59 MHz, from 1.773 to 1.832 GHz. This compares very well with the predicted values obtained by IE3D. The impedance matched antenna had a VSWR < 1.5:1 between 1.728 and 1.855 GHz, presenting a 127 MHz bandwidth, again corresponding very closely with the simulated result.

In the measured result a slight asymmetry can be observed in the return loss plot shown in Figure 5.8. This is due to a minor reactive component in the input impedance, most probably caused by assembly inaccuracies. On the Smith chart one would be able to notice that the "eye" is not perfectly placed around the centre of the chart, but moved slightly upward or downward. If this becomes a problem, it can be resolved by tweaking either the capacitor or the inductor used in the LC-match. The match itself increased the VSWR bandwidth from 59 MHz to 127 MHz. This is an increase of 68 MHz, or 115%. Table 5.1, included at the end of the chapter, summarises all the results presented in this chapter, expressing the results both in terms of frequency bandwidth and percentage improvement.

The impedance bandwidth of the patch antenna increased to more than double the original value. This is very promising, but in order to be able to characterise the improved patch antenna, the radiation patterns are also considered. The patterns are calculated using IE3D and compared to the patterns measured for the patch antenna with and without the matching circuit. The normalised E-plane patterns for 1.8 GHz are presented in Figure 5.9. The H-plane co-pol patterns are shown in Figure 5.10 and the cross-pol patterns in Figure 5.11, both at 1.8 GHz.

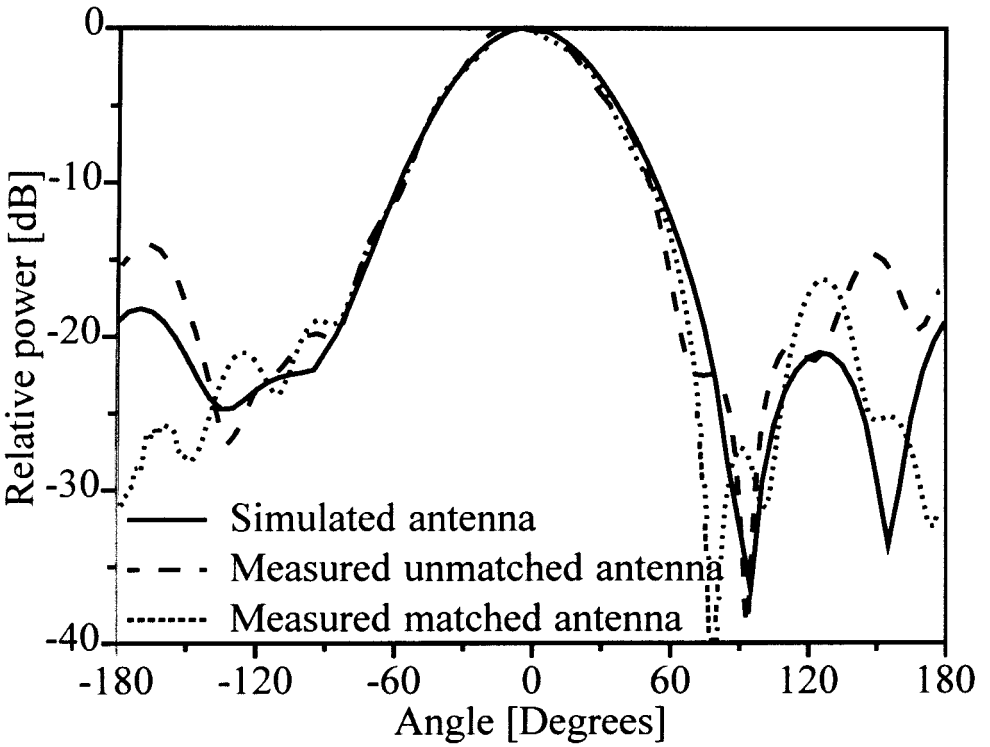

Figure 5.9 E-plane radiation patterns (1.8 GHz) of the patch antenna, comparing the results obtained for the simulated patch against the two measured unmatched and matched antennas. The simulated antenna is considered without a feed network, only a finite ground plane

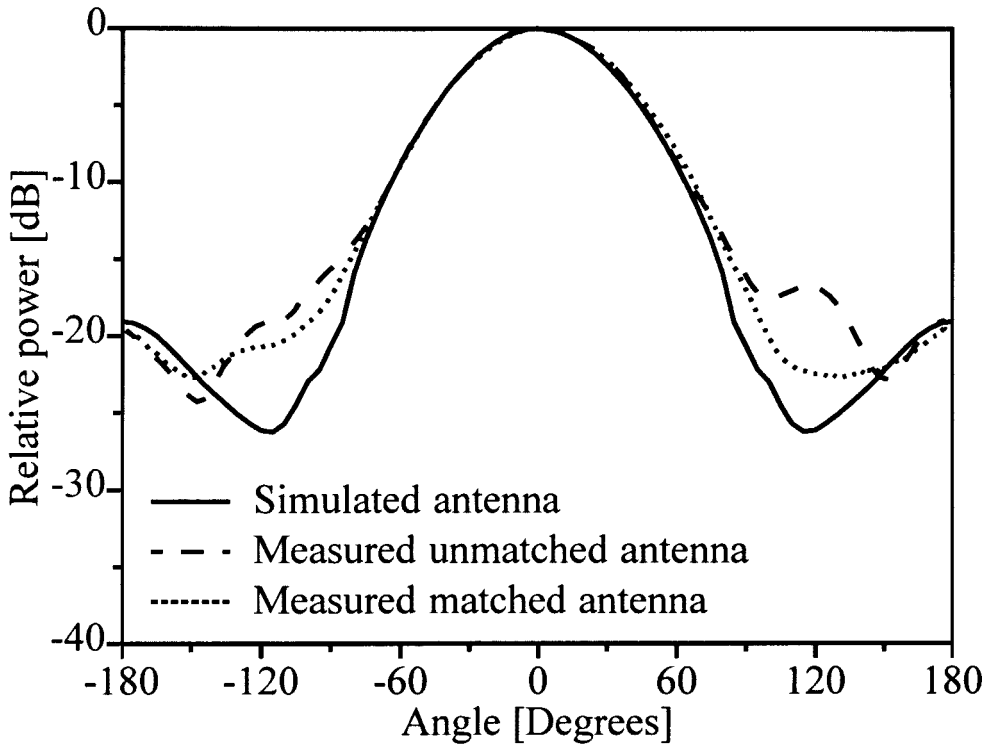

Figure 5.10 H-plane co-pol radiation pattern for the different types of antennas at 1.8 GHz

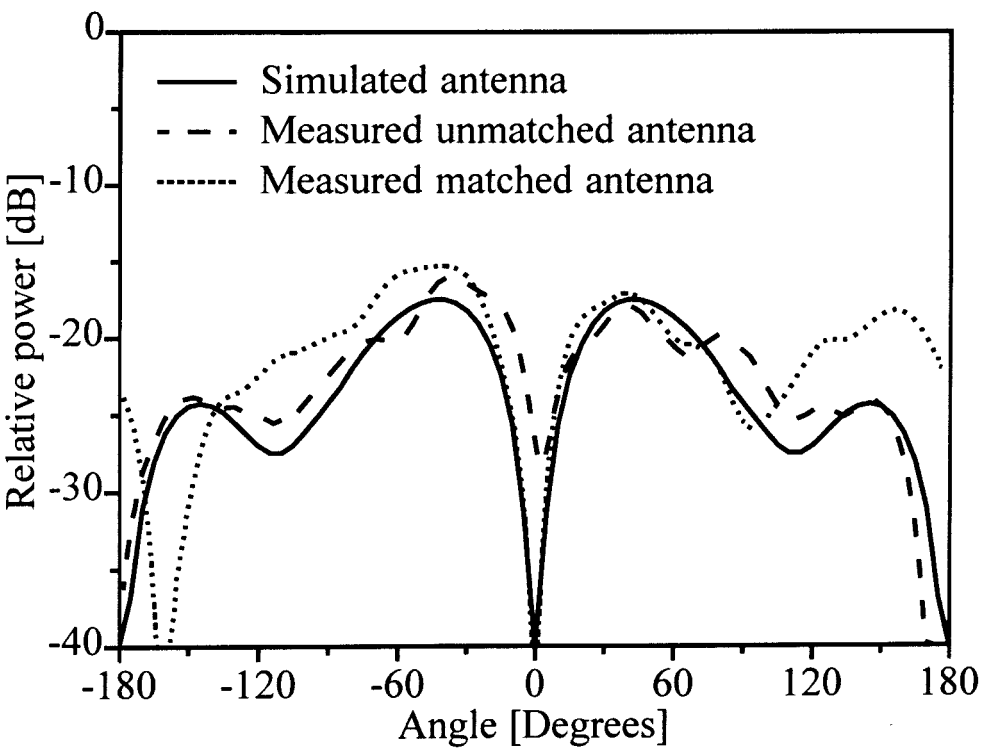

Figure 5.11 H-plane cross-pol radiation pattern for the three antennas considered, all at 1.8 GHz

It is evident that the radiation pattern obtained using the simulation software is, as was the case for the return loss results, very close to the measured results. In all three figures one can clearly see that the difference obtained is very small, and most often the main differences are encountered at levels of 15 dB or more down from the peak value. The possibility that unwanted radiation is encountered as a result of the addition of the open- and shorted stub is unlikely, and Figure 5.9 to Figure 5.11 shows this clearly. The only real noticeable deviation is visible in the H-plane cross-pol pattern, although the levels still remain nominally below –15 dB. The main lobe remains virtually unchanged when compared in the three antennas. This proves that the uncertainty in respect of the differences in the back lobe regions might be part of the feed network, as well as radiation obtained from the edges of the ground plane and construction errors.

Patch antennas in general have a relatively wide radiation pattern bandwidth [3]. The bandwidth operation is most often limited by the specified return loss bandwidth. In order to evaluate the radiation pattern as a function of frequency for the matched patch antenna, three radiation pattern graphs are presented in Figures 5.12 to 5.14. Only the graphs of the measured SRMT-matched antenna are included. Three different frequencies are shown, namely 1.74, 1.8 and 1.86 GHz.

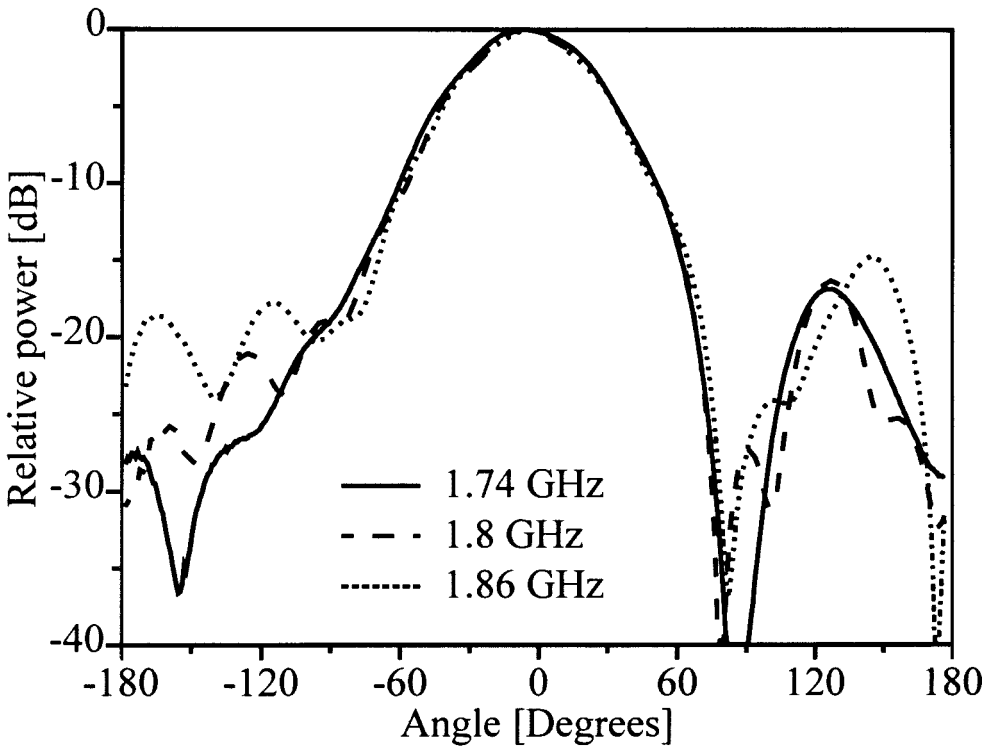

Figure 5.12 Measured E-plane radiation pattern of the SRMT-matched patch antenna at three operating frequencies

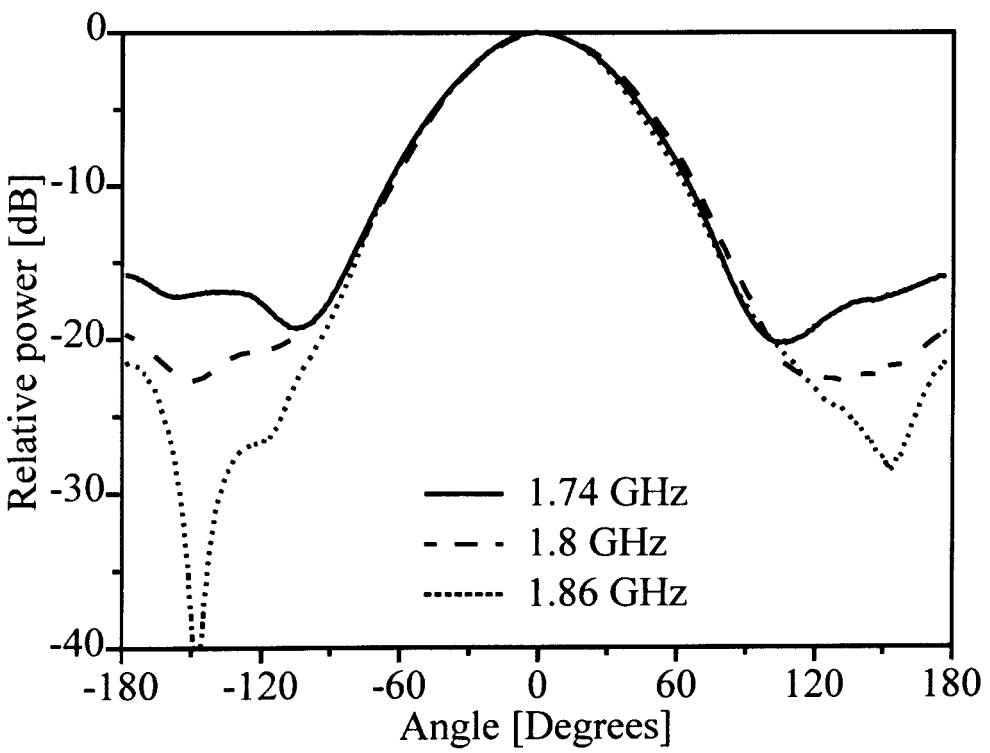

Figure 5.13 Measured H-plane co-pol radiation pattern of the patch antenna

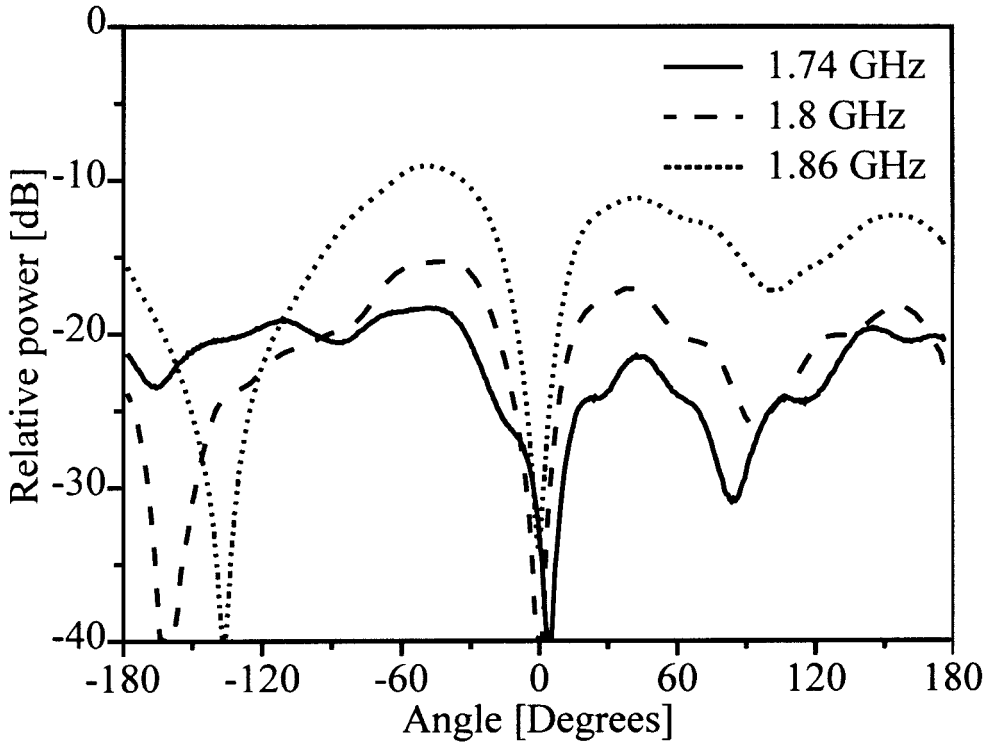

Figure 5.14 Measured H-plane cross-pol radiation pattern of the antenna

The main beam co-pol patterns for the different frequencies in both the E- and H-plane are relatively constant over the frequency range considered. In both Figures 5.12 and 5.13 the beam remains the same for the range ±90°, with minor differences visible at the edges very close to 90°. The variation that is visible in the E-plane pattern shown in Figure 5.12 in the vicinity of –90°, is the location where the connector was placed. Therefore the slight variation in pattern may be attributed to scattering from the connector interface, as well as the cable position during the measurement setup. The measured H-plane cross-polarisation measured for the patch antenna seems somewhat untidy. Some of the problems encountered can be attributed to construction errors and scattering from the finite ground plane edges as well as the connector and feed cable. Despite all this, the H-plane cross-polarisation has the standard shape that is associated with it, namely a null in the 0° direction, as well as maximum levels in the region of ±45° to ±60°. Also clear is the fact that the maximum value increases as the frequency increases. To correlate this with theory, the simulated cross-polarisation patterns are shown in Figure 5.15.

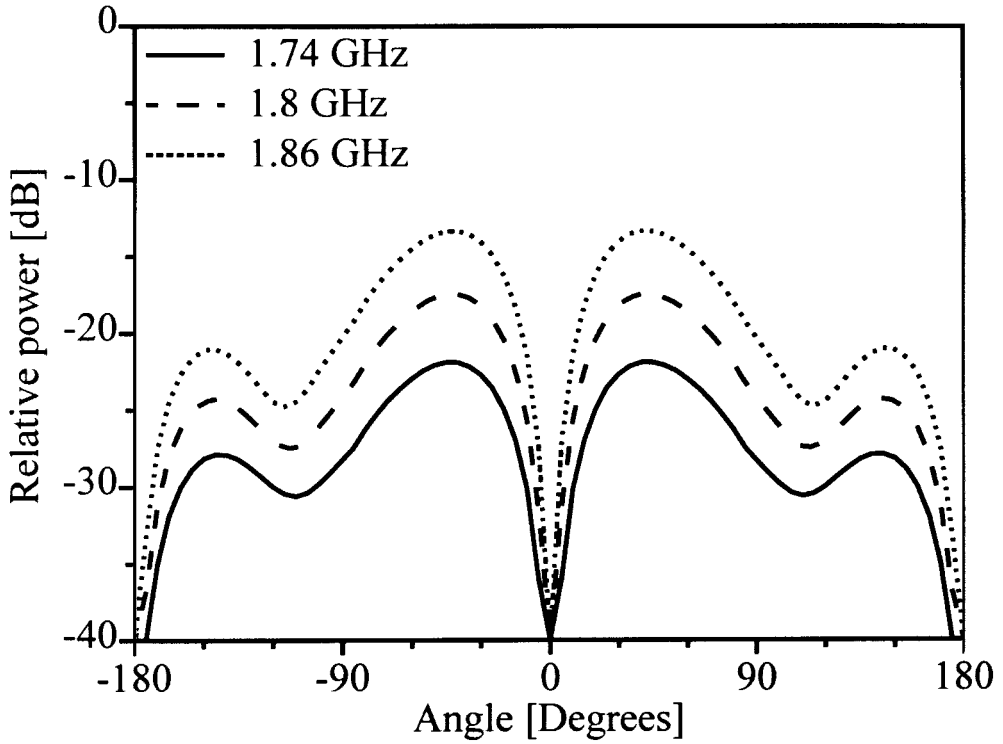

Figure 5.15 Simulated H-plane cross-polarisation with a finite ground plane

Despite the slight asymmetry of the radiation patterns in Figure 5.14, the resemblance between the simulated data in Figure 5.15 and the measured data is still visible and quite acceptable. The overall results prove that the addition of the matching network had a negligible effect on the radiation properties of the patch antenna.

Figure 5.16 presents the measured gain for the unmatched and matched patch antennas. The gain was measured between 1.7 and 1.9 GHz since this was mainly the frequency range of interest. According to the IEEE Standards (Page 59 in [36]): "gain does not include losses arising from impedance mismatches and polarisation mismatches". Therefore the term 'gain' used in this dissertation should strictly be considered measured gain with reference to the standard gain antenna (the measured gain presented here does include mismatch losses) and not the IEEE Standards definition of gain.

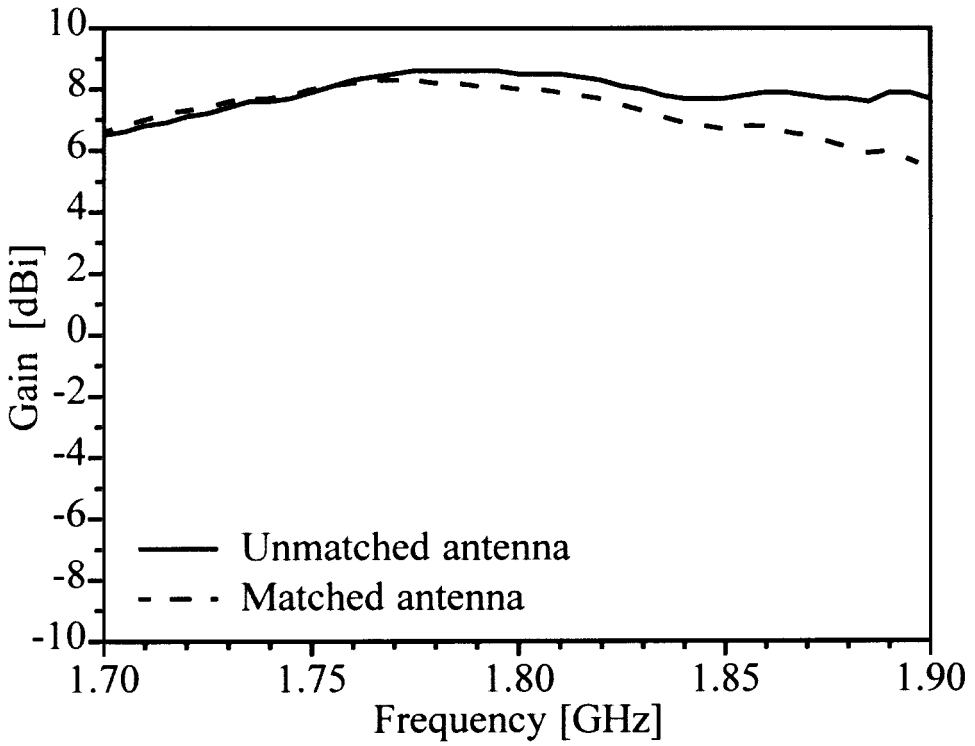

Figure 5.16 Measured gain response for the 5 mm air substrate antenna

An important note on this result is the fact that is seems as if the gain drops slightly for the antenna to which the SRMT-circuit was added. The maximum gain value measured for the patch without the SRMT-circuit is 8.6 dBi, and for the antenna with the LC-section added a maximum gain of 8.3 dBi was measured. The main difference is the fact that the gain peak for the matched antenna is at a lower frequency than the patch antenna without the SRMT circuit. In Figure 5.8 the slight frequency shift between the matched and unmatched antenna is illustrated. It is reasoned that this is mainly due to the additional losses added by the SRMT-circuit, and to a lesser extend the fact that the resonance of the actual load (the patch antenna) and the resonance of the LC-circuit are slightly displaced in frequency from one another. The combined resonance results in a final intermediate resonance with slightly compromised gain.

5.2 Example 2: Narrow band patch antenna

The outline of the second example patch antenna built is shown in Figure 5.17. The antenna is made with dielectric substrate only, and no air gaps are included. It is referred to as the "substrate-only" patch antenna. The dielectric substrate used for both the patch antenna and the feed network is GML-1000 [38].

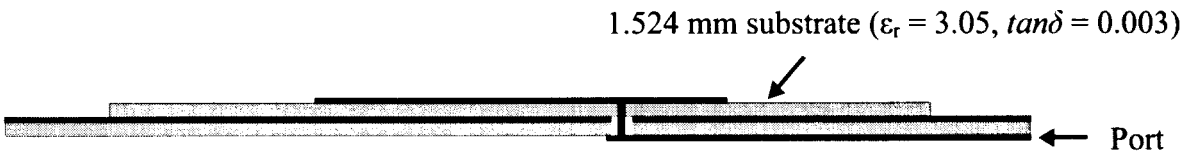

Figure 5.17 Outline of the "substrate-only" patch antenna

The design parameters for the patch antenna to have a minimum return loss at a centre frequency of 1.8 GHz are as follows (all dimensions in millimeters): d = 14.15, W = 60 and L = 46.3. The patch was designed and simulated in IE3D, after which it was built as shown in Figure 5.17. The simulated and measured results are shown in Figure 5.18.

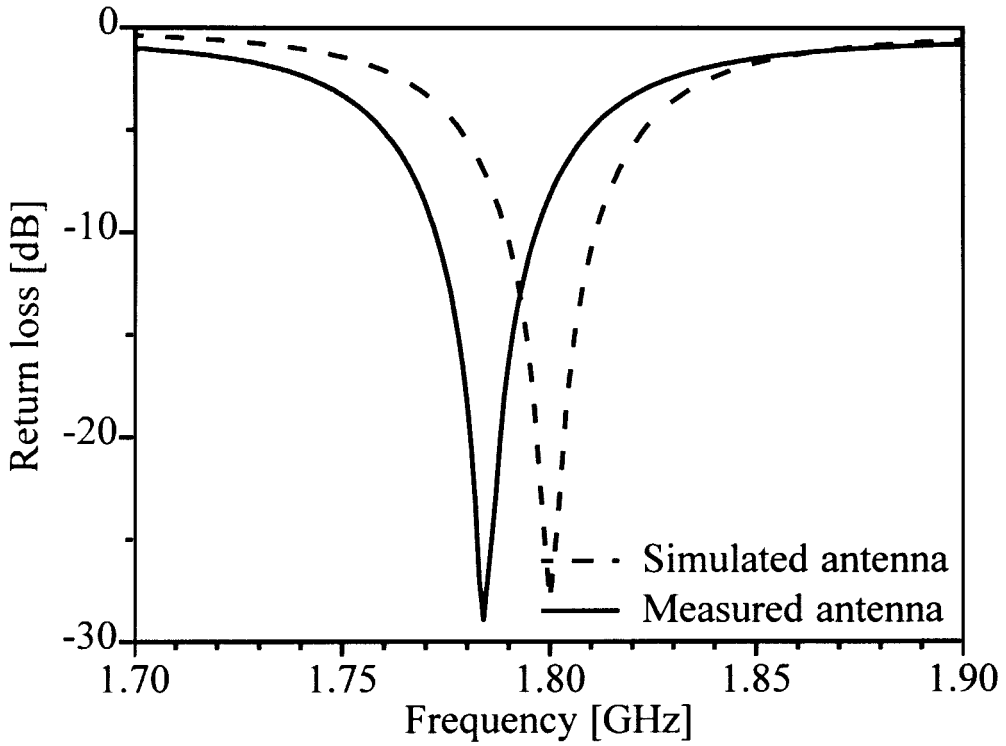

Figure 5.18 Measured and simulated return loss of the "substrate-only" patch antenna

In Figure 5.18 a frequency shift between the simulated prediction and the actual patch antenna is evident. The frequency shift obtained is 1%, and the VSWR bandwidth (1.5:1) of the patch antenna is also in the order of 1%. The "substrate-only" patch antenna is extremely sensitive to any type of variation in either the construction or the properties of the dielectric substrate. Although this 1% deviation might pose a problem in practice, the aim with this patch antenna is to prove an experiment and not so much to design a nearly perfect antenna. Therefore it was decided to keep the patch antenna as it is, and rather design a matching network that will work for the patch antenna example considered. The resonant frequency of the patch antenna is now 1.785 GHz. The design of the patch antenna's matching network was based on the measured data. In illustration, the theoretical predictions are included for the original simulation, and the full wave simulation as well as the measured matching results for the physical patch antenna.

The simulated "substrate-only" patch antenna, with and without the theoretical matching network, is presented in Figure 5.19. The matched specification is considered for a VSWR < 1.5:1. The original (unmatched) antenna has a bandwidth of 14 MHz (1.793 – 1.807 MHz), and the inclusion of the theoretical matching network improved the bandwidth to 33 MHz (1.784 – 1.817 MHz).

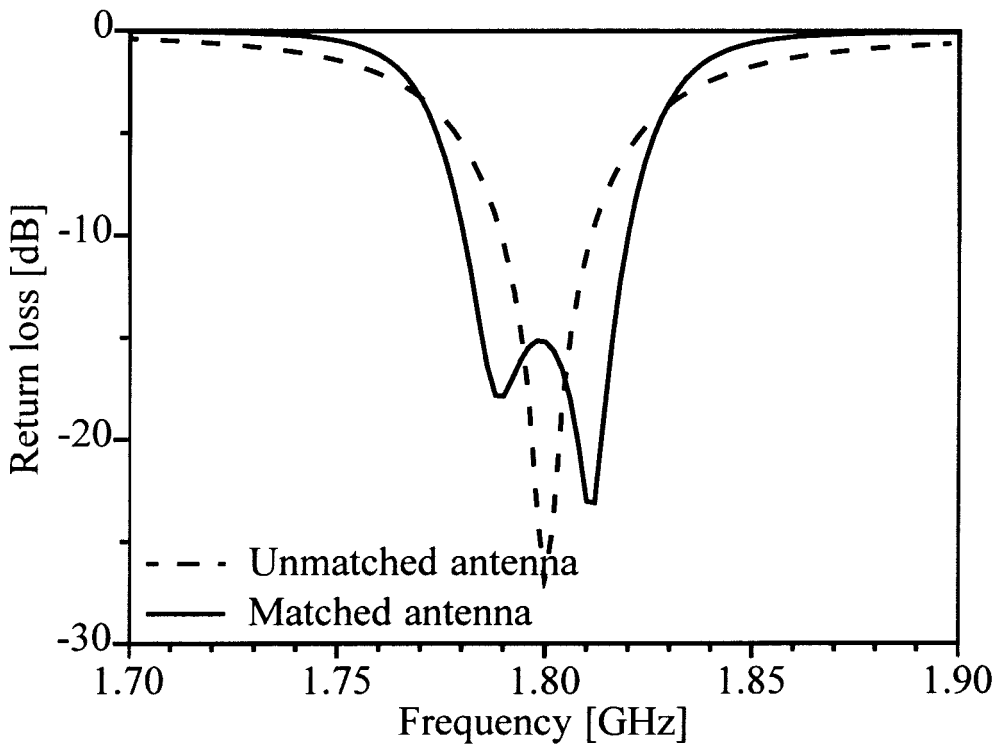

Figure 5.19 Theoretical bandwidth improvement of the "substrate-only" patch antenna

The measured antenna's input impedance has been used for the design of the actual matching network. Despite the slight frequency shift of 1% the component values are very close to those obtained for the theoretical design. The phase-transforming transmission line is 77.5° and the quarterwave matching line impedance 58 Ω. The capacitor used in the matching circuit is 27.807 pF and the inductor 0.286 nH.

In the previous section it was stated that the admittance response can be considered satisfactory in the initial design once the centre frequency and the admittance levels are within a 10% margin. For the "substrate-only" patch antenna this is not good enough. It

was found the final result must be extremely close to the required levels. For the theoretical values of the capacitor and the inductor, variation on the third decimal made a difference to the final result. For the microstrip simulation done in IE3D and Sonnet Lite a change in stub length in the order of 0.05 mm resulted in considerable variation in the final return loss. With this in mind, it must also be said that the measurement results presented in this section required a lot of patience to find the exact length of the stubs.

Figure 5.20 presents the final simulated resonant admittance curve for the above-mentioned LC-section as well as the microstrip resonant section for the "substrate-only" patch antenna example.

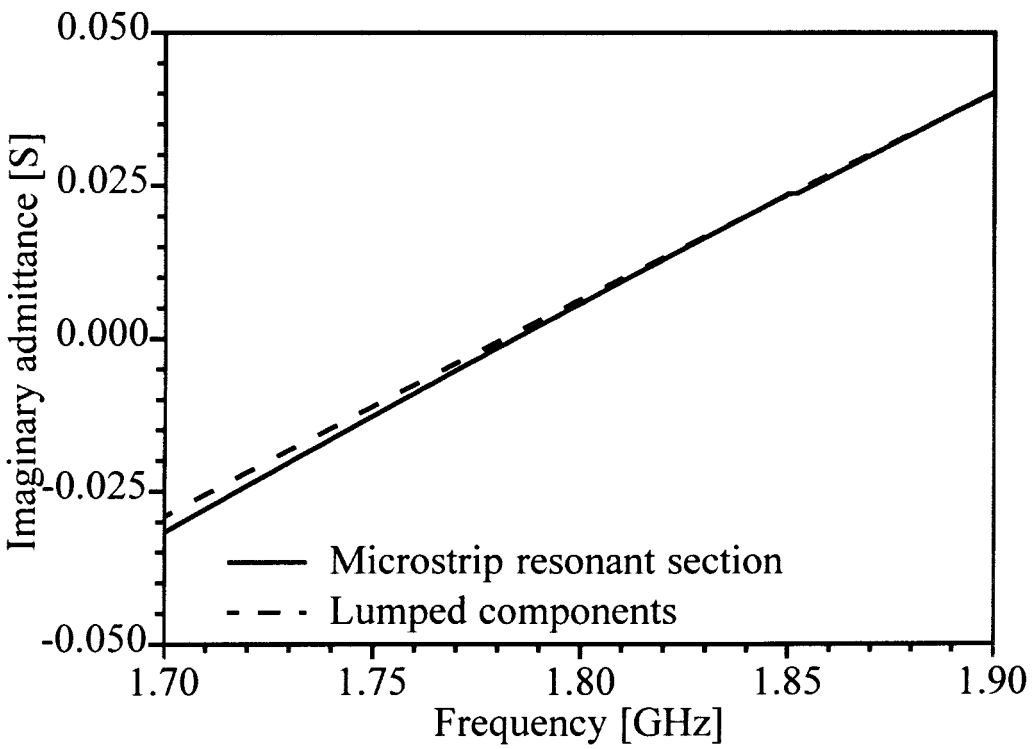

Figure 5.20 Theoretical and microstrip equivalent admittance response for the parallel-LC combination required for the "substrate-only" patch antenna

Figure 5.20 illustrates how the open- and shorted stubs implemented as equivalent circuit elements can result in very accurate circuit components. One phenomenon that is not evident from Figure 5.20, but was observed during the study, is that there is always a remarkable improvement between the theoretical predictions made and the final full wave

simulation and measurement. Figure 5.20 illustrates that this is probably not due to the difference in admittance response between an ideal LC-circuit and the stubs, but rather to the interfaces between the stubs and the various transmission lines.

Figure 5.21 presents the results obtained with IE3D for the matching network applied to the measured patch antenna. This was done because the measured antenna had a slight frequency shift, and by taking this frequency shift into account one will achieve a more reliable design.

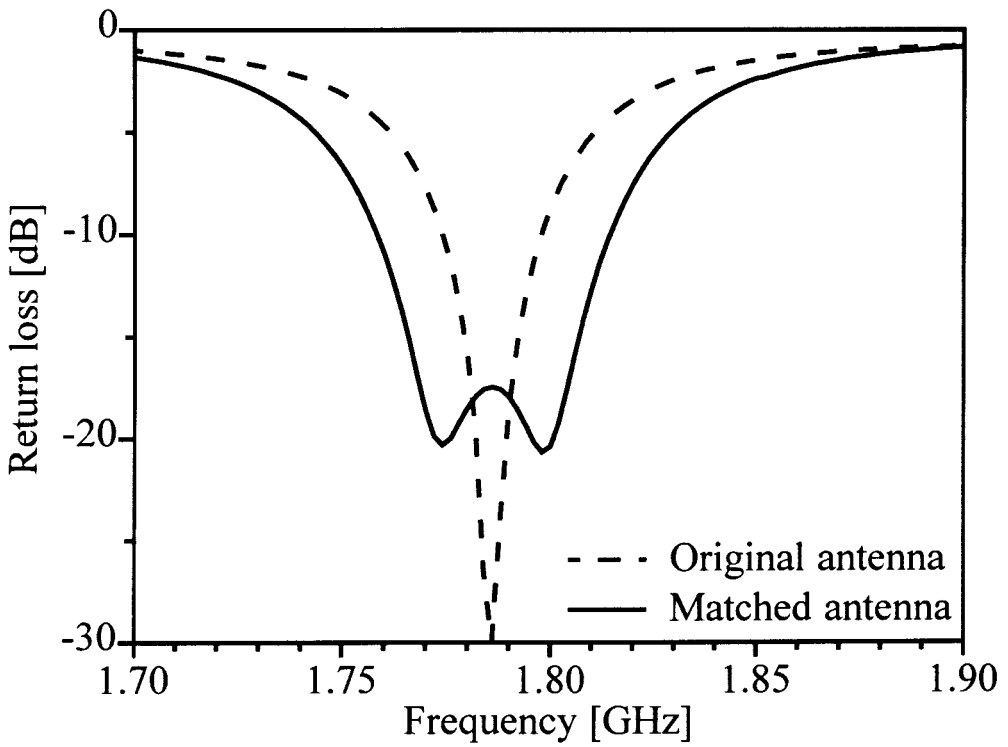

Figure 5.21 Simulated matched response, with the return loss of the measured antenna included, and also used as load for the simulation of the circuit

The simulated results for the matching network predicts a –14 dB bandwidth of 43 MHz (1.765 GHz – 1.808 GHz). The original antenna bandwidth is 15 MHz. This results in an improvement close to three times the original bandwidth.

Figure 5.22 presents the measured return loss for the matching network. The original antenna considered in this figure is the same one as in Figure 5.21.

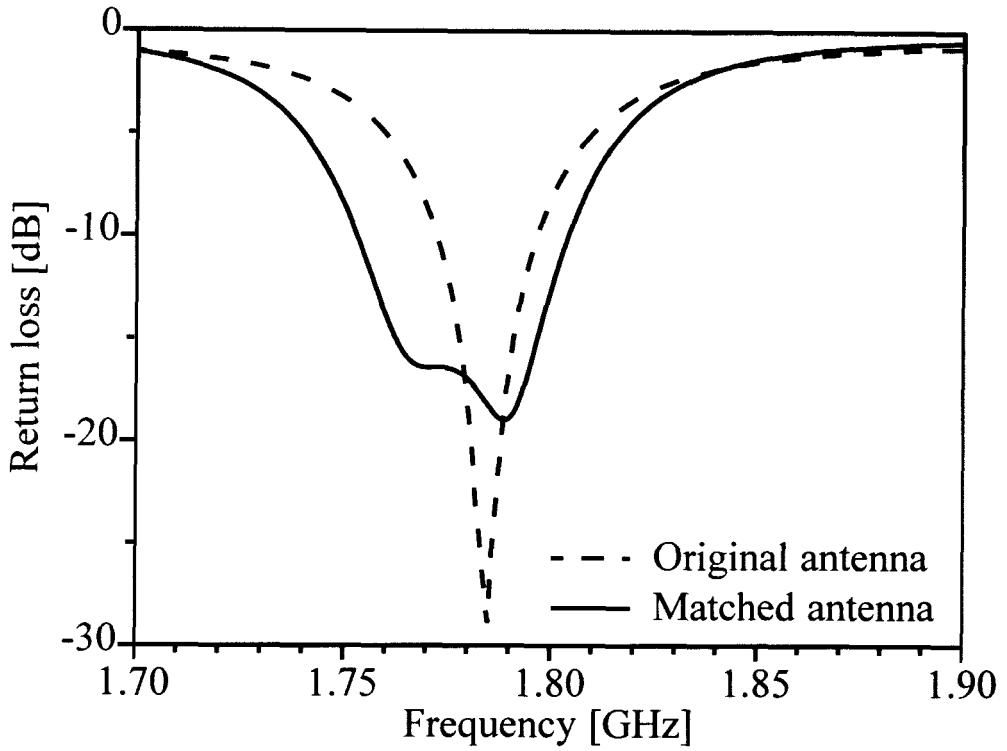

Figure 5.22 Measured bandwidth improvement of the "substrate-only" patch antenna

The measured improvement with the inclusion of the SRMT matching network is 37 MHz (1.761 – 1.798 GHz). The improvement is slightly less than the predicted improvement, but the factor is still much more than double the original return loss bandwidth. A slight asymmetry can be observed in the return loss result, similar to the measured result presented in Figure 5.8. This is once again probably caused by construction errors, as well as possible inaccuracies encountered by the simulation software. Although this might be the case, the results are still acceptable since a remarkable improvement in bandwidth is observed.

The gain of the patch antenna for unmatched and matched case is presented in Figure 5.23. The gain curve presented in Figure 5.23 differs from the gain presented in Figure 5.16. The main difference is in the fact that the "substrate-only" antenna is much narrower in its operating bandwidth, and the frequency range considered is thus much wider in comparison to the antenna bandwidth.

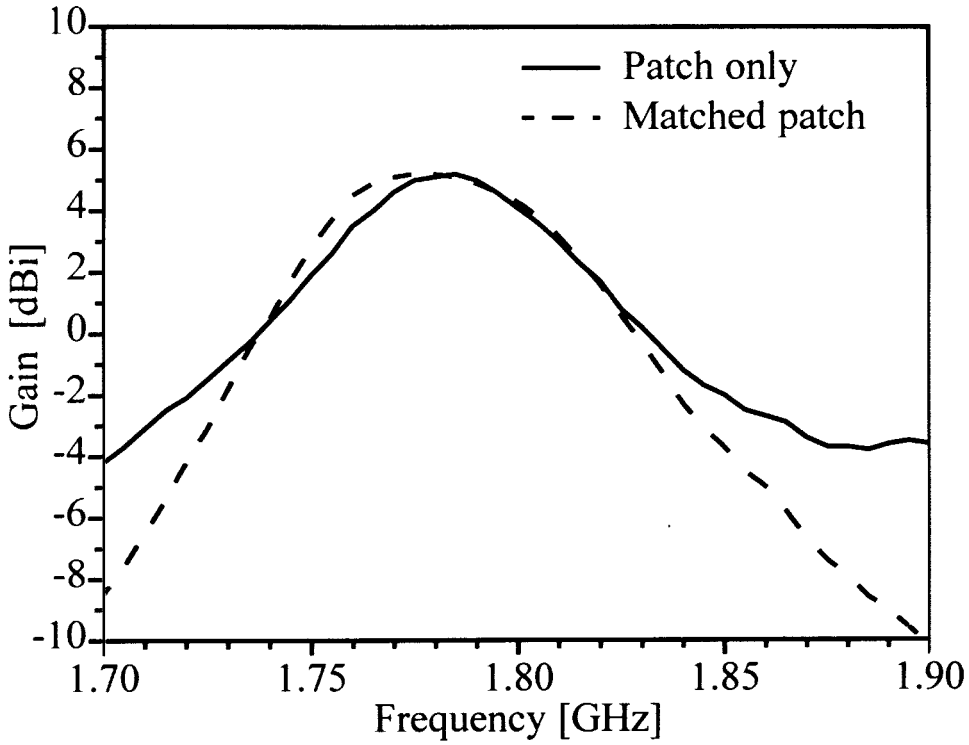

Figure 5.23 Measured gain for the "substrate-only" patch antenna

With the data shown in Figure 5.23 a number of important observations can be made, which is not evident in Figure 5.16. Note that a slight frequency shift similar to the shift obtained between the matched and unmatched antenna in Figure 5.19 is evident in the gain response. The centre frequency of the matched antenna is slightly lower than that of the unmatched antenna. The addition of the SRMT-circuit not only results in a wider return loss frequency range, but in Figure 5.23 one can see that the gain tends to remain close to the maximum value over a wider frequency range. If the frequency band is considered where the gain drops by 1 dB from the maximum, the unmatched patch antenna has a 35 MHz bandwidth around 1.785 GHz and the matched antenna 43 MHz with a centre frequency of 1.778 GHz. Both antennas have a maximum gain of 5.2 dBi. The out-of-band gain is lower when the SRMT-circuit is added. This is generally not a problem, since the antenna is not supposed to be operating at these frequencies.

5.3 Example 3: 10 mm air patch antenna

The SRMT was also applied to a patch antenna that is in itself already wideband. It is important to note that the usage of wideband in this dissertation is a relative term. When this antenna is called wideband, it is done so in comparison to the first two example patches. In itself, when compared to other wideband antennas, this example might prove rather narrowband. A patch antenna with the feed technique proposed by Mayhew-Ridgers et al. in [5] was designed for a resonant frequency of 1.8 GHz with an air gap of 10 mm between the ground plane and the supporting patch antenna substrate. The design and layout are shown in Figure 5.24. The parameters for the patch are as follows (all dimensions in millimetres): $w = 5$, $l = 24.6$, $y = 5.2$, $W = 58.2$, $L = 64$. The patch as well as the matching transmission line is etched on MC3D [39]. Please take note that the parameters for the main radiating patch are not defined in the same way as for the previous two patches, see Figure 5.24. The dimensions for this patch antenna are considered with respect to the small coupling patch that is connected to the probe.

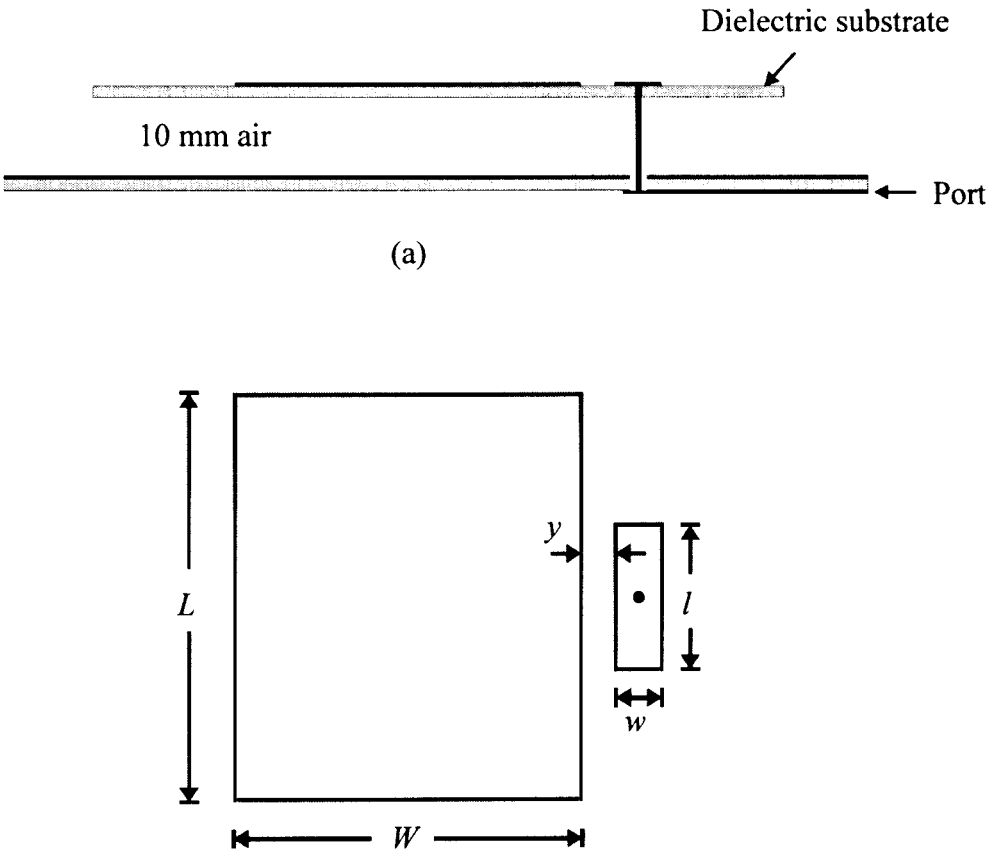

Figure 5.24 Design parameters for the capacitive-fed patch antenna with a 10 mm air gap. (a) presents the side view, and the top view with the inclusion of the parameters is given in (b)

The patch antenna was designed and simulated in IE3D. The capacitor required for the antenna is 1.77 pF and the inductor 4.4 nH. The admittance response for both the lumped components and the preliminary microstrip resonant section (i.e. before integration with the phase and impedance transforming transmission lines and the antenna itself) is shown in Figure 5.25. As was the case with both previous patch antenna examples, the resonant behaviour of the lumped LC-section can be obtained very accurately with the microstrip stubs.

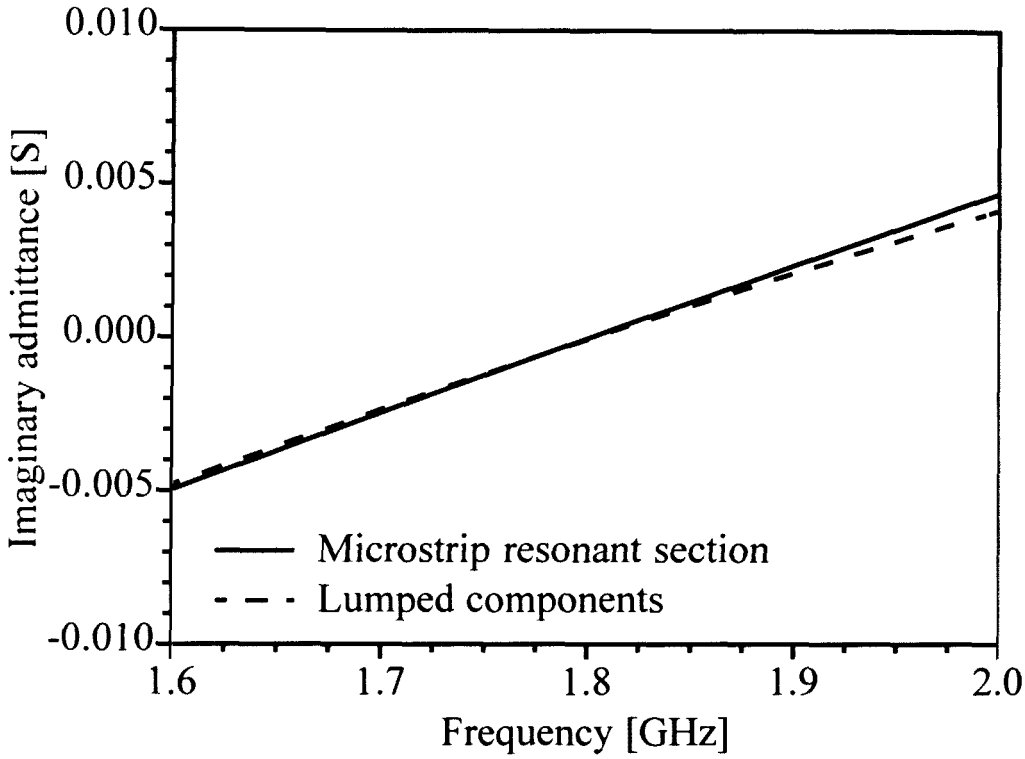

Figure 5.25 Resonant section design for the 10 mm air gap patch antenna example

The simulated return loss and the improvement with the addition of the matching circuit are shown in Figure 5.26. The original patch antenna has a VSWR < 1.5:1 frequency range between 1.723 and 1.879 GHz, presenting a 156 MHz band. The inclusion of the matching network increases the frequency band to 290 MHz (1.66 – 1.95 GHz). This is a very large frequency band, much larger than the previous two example patch antennas. The improvement obtained with the addition of the matching network is 86%, not exceeding more than double the original band. Figure 5.27 presents the measured results obtained for the antenna. A slight downward frequency shift is evident with the addition of the matching circuit. This is also evident in the previous two measured examples, implying that the occurrence might be attributed partly to the simulation software or the specific way all three the example patches were constructed. The original antenna has a VSWR < 1.5:1 bandwidth of 159 MHz, from 1.716 to 1.875 GHz. The addition of the matching network resulted in a new frequency bandwidth of 261 MHz between 1.656 and 1.917 GHz. The increase in bandwidth is 64%.

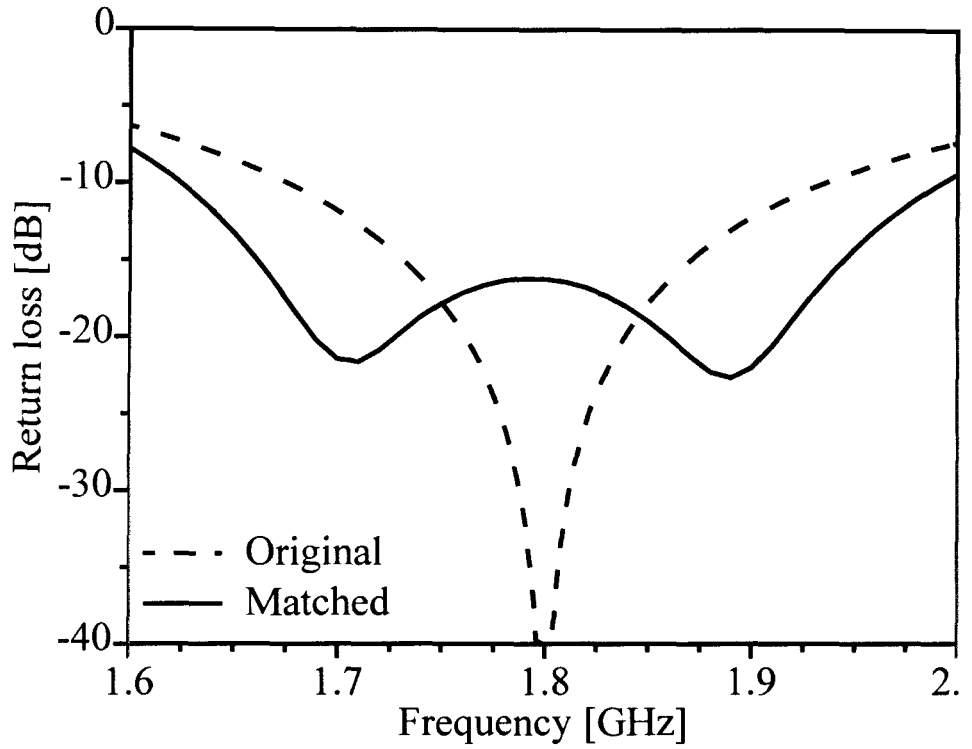

Figure 5.26 Simulated return loss for the 10 mm air patch antenna

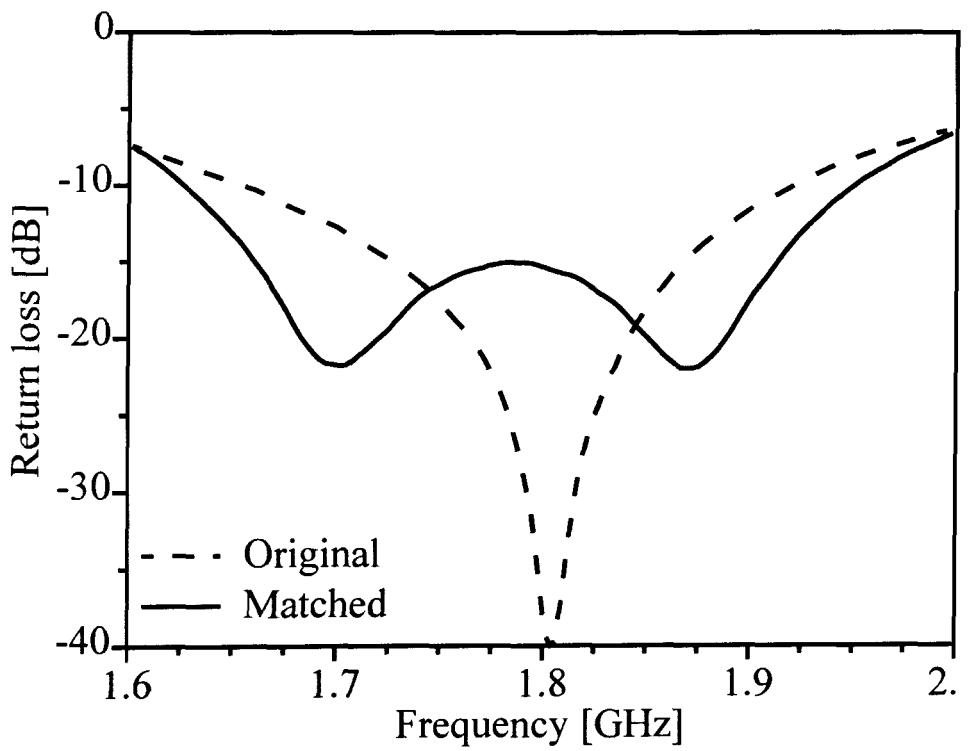

Figure 5.27 Measured return loss for the 10 mm air patch antenna

In the three examples presented in the last three sections, it was proven that the technique for impedance bandwidth improvement works very effectively. One conclusion that does, however, stand out is the fact that it seems as if the SRMT-circuit tends to work less effectively as the patches become more wideband. The percentage improvement obtained for the patches differs from the best improvement for the "substrate-only" patch (164%), to 80% for the 10 mm air patch antenna example. A possible explanation for this is shown in Figure 5.28. The phase transformed imaginary admittance of all three patch antennas is presented in Figure 5.28. The curves are all scaled relative to their VSWR 1.5:1 bandwidth.

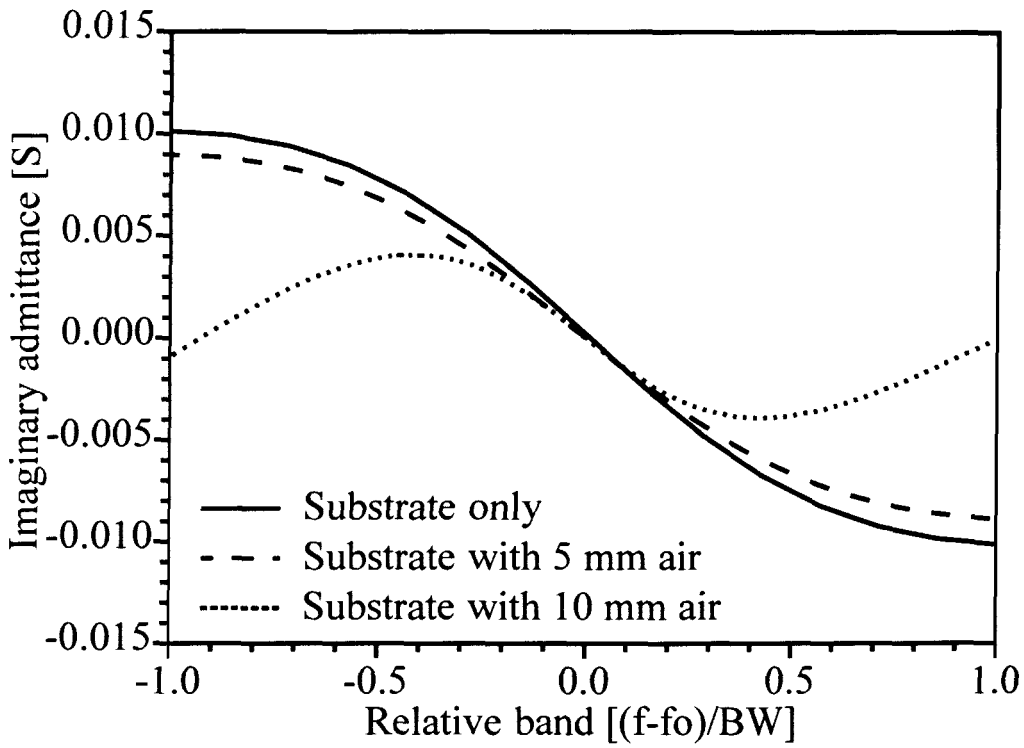

Figure 5.28 Bandwidth scaled version of the phase transformed imaginary admittance for the different patch antennas

In Figure 5.28 the maximum values of the imaginary admittance are of interest. The "substrate-only" patch antenna reaches a maximum value of ±0.01 S. The 5 mm air spaced patch antenna has a maximum of 0.009 S, and the 10 mm air substrate patch antenna only 0.004 S. The main purpose of the SRMT-matching network is to reduce the imaginary admittance for better antenna bandwidth. The "substrate-only" patch antenna has a relatively large reactive component in its input impedance very close to the resonant

frequency. Reducing the reactive component will then inevitably have a substantial effect on the overall performance. That is why the SRMT-circuit is very effective for this type of antenna. On the other hand, the 10 mm air patch antenna has a much-reduced reactive component in its input impedance. Therefore removing this reactive part will not yield the same improvement as in the case of the "substrate-only" patch antenna.

5.4 Coupled lines matching circuit performance compared to the SRMT

In Chapter 2 a matching circuit that implements a coupled line structure is shown [18]. This technique is similar to the coupled lines used for antenna arrays first discussed in [17]. The equivalent circuit of the quarterwave coupling section is a parallel LC-circuit in conjunction with a series transformer [21]. This resonant behaviour, which is present in both the quarterwave coupling structure and the SRMT, shows that the basic principles of both circuits are similar. In [18] it is illustrated how the VSWR bandwidth of an edge-fed patch antenna is increased by adding a quarterwave coupling line to the feed circuit whilst simultaneously feeding the patch antenna with another coupling section (Figure 2.8). The published result of the patch when fed normally and with the edge-fed coupled line is shown in Figure 5.29.

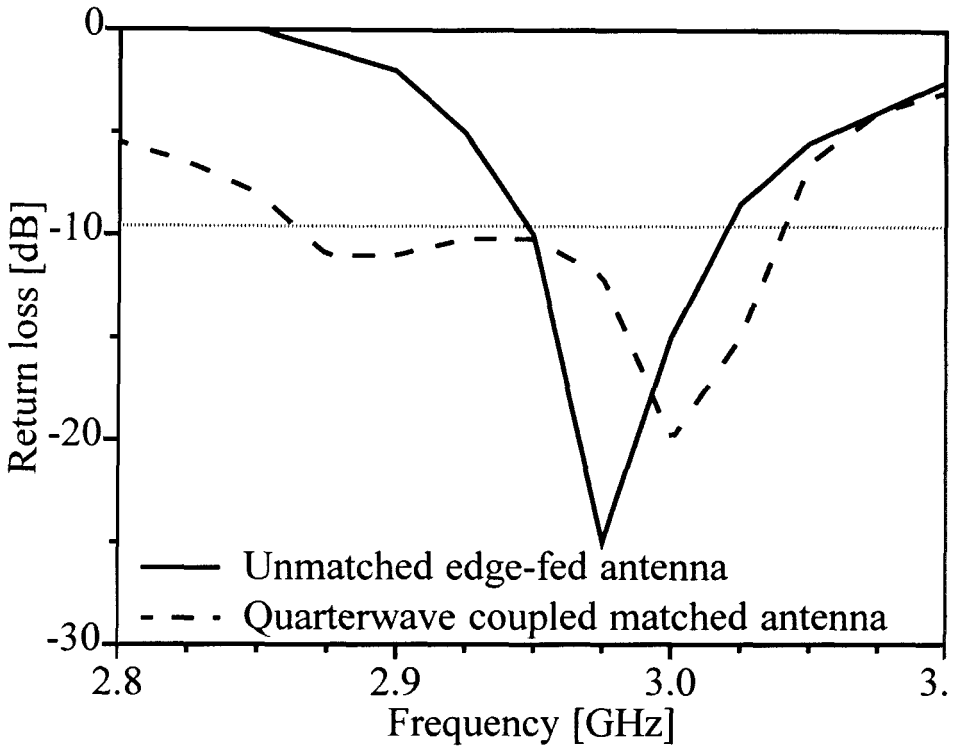

Figure 5.29 Return loss published in [18] for the edge-fed patch and the quaterwave coupled feed line implemented on the patch

The data shown in Figure 5.29 is taken from [18], but only discrete values every 25 MHz are reproduced. The data is not perfectly accurate, but the frequency range below a VSWR of 2:1 is still represented accurately in Figure 5.29. The design frequency of the patch antenna is 3 GHz, and the effective bandwidth obtained for the patch antenna is in the order of 65 MHz. The antenna with the quarterwave coupled lines included has a bandwidth of close to 150 MHz. Note that the values are all approximate since they are read from the published graph [18]. The co-pol radiation pattern of the two patch antennas, shown in [18], exhibits slight beam squint with the addition of the feed structure. Both in the E-plane and H-plane a squint in the order of 7° is obtained. No statements are made regarding possible cross-pol degradation.

The input impedance of the edge-fed patch antenna in the publication [18] is matched to 50 Ω with the addition of a quarterwave matching transmission line. This impedance transforming function is incorporated in the design of the quarterwave coupled line

sections. In Figure 2.8 it is evident that there are two quarterwave coupled sections in the feed network. One section couples to the patch antenna, while the second section couples to the feed line. The equivalent circuit mentioned in [18] is somewhat more complex than the SRMT circuit. To evaluate how the additional complexity affects the circuit's performance in comparison to the SRMT circuit, a similar patch antenna was designed and matched. The design frequency used is 3 GHz. The final antenna prototype obtained with IE3D is shown in Figure 5.30.

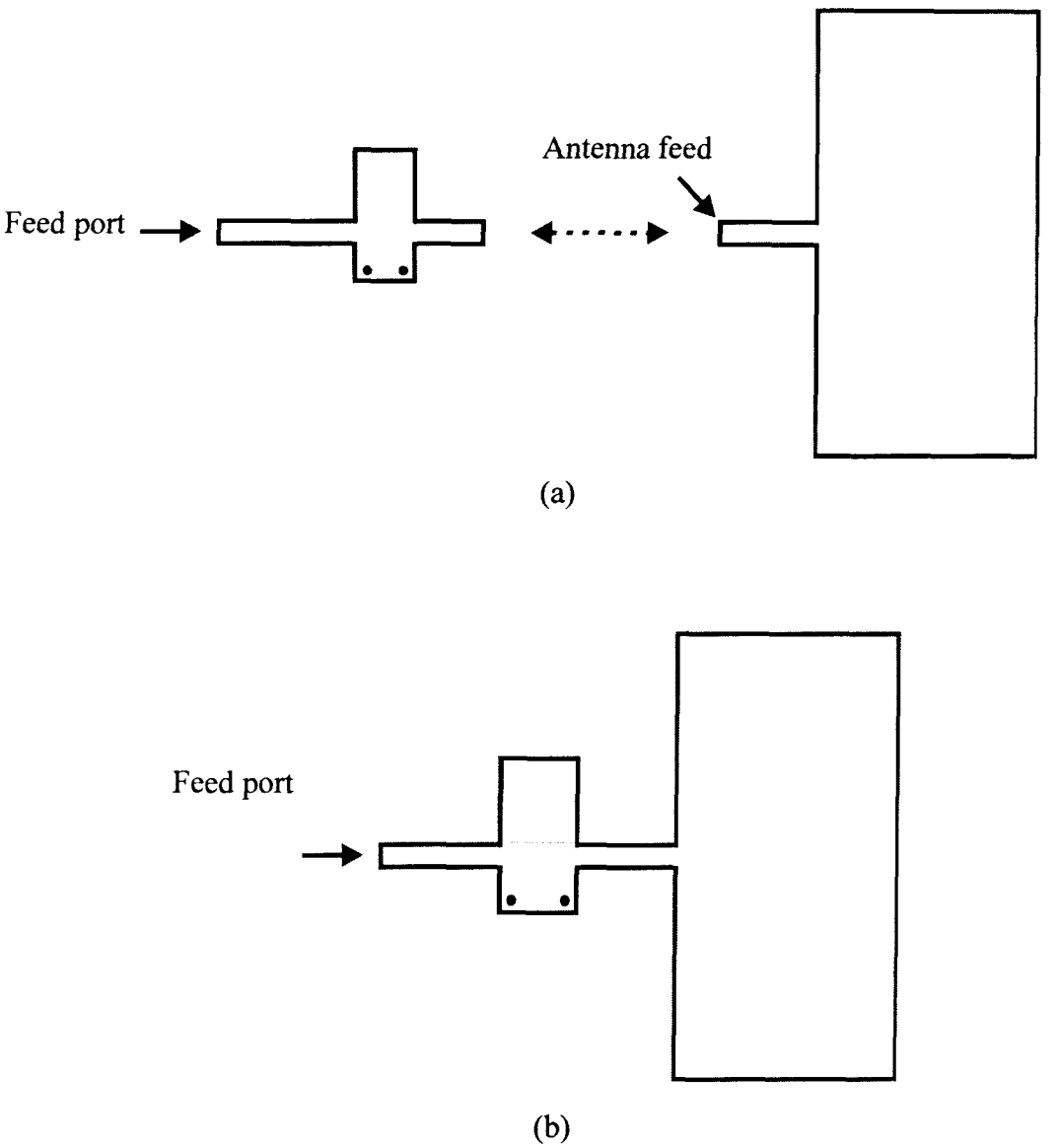

Figure 5.30 Edge-fed patch antenna with matching section. In (a) the matching designed was done separately while (b) has the matching section included as part of the design

Figure 5.30 shows two topologies for the matching of the patch antenna. In all the probe-fed patch antenna examples presented and discussed so far in this chapter, the feed section and the antenna could be separated during simulation because of the intervening ground plane. The edge-fed patch antenna was first designed in a similar fashion, as illustrated in Figure 5.30(a). The patch was considered on its own, and the S-parameters obtained from the simulation were then used for the design and optimising of the LC-resonant section. In principle this would lead to an answer that would show the validity of the matching circuit. It was, however, not the case. The fact that the SRMT-circuit is on the same side of the ground plane as the radiating patch antenna forced the researchers to have the antenna included in the simulation of the matching circuit. This setup is illustrated in Figure 5.30(b). The Smith chart illustration of the results obtained for the SRMT-match is shown in Figure 5.31.

The results for the designed matching circuits for both the separate theoretical design and the combined simulated circuit are presented in Figure 5.31.

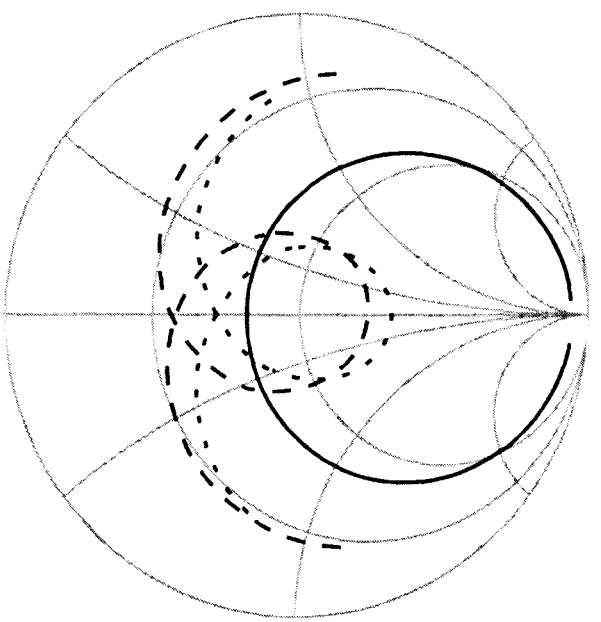

—— Phase transformed unmatched edge-fed

- - - Theoretical SRMT

– – Complete matched

Figure 5.31 Smith chart impedance curves for the edge-fed antenna, shown together with the theoretical circuit design and the combined simulation

The unmatched antenna shown in Figure 5.31 has a resonant frequency input impedance of 83 Ω. The impedance locus shown is already phase-transformed for the SRMT, in order for all the curves on the Smith chart not to lie on top of one another. The unmatched antenna is considered without a quarterwave matching transmission line, since this can be an integral part of the SRMT-design and the antenna already exhibits a VSWR 2:1 bandwidth (Figure 5.32). The first attempt at matching the antenna was made in theory with the raw edge-fed antenna input impedance data. The locus is shown with the dotted line in Figure 5.31 and 5.32. The circuit was created in IE3D for simulation, as shown in Figure 5.30(b). The best response obtained with additional tweaking is shown in Figures 5.31 and 5.32 with the dashed lines.

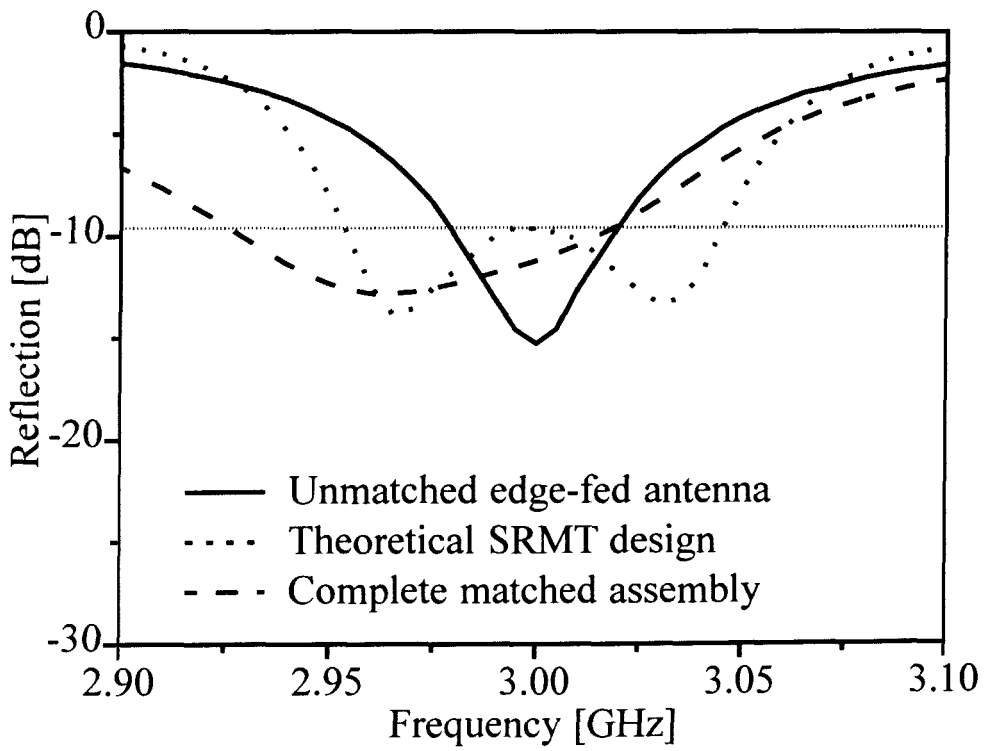

Figure 5.32 Return loss for the edge-fed patch antenna

The unmatched antenna has a VSWR < 2:1 bandwidth of 40 MHz, between 2.98 and 3.02 GHz. The bandwidth increased to 90 MHz with the addition of the theoretically calculated SRMT-match, and the complete simulation also reached a bandwidth of 90 MHz. Although the results for the theoretical design and the full-wave simulation are both 90 MHz, Figures 5.31 and 5.32 show a problem in the response curve. The problem

seemed to be substantial coupling between the patch antenna and the SRMT-circuit. The extra stubs close to the radiating element interfered with the antenna's input parameters and simultaneously the antenna induced currents on the open and shorted stub so that varying the width or length of the stub had little or no effect on the matching of the circuit. The stubs in turn introduced substantial unwanted radiation, as can be seen in the cross-polarisation levels presented in Figure 5.33 and 5.34.

The improvement results are, percentage-wise, very close to the results presented in [18]. The SRMT presented a bandwidth improvement of 125%, from 40 MHz to 90 MHz. The quarterwave match example in [18] improved the edge-fed patch antenna from 65 MHz to 150 MHz, an improvement of 131%. Despite the difficulties encountered in the software implementation of the edge-fed SRMT-match, the result for the circuit is only 6% less in improvement than the published structure. The published structure, on the other hand, is limited in terms of generality, since it is only an option for edge-fed patch antennas. These antennas can only be implemented where no air substrate is considered, thus already limiting the possible bandwidth of the antenna. Secondly the quarterwave-coupled structure has two resonators, since there are two coupled sections. The SRMT aims to match with only one resonant circuit. Space occupancy is also a problem for the quarterwave-coupled structure, as has been explained in [17]. In this section the difficulty in obtaining the resulting match is described, but in [18] only the final result is published. Therefore, it is unknown whether strong coupling between the patch and the matching coupled lines also influenced the results in [18], as was the case with this example.

The simulated radiation pattern of the matched and unmatched edge-fed patch antenna is shown in Figure 5.33 and Figure 5.34. In Figure 5.33 the E-plane pattern is shown. The simulation is presented with an infinite ground plane and no pattern is available from +90° to –90°. The E-plane without the matching circuit has no cross-polarised radiation component. The addition of the matching circuit introduced cross-polarised radiation reaching –20 dB, still acceptably low. The co-pol radiation pattern is changed slightly. The H-plane radiation pattern, presented in Figure 5.34, shows even less radiation distortion in co-pol. The cross-polarisation levels increase from about –34 dB to close to –19 dB. Note that no statements are made regarding cross-polarisation in [18]. In [18] a beam squint is

obtained with the addition of the quarterwave coupled lines. The addition of the SRMT-circuit did not change the co-pol radiation beam squint, and the cross-pol radiation pattern is changed slightly, but the levels still remain well below the co-pol maximum values.

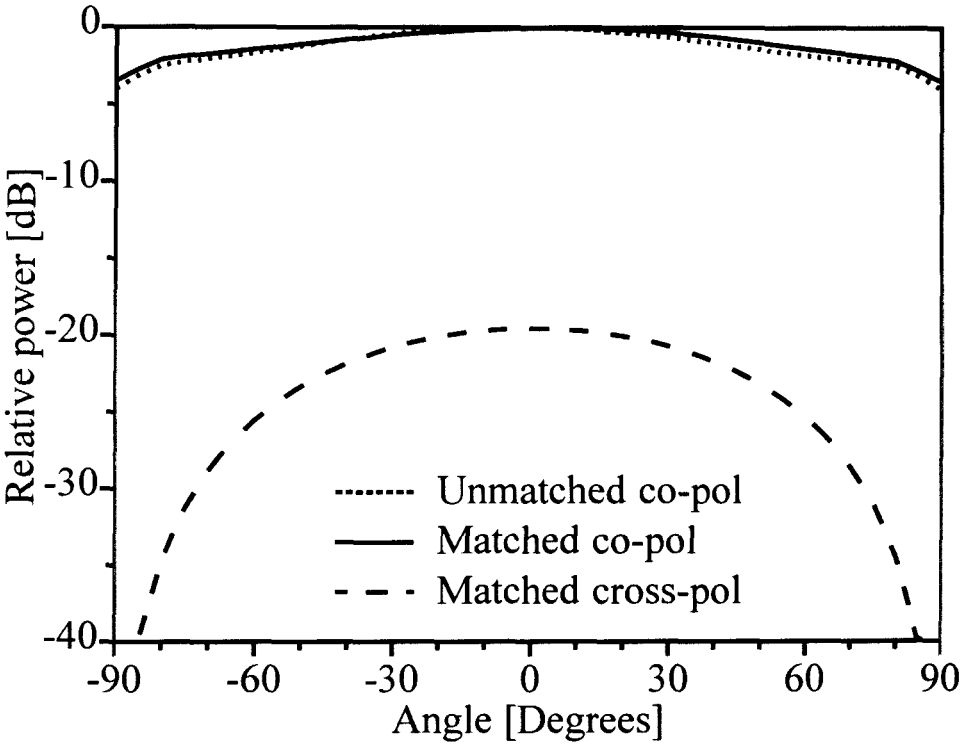

Figure 5.33 E-plane radiation pattern of the edge-fed patch antenna

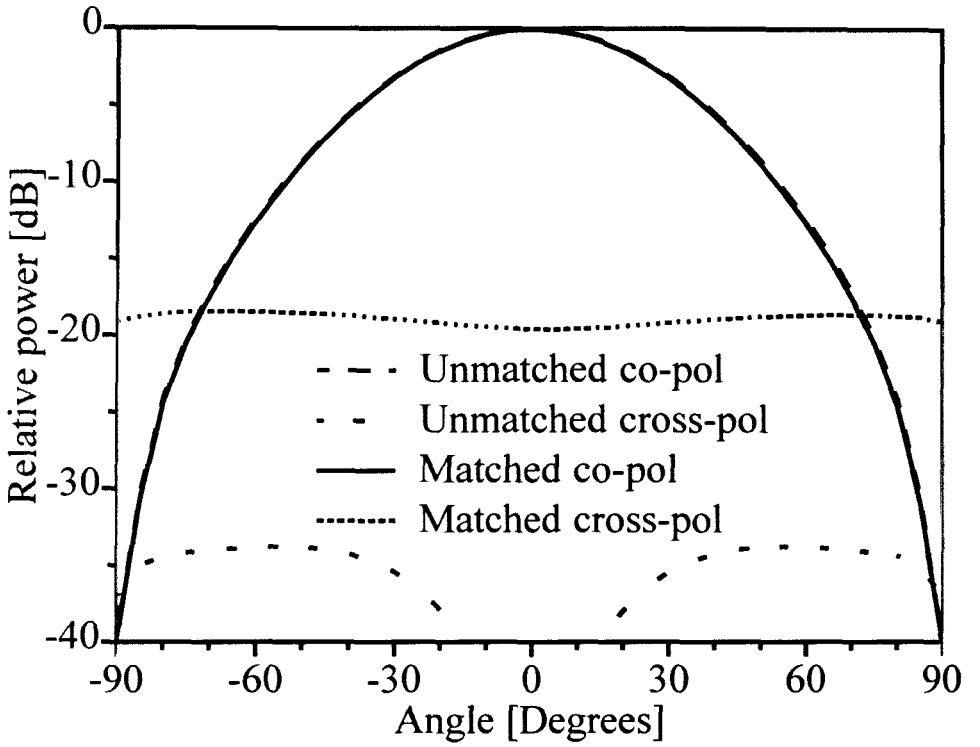

Figure 5.34 H-plane radiation pattern of the edge-fed patch antenna

5.5 Summary of bandwidth enhancement results

In the previous few sections a number of examples were given where the SRMT was implemented on different patch antennas. The results are summarised in Table 5.1. Explanations for the variations were discussed in Section 5.3. Only the edge-fed patch antenna is not verified experimentally, but the main aim with this antenna was to compare the matching circuit in a different setup. It is shown in principle that the SRMT can also work with other types of patch antennas than the probe-fed version.

Table 5.1 Bandwidth operation of the matching network with the patch antenna, expressed in percentage bandwidth and percentage improvement

Antenna	VSWR	Own simulated results			Measured results		
		Original band (%)	Matched band (%)	Improvement factor (%)	Original band (%)	Matched band (%)	Improvement factor (%)
5 mm air	1.5:1	2.78	7.22	160	3.22	6.89	113.8
Substrate only	1.5:1	0.78	1.83	136	0.78	2.06	164
10 mm air	1.5:1	8.67	16.11	85.6	8.83	14.5	64.2
Edge-fed	2:1	1.33	3	125	2.17 [18]	5 [18]	131 [18]

Chapter 6

Conclusion

6.1. Background

The use of microstrip antennas has become increasingly popular. Despite the advantages promised by microstrip patch antennas, their inherent narrow impedance bandwidth often comes as a drawback limiting the antennas' usability. A number of proposals to enhance the antenna's impedance bandwidth performance by physically altering the antenna have been presented and are mentioned briefly in Chapter 2. The viability of a matching feed network to improve the bandwidth was also considered in the open literature, and the most common matching techniques were listed in Chapter 2. In Chapter 3 an alternative matching idea named the SRMT (Optimum Bandwidth Simple LC-Resonant Matching Technique) was presented. The SRMT was originally considered for probe-fed microstrip patch antennas. A number of well-known standard matching circuits were implemented in Chapter 4 to compare the SRMT with these techniques, while Chapter 5 presented examples where the matching technique was applied to various types of patch antennas both in simulation and measurement. The resulting improvement in impedance bandwidth was shown, and the different effect the SRMT has on the various types of antennas is highlighted.

In this, the final chapter, a retrospective overview of the work done in this dissertation is given. In the next section conclusions on the performance of the feed networks presented in this dissertation are drawn. Section 6.3 elaborates on the knowledge gained in this study and presents a number of ideas for future work.

6.2. Contributions

In Chapter 3 the design of a resonant circuit was explained. Theoretically predicted results were presented. It was evident in Chapter 3 that the SRMT is able to double the original antenna VSWR bandwidth. Chapter 5 presented a number of examples. The electrically thin patch antenna ("substrate-only" patch) ended up with a bandwidth improvement factor in excess of 150%, and for the electrically thick patch (10 mm air patch) an improvement of 85% was obtained. Although the improvement is less drastic, the electrically thick patch antenna presents a reasonably wide operating bandwidth in comparison to other types of microstrip patch antennas. In Chapter 4 the SRMT was compared to results obtained by the SRFT in [2, 4], and in Chapter 5 the SRMT was compared to the quarterwave coupled matching network, presented in [18]. The SRMT-matching network compared well with these matching techniques.

The SRMT-network is fairly simple to design and realise in microstrip line. The predefined circuit layout ensures that possible space occupancy is roughly known early in the antenna design process. The aim of the matching network is to reach a compact and effective solution. The SRMT-circuit succeeds in that only four components are used and the results are comparable with published results obtained for previous antenna matching techniques.

The SRMT works on the basic principle that the input impedance of a probe-fed patch antenna represents an equivalent parallel-RLC circuit with a series inductance. The impedance frequency behaviour obtained for the probe-fed patch is not limited to this type of antenna, but other patch antennas, as well as dipoles and almost any type of single element antenna can benefit from this matching technique. For other antennas without the

equivalent series inductance the level of phase transforming will probably be the main variable.

In this study it was illustrated how the feed network can be integrated as part of the design process of the antenna. Once the feed network is considered an integral part of the antenna, a newly defined system (i.e. feed network and antenna integrated) can be designed with enhanced performance. The matching feed network enables one to reach a specific impedance bandwidth without necessarily altering the antenna itself.

6.3. Challenges and issues for future work

The main focus of this study was to find a relatively simple way to solve the narrow impedance bandwidth problem of microstrip patch antennas. The use of the SRMT-network was proposed and analysed. The SRMT-circuit worked very effectively for narrowband patches, with the antennas obtaining more than double the original impedance bandwidth. The wideband patch, on the other hand, has shown less drastic improvement. A topic for future work might be to investigate the possibility of two or more resonators in the circuit.

The antennas presented in the dissertation are all single element radiators. In the case of an array of radiators the SRMT-circuit will be able to enhance the impedance bandwidth of each of the individual elements in the array. Another possible option for further investigation would be to look at how a single LC-resonator would be able to improve the impedance bandwidth of an array of antennas.

References

[1] H.F. Pues and A.R. van de Capelle, "An Impedance-Matching Technique for Increasing the Bandwidth of Microstrip Antennas", IEEE Transactions on Antennas and Propagation, Vol. 37, No. 11, November 1989, pp. 1345-1353.

[2] H. An, B. Nauwelaers and A.R. van de Capelle, "Matching Network Design of Microstrip Antennas with Simplified Real Frequency Technique", Electronic Letters, Vol. 27, No. 24, November 1991, pp. 2295-2297.

[3] E. Chang, S.A. Long and W.F. Richards, "An Experimental Investigation of Electrically Thick Rectangular Microstrip Antennas", IEEE Transactions on Antennas and Propagation, Vol. AP-34, No. 6, June 1986, pp. 767-772.

[4] H. An, B. Nauwelaers and A.R. van de Capelle, "Broadband Microstrip Antenna Design with the Simplified Real Frequency Technique", IEEE Transactions on Antennas and Propagation, Vol. 42, No. 2, February 1994, pp. 129-136.

[5] G. Mayhew-Ridgers, J.W. Odendaal and J. Joubert, "New Feeding Mechanism for Annular_Ring Microstrip Antenna", Electronic Letters, Vol. 36, No. 7, March 2000, pp. 605-606.

[6] G.A.E. Vandenbosch and A.R. van de Capelle, "Study of the Capacitively Fed Microstrip Antenna Element", IEEE Transactions on Antennas and Propagation, Vol. 42, No. 12, December 1994, pp. 1648-1652.

[7] R.B. Waterhouse, "Design of Probe-fed Stacked Patches", IEEE Transactions on Antennas and Propagation, Vol. 47, No. 12, December 1999, pp. 1780-1784.

[8] P.S. Hall, "Probe Compensation in Thick Microstrip Patches", Electronic Letters, Vol. 23, No. 11, May 1987, pp. 606-607.

[9] K. Levis, A. Ittipiboon and A. Petosa, "Probe Radiation Cancellation in Wideband Probe-fed Microstrip Arrays", Electronic Letters, Vol. 36, No. 7, March 2000, pp. 606-607.

[10] A. Ittipiboon, R. Oostlander, Y.M.M. Antar and M. Cuhaci, "A Modal Expansion Method of Analysis and Measurement on Aperture-Coupled Microstrip Antenna", IEEE Transactions on Antennas and Propagation, Vol. 39, No. 11, November 1991, pp. 1567-1573.

[11] D.M. Pozar, "Microstrip Antenna Aperture-coupled to a microstripline", Electronic Letters, Vol. 21, No. 2, January 1985, pp. 49-50.

[12] S. Maci and G. Biffi Gentili, "Dual-Frequency Patch Antennas," IEEE Antennas and Propagation Magazine, Vol. 39, No. 6, December 1997.

[13] D.M. de Haaij, J. Joubert and J.W. Odendaal, "Wideband dual-Frequency Stacked Microstrip Patch Antenna," Microwave and Optical Technology Letters, Vol. 31, No. 4, November 2001, pp. 289-292.

[14] D.M. de Haaij, J. Joubert and J.W. Odendaal, "Diplexing Feed Network for Wideband Dual-Frequency Stacked Microstrip Patch Antenna," Microwave and Optical Technology Letters, Vol. 36, No. 2, January 2003, pp. 100-102.

[15] J.R. James and P.S. Hall, "Handbook of Microstrip Antennas," Peter Peregrinus Ltd., London, 1989, Vol. 1, Chapter 6, pp. 311-351.

[16] H. An, B. Nauwelaers and A.R. van de Capelle, "Broadband Active Microstrip Antenna Design with the Simplified Real Frequency Technique", IEEE Transactions on Antennas and Propagation, Vol. 42, No. 12, December 1994, pp. 1612-1619.

[17] J.I. Kim and Y.J. Yoon, "Design of Wideband Microstrip Array Antennas Using the Coupled Lines", IEEE Antennas and Propagation International Symposium Digest, 2000, Salt Lake City, Utah.

[18] M.D. van Wyk and K.D. Palmer, "Bandwidth enhancement of microstrip patch antennas using coupled lines", Electronics Letter, Vol. 37, No. 13, 21 June 2001.

[19] D.M. de Haaij, J. Joubert and J.W. Odendaal, "Impedance Matching of Microstrip Antennas with a Parallel Resonant Circuit", IEEE Antennas and Propagation International Symposium Digest, 2001, Boston, Massachusetts.

[20] D.M. de Haaij, J.W. Odendaal and J. Joubert, "Increasing the Bandwidth of a Microstrip Antenna with a Parallel Resonant Circuit", IEEE Africon Conference Digest 2002, George, South Africa.

[21] D.M. Pozar, "Microwave Engineering, 2nd Edition," John Wiley and Sons, 1998

[22] G. Gonzales, "Microwave Transistor Amplifiers – Analysis and Design, 2nd Edition," Prentice Hall, 1997.

[23] H.J. Carlin, "A new Approach to Gain-Bandwidth Problems", IEEE Transactions on Circuits and Systems, Vol. CAS-24, No. 4, April 1977, pp. 170-175.

[24] H.J. Carlin and J.J. Komiak, "A new Method of Broad-Band Equalization Applied to Microwave Amplifiers", IEEE Transactions on Microwave Theory and Techniques, Vol. MTT-27, No. 2, February 1979, pp. 93-99.

[25] H.J. Carlin and P. Amstutz, "On Optimum Broad-Band Matching", IEEE Transactions on Circuits and Systems, Vol. CAS-28, No. 5, May 1981, pp. 401-405.

[26] B.S. Yarman and H.J. Carlin, "A Simplified "Real-Frequency" Technique Applied to Broad-Band Multistage Microwave Amplifiers", IEEE Transactions on Microwave Theory and Techniques, Vol. MTT-30, No. 12, December 1982, pp. 2216-2222.

[27] H.J. Carlin and B.S. Yarman, "The Double Matching Problem: Analytic and Real Frequency Solutions", IEEE Transactions on Circuits and Systems, Vol. CAS-30, No. 1, January 1983, pp. 15-28.

[28] E. Kerherve, P. Jarry and P-M Martin, "Design of Broad-Band Matching Network with Lossy Junctions Using the Real Frequency Technique", IEEE Transactions on Microwave Theory and Techniques, Vol. MTT-46, No. 3, March 1998, pp. 242-249.

[29] H.J. Carlin and P.P. Civalleri, "An Algorithm for Wideband Matching using Wiener-Lee Transforms", IEEE Transactions on Circuits and Systems, Vol. 39, No. 7, July 1992, pp. 497-505.

[30] H. Dedieu, C. Dehollain, J. Neirynck and G. Rhodes, "A New Method for Solving Broadband Matching Problems", IEEE Transactions on Circuits and Systems, Vol. 41, No. 9, September 1994, pp. 561-571.

[31] H. Oraizi, "Design of Impedance Transformers by the Method of Least Squares", IEEE Transactions on Microwave Theory and Techniques, Vol. 44, No. 3, March 1996, pp. 389-399.

[32] Y. Sun and J.K. Fidler, "Design Method for Impedance Matching Networks", IEE Proceedings – Circuits Devices and Systems, Vol. 143, No. 4, August 1996, pp. 186-194.

[33] P.L.D. Abrie, "Design of RF and Microwave Amplifiers and Oscillators", Artech House, 2000, pp. 333.

[34] Hongming An, "Broadband Active and Passive Microstrip Antennas," Ph.D Thesis, Katholieke Universiteit Leuven, Departement Elektrotechniek, May 1993.

[35] S. M. Duffy, "An Enhanced Bandwidth Design Technique for Electromagnetically Coupled Microstrip Antennas," IEEE Transactions on Antennas and Propagation, Vol. 48, No. 2, February 2000, pp. 161-164.

[36] C.A. Balanis, " Antenna Theory. Analysis and Design, 2nd Edition", John Wiley & Sons, 1997. Chapter 14.

[37] D.M. Pozar and D.H. Schaubert, "Microstrip Antennas. The Analysis and Design of Microstrip Antennas and Arrays", IEEE Press, 1995, Chapter 4, p.155.

[38] GML-1000 Data sheet, GIL Technologies, gilam@gilam.com.

[39] MC3 and MC3D Data sheet, GIL Technologies, gilam@gilam.com.

[40] IE3D user's manual, Release 8, Zeland Software Inc.

[41] Sonnet user's manual, Release 7.0a-Lite. http://www.sonnetusa.com.